Apd1 and Aim32 are prototypes of bis-histidinyl-coordinated non-Rieske [2Fe-2S] proteins

Kathrin Stegmaier[§‡], Catharina M. Blinn[§‡], Dominique F. Bechtel[§], Carina Greth[§], Hendrik Auerbach[†], Christina S. Müller[†], Valentin Jakob[§], Daili J. A. Netz[§], Volker Schünemann[†] & Antonio J. Pierik[§*]

Technische Universität Kaiserslautern, [§]Fachbereich Chemie and [†]Fachbereich Physik, Erwin-Schrödinger-Str. 54/56, D67663 Kaiserslautern, Germany

ABSTRACT: Apd1, a cytosolic yeast protein, and Aim32, its counterpart in the mitochondrial matrix, have a C-terminal thioredoxin-like ferredoxin domain and a widely divergent N-terminal domain. These proteins are found in bacteria, plants, fungi and unicellular pathogenic eukaryotes, but not in Metazoa. Our chemogenetic experiments demonstrate that the highly conserved cysteine and histidine residues within the C-X_8-C-X_{24-75}-H-X-G-G-H motif of the TLF domain of Apd1 and Aim32 proteins are essential for viability upon treatment of yeast cells with the redox potentiators gallobenzophenone or pyrogallol, respectively. UV-Vis, EPR and Mössbauer spectroscopy of purified wild type Apd1 and three His to Cys variants demonstrated that Cys207 and Cys216 are the ligands of the ferric ion and His255 and His259 are the ligands of the reducible iron ion of the [2Fe-2S]$^{2+/1+}$ cluster. The [2Fe-2S] center of Apd1 ($E_{m,7}$ = −164±5 mV, $pK_{ox1,2}$=7.9±0.1 and 9.7±0.1) differs from both dioxygenase ($E_{m,7}$ ≈ −150 mV, $pK_{ox1,2}$=9.8 and 11.5) and cytochrome bc_1/b_6f Rieske clusters ($E_{m,7}$ ≈ +300 mV, $pK_{ox1,2}$= 7.7 and 9.8). Apd1 and its engineered variants represent an unprecedented flexible system for which a stable [2Fe-2S] cluster with two histidine ligands, (two different) single histidine ligands or only cysteinyl ligands is possible in the same protein fold. Our results define a remarkable example of convergent evolution of [2Fe-2S] cluster containing proteins with bis-histidinyl coordination and proton-coupled electron transfer.

INTRODUCTION

Iron-sulfur (Fe/S)-cluster-containing proteins are found across all kingdoms of life, where they participate in fundamental cellular processes, such as respiration, photosynthesis and nitrogen fixation.[1] Fe/S proteins involved in electron-transfer processes can be classified on basis of their structural and electrochemical properties.[2] A prominent class of such proteins are the [2Fe-2S] ferredoxins, containing two iron ions that are bridged by two inorganic sulfides and usually coordinated by four cysteine thiolates. [2Fe-2S] ferredoxins share a β-grasp structure composed of 3-5 β-strands with 1-3 α-helices. They are further divided into the classical plant and vertebrate (or adrenodoxin) type ferredoxins and the thioredoxin-like ferredoxins (TLF).[3] In multiple domain redox enzymes exemplified by NADH and succinate dehydrogenases ferredoxin-like modules are responsible for internal electron transport. A subset of the structurally-related glutaredoxins bind a bridging [2Fe-2S] cluster with two cysteine residues as internal and two glutathione molecules as external ligands.[4] Ferrochelatases, SoxR and IscR[1] are examples of natural systems which a bind [2Fe-2S] cluster in a protein fold different from the ferredoxin or thioredoxin fold. [2Fe-2S] clusters can occur as artifact from breakdown of labile [4Fe-4S] clusters in SAM radical enzymes and other enzymes.[5]

Rieske-type proteins differ from other [2Fe-2S]-containing systems by their double β-sandwich fold composed of three antiparallel β-sheets and their coordination of the cluster by two cysteine thiolates and $N_δ$ of two histidine residues.[6-7] The reduction potentials of Rieske centers (−150 to +400 mV) are higher than those observed for [2Fe-2S] ferredoxins (−450 to −150 mV).[8-9] The human proteins MitoNEET, Miner1 and Miner2 belong to a third [2Fe-2S] protein family, characterized by a unique β-cap fold.[10] Coordination of the cluster by three cysteine residues and histidine $N_δ$ leads to a reduction potential of ~0 mV. Other biological systems with monohistidinyl coordination of a [2Fe-2S] cluster are IscR,[11] and the heterodimeric glutaredoxin-BolA-like protein complexes.[12] Histidine coordination not only modulates the stability and shifts the redox potential, but also enables proton-coupled electron transfer (PCET) by deprotonation of histidine ligand(s) in the oxidized state.[13]

Several cytosolic Fe/S proteins have a C-terminal tryptophan residue.[14-16] Bioinformatic analysis shows that Apd1, a 35.7 kDa protein from *Saccharomyces cerevisiae* named after the change of actin localization upon deletion (Actin patches distal gene 1)[17] has a C-terminal tryptophan and several conserved cysteine residues. Loss of the Apd1-encoding gene results in hydroxyurea susceptibility.[18] Yeast has a second protein (Aim32), which has a ~100 amino acid C-terminal TLF domain similar to Apd1. Deletion of the Aim32-encoding gene resulted in a slightly Altered Inheritance rate of Mitochondria, hence its name Aim32.[19] Overexpression of Aim32 protected yeast lacking the mitochondrial manganese superoxide dismutase (Δ*sod2*) against the drug primaquine under respiratory growth conditions.[20] Amino acid sequence analysis of Apd1 and Aim32 from fungi shows two highly conserved cysteine and two highly conserved histidine residues within the C-terminal TLF domain (Figure S1 and S2). UV-visible spectra have been reported for Apd1, but evidence for the cluster type and coordination is lacking.[18] Using chemogenetic screens and analysis by UV/Vis,

EPR and Mössbauer spectroscopy, we identified a unique redox-active [2Fe-2S] cluster with bis-histidinyl coordination. Our results define Apd1 and Aim32 as founding members of a widespread class of [2Fe-2S] proteins with proton-coupled electron transfer properties.

RESULTS

Chemogenetic identification of Fe/S ligands. Since deletion of *apd1* or *aim32* genes does not result in an apparent growth defect of yeast cells (Figure S3a), we searched the yeast haplo insufficiency and homozygous profiling database.[21] This dataset contains fitness signatures for growth in the presence of 3356 small molecules of 4812 yeast strains with individually deleted genes. In this screen the redox potentiator gallobenzophenone perturbed growth of Δ*apd1* cells at 84 µM. Our results show that even at lower concentration gallobenzophenone is lethal for Δ*apd1* cells on solid (25 µM) and liquid media (50 µM), but not for Δ*aim32* cells (Figure 1a and S3). This phenotype is 10,000–fold more specific than the previously reported effect of hydroxyurea (0.24 M) on Δ*apd1* cells.[18] The growth defect of Δ*apd1* cells could be rescued by Apd1 expressed from a plasmid, but not by Aim32 (Figure 1a). Gallobenzophenone and other compounds including harmaline[21] or primaquine[20] did not cause a selective growth defect for Δ*aim32* cells (Figure 1a and S4). If overexpression of Aim32 protects Δ*sod2* yeast cells against oxidative stress,[20] then Δ*sod2*/Δ*aim32* could be more sensitive to redox potentiating compounds. Indeed, we noted that wild type and Δ*sod2* yeast cells were resistant to 50 µM pyrogallol, but that Δ*sod2*/Δ*aim32* cells did not survive (Figure 1b). Notably, growth of Δ*sod2*/Δ*aim32* cells could be rescued by Aim32 expression from a plasmid, but not by Apd1 (Figure 1b). When gallobenzophenone was used, the pronounced growth defect on Δ*sod2*/Δ*aim32* cells could be partially rescued by expression of Aim32 but not of Apd1 (Figure S5a).

The strong growth phenotypes of Δ*apd1* cells treated with gallobenzophenone and Δ*sod2*/Δ*aim32* cells with pyrogallol are excellent tools to *in vivo* screen amino acid residues potentially involved in metallocenter coordination in Apd1 and Aim32. Apd1 has nine cysteine residues, of which the highly conserved C207 and C216 residues correspond to the first two cysteines of the TLF motif ($CX_{4\text{-}12}C\text{-}X_n\text{-}CX_3C$).[22] Aim32 has five cysteine residues, of which the highly conserved C213 and C222 residues match C207 and C216 of Apd1 (Figure 1c and d, S1 and S2). Remarkably, the cysteine residues at the third and fourth position of the TLF motif are histidine residues in Apd1 and Aim32 ($C\text{-}X_8\text{-}C\text{-}X_n\text{-}H\text{-}X_3\text{-}H$). From the eleven amino acid residues tested for Apd1 only residues C207, C216, H255 and H259 were required for cell growth in the presence of 50 µM gallobenzophenone (Figure 1e). C44 and C48 were not required for survival in the presence of gallobenzophenone (Figure 1e), pyrogallol (Figure S5b) or hydroxyurea (Figure S5c, contrary to previous findings[18]). For Aim32 only residues C213, C222,

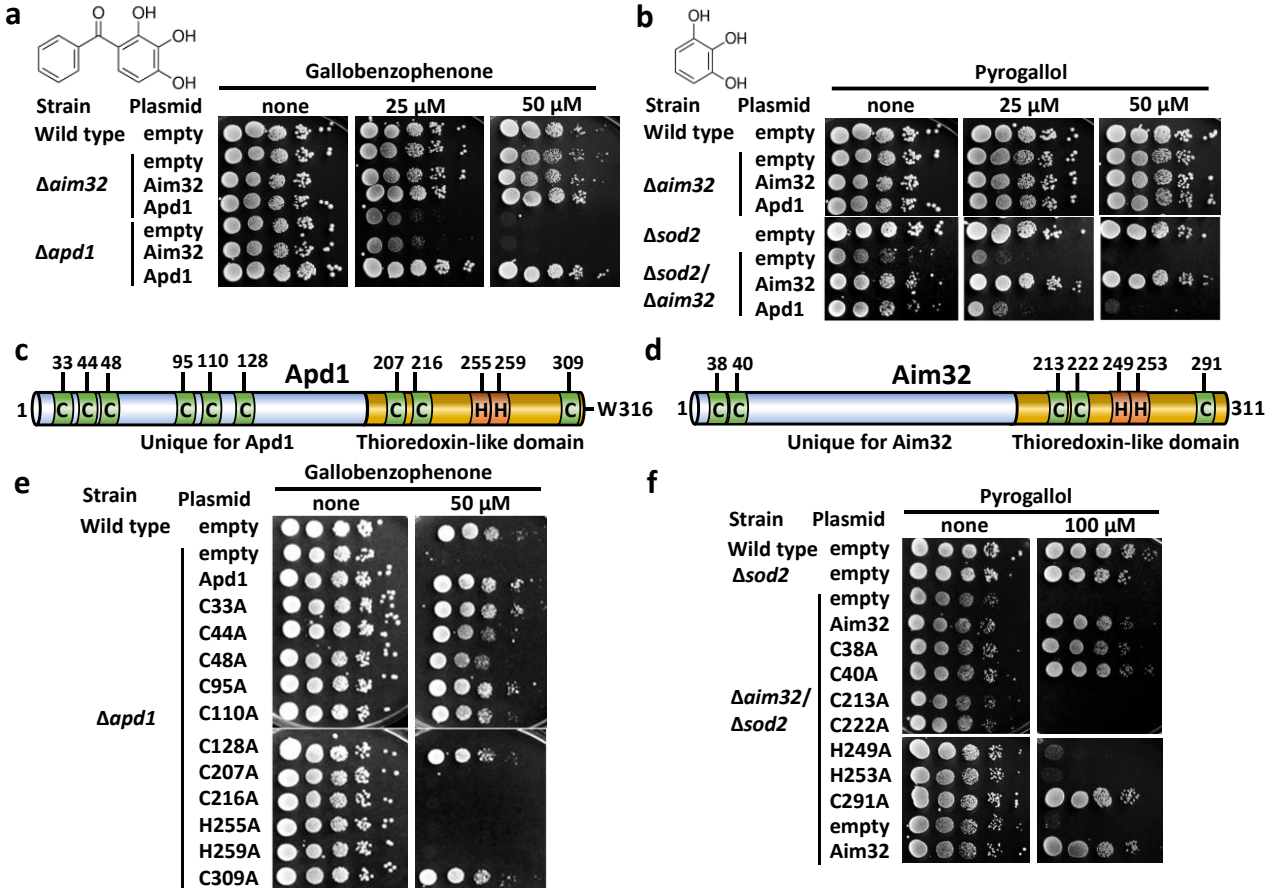

Figure 1. Chemogenetic screening of Fe/S ligands of Apd1 and Aim32 by conditional synthetic lethality of Δ*apd1* and Δ*aim32* strains. Wild type or indicated yeast deletion strains were transformed with empty plasmids or 416NP plasmids expressing Apd1 or Aim32 proteins. Serial 10-fold dilutions of liquid precultures were spotted onto agar plates with minimal glucose media and freshly-added gallobenzophenone (a) or pyrogallol (b). Photographs were taken after 2 days at 30 °C. (c) and (d) cartoons depicting potential ligands. (e) and (f) Growth sensitivity of wild type or yeast deletions strains with empty plasmids or 416NP plasmid-encoded Apd1 and Aim32 variants.

H249 and H253 were critical for cell survival of Δ*aim32*/Δ*sod2* cells treated with 100 μM pyrogallol (Figure 1f). All other cysteine residues, including C38 and C40, were not required for cell viability. These findings strongly suggest that the $CX_8CX_nHX_3H$ motif is responsible for metal binding of Apd1 and Aim32 *in vivo*.

[2Fe-2S] bis-histidinyl coordination of Apd1. Recombinant N-terminally hexa-His-tagged Apd1 and Aim32 expressed in *E. coli* were purified to homogeneity via Ni-NTA affinity chromatography (Figure S6). Both proteins as isolated exhibited a red color and had a well-structured UV-Vis absorption spectrum with maxima at 325, 455 and 550 nm (Figure S6c), indicative of a [2Fe-2S] cluster. Determination of non-heme iron and acid-labile sulfide ions identified 1.3-2.1 Fe/S per monomer of Apd1 or Aim32 (Figure S6c). Comparison with visible spectra of human adrenodoxin,[23] MitoNEET[24] and a Rieske protein[25] shows that Apd1 (and Aim32) lacks the pronounced peaks at 415 and 455 nm typical for the $[2Fe\text{-}2S]^{2+}$ cluster of adrenodoxin, which is coordinated by four cysteine residues (Figure S7). The prominent shoulder at 570 nm of the Apd1 protein is shared with the Rieske protein, but is lacking in the MitoNEET protein. Since the yield of Apd1 was 5-fold higher (25 mg/L culture) than that of Aim32, further spectroscopic studies focused on Apd1. Coordination of the [2Fe-2S] cluster in Apd1 was investigated in variants of which the two histidine residues were replaced individually (H255C or H259C) or as a pair (H255C/H259C) by cysteine residues. This ligand replacement strategy circumvents the disadvantages of alanine substitution, which frequently yields unstable apoproteins.[26] All three Apd1 variants could be purified to homogeneity (Figure S6a) with reasonable yields (~10 mg/L culture). We observed remarkable spectral differences: the red color of wild type Apd1 changed to red-brown for the H255C and H259C variants and to olive-brown for the H255C/H259C variant (Figure S6d and e). The visible spectra of the H255C and H259C variants were similar to each other and both lacked a pronounced 570 nm shoulder. A more substantial change was observed for the H255C/H259C variant which acquired maxima at 415 and 455 nm similar to adrenodoxin (Figure S7).

We further applied EPR spectroscopy to investigate the cluster coordination in Apd1 and its variants. Anaerobic reduction by sodium dithionite at pH 8.5 quantitatively converted the cluster into a paramagnetic EPR-active S=1/2 state (Figure 2). At 10 K well-resolved rhombic signals from a single species were observed, which could be simulated with g_z=2.009, g_y=1.906 and g_x=1.861 for Apd1 (Figure 2a, Table S1) and g_z=2.011, g_y=1.903 and g_x=1.860 for Aim32 (Figure S8, Table S1). Both EPR signals are detectable with slight broadening up to 77 K, which is typical for $[2Fe\text{-}2S]^{1+}$ clusters.[27] ^{57}Fe enrichment of Apd1 by *E. coli* growth on ^{57}Fe-citrate led to hyperfine broadening of the linewidths along all three axes of the g-tensor (Figure S9). We restrained the number of EPR simulation parameters by a fitting procedure with fixed g-values and linewidths derived from the non-enriched sample. The number of $\boldsymbol{A}(^{57}Fe)$ parameters was decreased from six to two by assuming isotropic $\boldsymbol{A}(^{57}Fe)$ values for the ferric and ferrous ions. With 85±5 % ^{57}Fe enrichment the spectrum could accurately be simulated with $|\boldsymbol{A}|(^{57}Fe^{3+})$=50±10 MHz and $|\boldsymbol{A}|(^{57}Fe^{2+})$=20±5 MHz. The EPR-derived $|\boldsymbol{A}|^{57}$Fe values for Apd1 are typical for antiferromagnetically coupled fer ric (S=5/2, $\boldsymbol{A}$ between -41 and -57 MHz) and ferrous sites (S=2, $\boldsymbol{A}$ between +9 and +35.5 MHz)

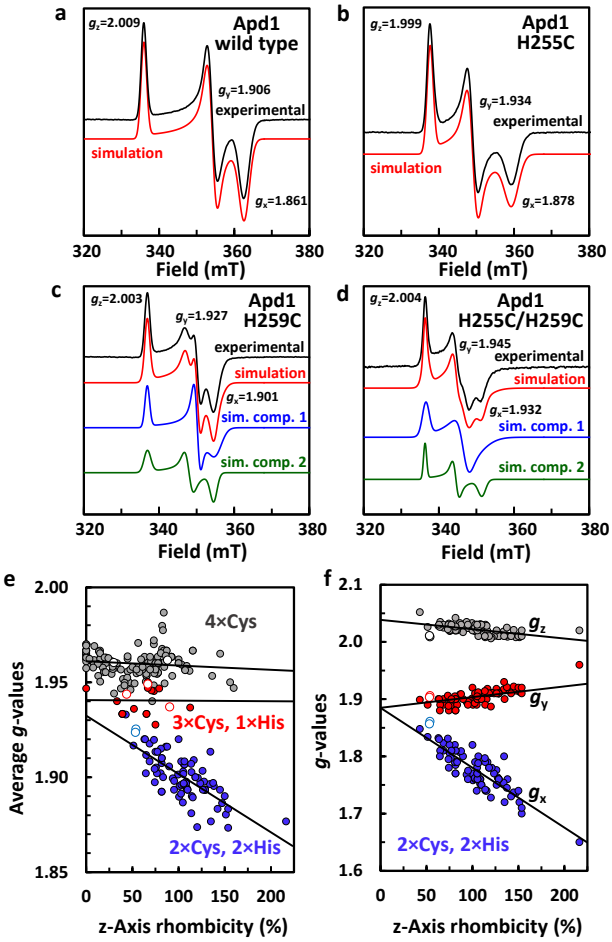

Figure 2. EPR spectroscopic evidence for bis-histidinyl coordination of the [2Fe-2S] cluster in Apd1. (a-d) EPR spectra of dithionite-reduced wild type Apd1 and variants (9.456 GHz, 10 K, 0.02 mW microwave power). Simulations (Table S1) are shown in colour. (e) Comparison of average g values as a function of z-axis rhombicity (R_z) for biological $[2Fe\text{-}2S]^{1+}$ clusters (closed symbols) with Apd1 wild type and variants (open symbols). (f) Comparison of g values as a function of R_z for Rieske centers (closed symbols) with Apd1 and Aim32 wild type (open symbols). Lines in (e) and (f) are linear regression curves. See Table S2-S4 for g-values.

of $[2Fe\text{-}2S]^{1+}$ clusters, as determined by Mössbauer and ENDOR spectroscopy.[6, 28-29] Comparison of the average g-value (g_{av}=1.925 and 1.924 for Apd1 and Aim32, respectively, Figure 2e) and the g-values (Figure 2f) as function of the z-axis rhombicity R_z $[300(g_y\text{-}g_x)/(2g_z\text{-}g_y\text{-}g_x)]$ in a Gibson plot demonstrates that wild type Apd1 g-values are at the low rhombicity extreme for Rieske-type $[2Fe\text{-}2S]^{1+}$ clusters (Table S2-S4). Note that R_z is used over the full range in Figure 2e and f to prevent changing axes (R_z values above 100 % are 200 % minus R_z along the x axis).[8] Single histidine to cysteine replacements substantially alter the coordination, as reflected by shifts of all g-values (H255C, g_z= 1.999, g_y=1.934, g_x=1.878 and g_{av}=1.938; H259C, g_z = 2.003, g_y=1.927, g_x=1.901 and g_{av}=1.944) (Figure 2b and c). Simulation indicates the presence of a second, minor component for the H259C variant with g_z=2.003, g_y=1.940, g_x=1.904 and g_{av}=1.949 and ~40% abundance (Table S1). The spectra of these variants are remarkably similar to human mitoNEET (g_z= 2.007, g_y=1.937, g_x=1.897 and g_{av}=1.947)[30] and other proteins featuring a $[2Fe\text{-}2S]^{1+}$ cluster with 3×Cys,1×His

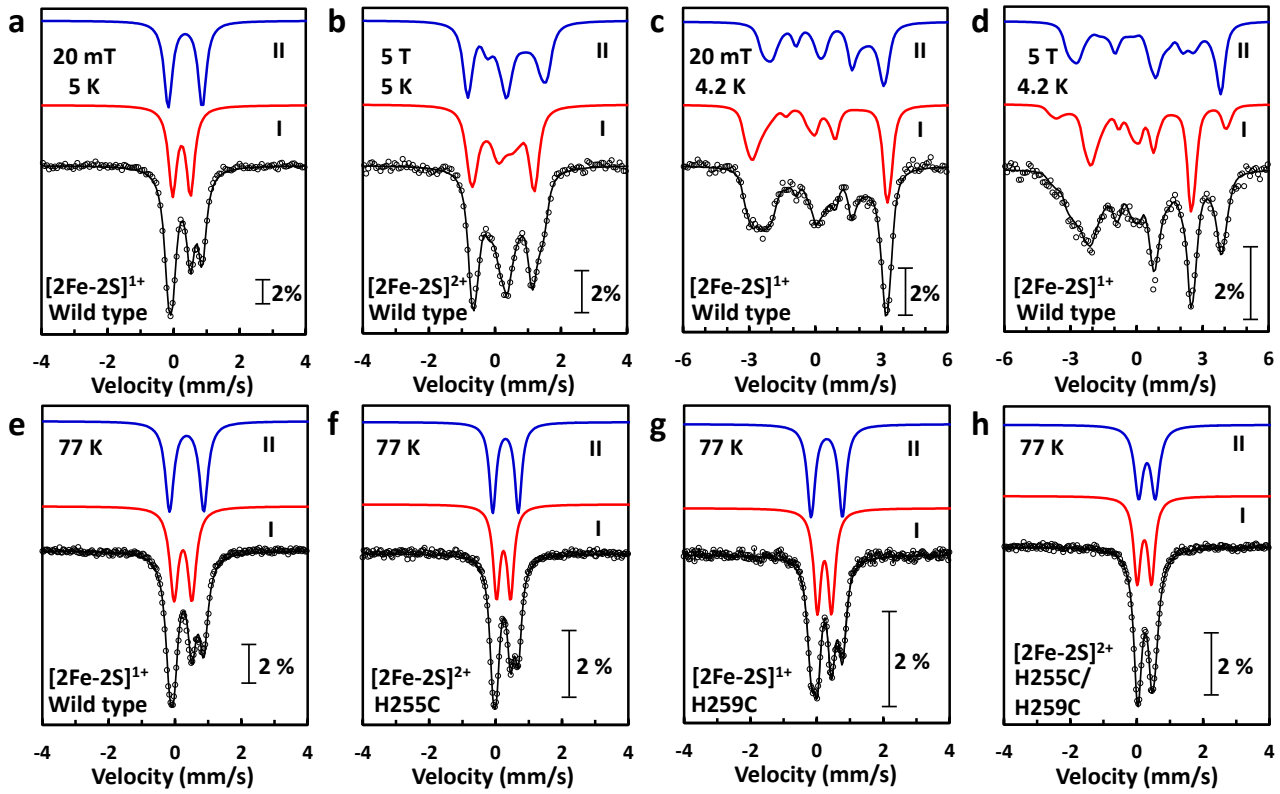

Figure 3. Mössbauer spectroscopy of wild type Apd1 (a-e), and its H255C, H259C and H255C/H259C variants (f-g). Samples (2-5 mM) as isolated ($[2Fe\text{-}2S]^{2+}$) or after dithionite reduction ($[2Fe\text{-}2S]^{1+}$), in 20 mM Tris/Cl, pH 9.0, 150 mM NaCl. The sum of the simulations (black line) of component I and II (red and blue lines) are superimposed on the experimental spectra (parameters are in Table 1).

coordination (Table S3). In the H255C/H259C variant the *g*-values change to g_z= 2.004, g_y=1.945, g_x=1.932 causing a shift of g_{av} to 1.960. For simulation a second component with slightly different *g*-values (g_z=2.006, g_y=1.959, g_y=1.920 (abundance of 32 %) with g_{av}=1.962 was required (Figure 2d and Table S1). These parameters are almost identical to the exclusively cysteinyl-coordinated $[2Fe\text{-}2S]^{1+}$ cluster of *Aquifex aeolicus* TLF (g_z=2.006, g_y=1.950, g_x=1.918 and g_{av}=1.958).[31] The $[2Fe\text{-}2S]^{1+}$ cluster in wild type Apd1 and the H255C variant were stable for 4 h at 25 °C (Figure S10). For the H259C and H255C/H259C variants 10-30% loss of double integrated EPR intensity indicated a slightly increased cluster lability. During a 4 h incubation of the H259C variant the relative abundance of the major EPR species increased from 60 % to ~ 71 % (Figure S11).

To address whether the two histidine ligands bind to one or two different iron ions, we performed Mössbauer spectroscopy of Apd1 and its variants isolated from ^{57}Fe-grown *E. coli* (Figure 3). As isolated, oxidized wild type Apd1 at 5 K with a parallel applied magnetic field of 20 mT exhibited two quadrupole doublets of equal integrated intensity, which could be simulated with isomer shifts (δ) of 0.24 and 0.35 mm/s with quadrupole splittings (ΔE_Q) of –0.54 and +1.06 mm/s for subspectra I and II, respectively. Spectra recorded at 5 K and a magnetic field of 5.0 T (Figure 3b, Table 1) determined the sign of the quadrupole splittings and demonstrated that the doublets arise from a diamagnetic antiferromagnetically coupled ferric ion pair. The parameters of the two quadrupole doublets are almost identical to those of the Rieske center in benzoate 1,2-dioxygenase from *Pseudomonas putida*[32] and similar to the *T. thermophilus* Rieske protein[6] (Table S5). Thus, both histidine residues (H255 and H259) coordinate the ferric ion with the higher isomer shift (subspectrum II, δ = 0.35 mm/s) due to lower covalencies of the Fe-N bonds. An exclusive sulfur coordination of the ferric ion by Cys207, Cys216 and the two bridging S^{2-} ions is compatible with the lower isomer shift of subspectrum I (δ = 0.24 mm/s). Upon dithionite reduction the signal of the all ferric $[2Fe\text{-}2S]^{2+}$ cluster disappeared beyond detection at 77 K and broad spectra from a paramagnetic species were detected at zero field. Because the electronic spin relaxation rate of the $[2Fe\text{-}2S]^{1+}$ cluster is slow in comparison to the nuclear precession frequency, individual quadrupole doublets of the ferric and ferrous ions could not be detected below 200 K. The quadrupole doublet of the ferrous ion became discernable (δ=0.67 mm/s and ΔE_Q=3.00 mm/s, Figure S12) raising the temperature up to 230 K. Lack of collapse into quadrupole doublets by slow Orbach relaxation in Apd1 is not unique. For the $[2Fe\text{-}2S]^{1+}$ clusters of adrenodoxin and mouse ferrochelatase strong exchange interaction (J>300 cm^{-1}) leads to the same phenomenon.[33] Analysis of the 4.2 K Mössbauer spectra at applied fields of 20 mT and 5 T allowed extraction of spin Hamiltonian parameters (Figure 3c and d). Assignment to ferric and ferrous site within the $[2Fe\text{-}2S]^{1+}$ cluster is straightforward (Table S6): the ferric site (subspectrum I) has δ= 0.32 mm/s and ΔE_Q=+0.81 mm/s, whereas the ferrous site (subspectrum II) has δ= 0.75 mm/s and ΔE_Q= –3.16 mm/s. The increase of the isomer shift of the ferric site from 0.24 to 0.32 mm/s is caused by shift of electron density by valence delocalization from the ferrous site.[11] ^{57}Fe hyperfine couplings ($\boldsymbol{A}_{xx,yy,zz}$) of –49, –57, –42 MHz for the ferric site and +22, +11, +34 MHz for the ferrous site were required for simulation. The difficulty to pinpoint a unique combination of asymmetry parameters and $\boldsymbol{A}$ values for the ferric and ferrous site was avoided

Table 1. Mössbauer parameters for the [2Fe-2S] cluster of Apd1.

species	pH	Temperature (K)	redox state	subspectrum I (all sulfur coordinated)				subspectrum II (histidine coordinated[a])			
				δ (mm/s)[b]	ΔE_Q (mm/s)[b]	Γ (mm/s)[bc]	η[bd]	δ (mm/s)[b]	ΔE_Q (mm/s)[b]	Γ (mm/s)[bc]	η[bd]
Wild type[e]	9.0	5	ox	0.24	–0.54	0.30	0.6	0.35	+1.06	0.30	0.3
	9.0	77	ox	0.23	0.53	0.31	NA[f]	0.34	1.03	0.31	NA
	9.0	4.2	red	0.32	+0.81	0.31	0	0.75	–3.16	0.35	-3.0
				^{57}Fe hyperfine couplings -49, -57, -42 MHz[g]				^{57}Fe hyperfine couplings +22, +11, +33 MHz[g]			
H255C	9.0	5	ox	0.24	–0.43	0.30	0.5	0.30	+0.77	0.30	0.5
	9.0	77	ox	0.24	0.42	0.25	NA	0.30	0.75	0.25	NA
H259C	9.0	5	ox	0.24	–0.45	0.30	0.5	0.31	+0.95	0.30	0.4
	9.0	77	ox	0.23	0.43	0.26	NA	0.31	0.95	0.28	NA
H255C/H259C	9.0	5	ox	0.26	–0.39	0.30	0.5	0.28	+0.58	0.30	0.4
	9.0	77	ox	0.25	0.37	0.25	NA	0.28	0.58	0.28	NA
Wild type, diprotonated	6.0	5	ox	0.24	–0.57	0.34	0.6	0.36	+1.11	0.29	0.3
	6.0	77	ox	0.23	0.56	0.26	NA	0.36	1.11	0.26	NA
Wild type, monoprotonated[h]	9.0	5	ox	0.24	–0.54	0.31	0.5	0.35	+1.05	0.29	0.4
	8.5	77	ox	0.23	0.52	0.26	NA	0.34	1.04	0.27	NA
Wild type, deprotonated[h]	10.5	5	ox	0.24	–0.51	0.29	0.7	0.33	+0.94	0.30	0.4
	10.5	77	ox	0.24	0.49	0.26	NA	0.33	0.94	0.29	NA

[a]For H255C/H259C these values are assigned to the ferric ion coordinated by C255 and C259. [b]Estimated uncertainties are ±0.01 mm/s for isomer shifts, ±0.02 mm/s for quadrupole splittings, ±0.01 mm/s for linewidths and ±0.3 for asymmetry parameters. [c]Linewidth at half height for the Lorentzian lines. [d]Asymmetry parameter. [e]Average parameters not corrected for contributions by diprotonated and deprotonated species. [f]Not applicable. [g]Along the g_x=1.861, g_y=1.906 and g_z=2.009 axis, orientation defined by preliminary ^{57}Fe Q-band ENDOR measurements, estimated relative errors 5%. [h]Refers to the parameters after iterative fitting of the pH 8.5, 9.0 and 10.5 data with the content of di-, mono- and deprotonated species calculated from experimental $pK_{ox1,2}$ values and fixed Mössbauer parameters from the diprotonated form.

by use of the EPR derived *g*-values and preliminary ^{57}Fe Q-band ENDOR data.

Comparison the Apd1 variants with wild type Apd1 was performed at 77 K in absence of an applied magnetic field (Figure 3e to g). Under these conditions the Mössbauer parameters of the Apd1 wild type spectrum were similar to those for the spectrum at 5 K (Figure 3a, Table 1). Single histidine to cysteine Apd1 variants (H255C and H259C) have Mössbauer parameters comparable with mitoNEET[34], with exception of a slightly different quadrupole splitting for the H255C variant (Figure 3f, g and Table S5). Upon exchange of the second histidine to cysteine (H255C/H259C) the isomer shifts (Figure 3h) became almost identical to the all cysteine coordinated [2Fe-2S] cluster of TLF.[35-36] For all variants the antiferromagnetic coupling was ascertained by measurement at 5 K with an applied field of 5 T (Figure S13, Table 1). Taken together, chemogenetic analysis of variants, visible, EPR and Mössbauer spectroscopy provide compelling evidence for two structurally different iron ions within the $[2Fe\text{-}2S]^{2+/1+}$ cluster: a ferric ion with an exclusive sulfur coordination and a reducible ferric site coordinated by the two bridging acid-labile sulfide ions and by H255 and H259.

Redox biochemistry of Apd1. In the oxidized state Apd1 remained stable over a broad pH range (pH 6 to 11, Figure S14). A biphasic hypsochromic shift of 13 nm with concomitant increase of the extinction coefficient by 9 % was observed upon deprotonation (Figure S15). Simulation of the pH-dependency of the absorbance difference between 445 and 465 nm with the Henderson-Hasselbalch equation for two single (de)protonations identified pK_{ox1}= 7.9 ± 0.1 and pK_{ox2}= 9.7 ± 0.1 (Figure 4a). We attribute these two pK_{ox} values to (de)protonation of the non-coordinating imidazole nitrogens of the two coordinating histidine residues. Consistently, upon conversion to a 3×Cys,1×His coordination in the H255C and H259C variants only a single (de)protonation event with a two-fold weaker absorbance difference was detected with pK_{ox}= 9.8 ± 0.1 and 9.4 ± 0.1, respectively (Figure 4a and S16). In agreement with the exclusive cysteinyl coordination revealed by EPR and Mössbauer spectroscopy the visible absorbance spectrum of the H255C/H259C variant was pH independent.

Next, Apd1 was submitted to anaerobic dye-mediated reductive titrations. Our results show that the $[2Fe\text{-}2S]^{2+/1+}$ redox couple in Apd1 has an almost pH-independent midpoint potential below pH 8 ($E_{m,\ low\ pH}$= –161±5 mV vs. SHE), but that the reduction potential becomes pH-dependent at higher pH values (Figure 4b and S17). At pH 10 the midpoint potential of Apd1 decreases down to –291 mV with a slope of -104 mV/pH unit, which demonstrates that up to two protonations accompany reduction of the $[2Fe\text{-}2S]^{2+}$ cluster. EPR spectra of dithionite reduced Apd1 exhibited minor changes of the *g*-values (Δg_z = +0.001, Δg_y = –0.001, Δg_x = –0.002) between pH 5.5 and 10.5 (Figure S18). Shifts of similar amplitude (Δg_z = –0.003, Δg_y = +0.001, Δg_x = +0.002), but in the opposite direction, were found for the *T. thermophilus* Rieske protein upon a pH change from 6.1 to 10.2. Such small changes are not associated with deprotonation of the N_ε atoms of the histidine ligands, since this Rieske protein has pK_{red} = ~12.5.[13] The minor changes likely derive from buffer-induced changes or deprotonation events beyond the direct coordination sphere. We therefore infer that Apd1 has pK_{red} values above 12 and apply an appropriate equation neglecting pK_{red}.[37-38] The pH dependency of the midpoint potential could be satisfactorily reproduced with a fit using the two pK_{ox} values from visible spectroscopy (pK=7.9 and 9.7) and $E_{m,low\ pH} \approx -161 \pm 5$ mV ($E_{m,7} \approx -164$ mV). The properties of the [2Fe-2S] center of Apd1 differ from both dioxygenase ($E_{m,7} \approx -150$ mV, $pK_{ox1,2}$= 9.8 and 11.5) and cytochrome bc_1/b_6f Rieske clusters ($E_{m,7} \approx +300$ mV, $pK_{ox1,2}$= 7.7 and 9.8)[13]. Conversion from 2×Cys,2×His to 3×Cys,1×His coordination caused a drop of the redox midpoint potential from –203 mV to –415 mV (H255C) or –395 mV (H259C). These experiments were carried out at pH 8.5, the pH value at which the variants were most stable. A further change to 4×Cys coordination lowered the midpoint potential to –525 mV (H255C/H259C). Thus-far the effect of His→Cys substitution in biological [2Fe-2S] clusters was only known for a very unstable H64C variant of the *Sulfolobus solfataricus* Rieske protein[39] and a H87C variant of MitoNEET.[40] In these systems His to Cys replacement led to a drop of the redox midpoint potential by ~350 mV and 315 mV, respectively. The average observed change of the redox midpoint potential for Apd1 is –188 mV per His→Cys substitution (–212, –192 and –322/2 mV). Thus, our data point out that stabilization of the ferric oxidation state by change from histidine to the more electronegative cysteinate is not as pro-

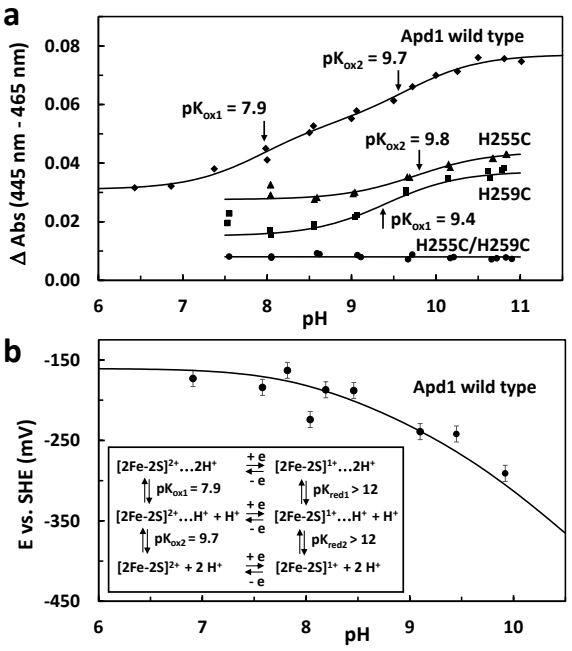

Figure 4. Protonation events and PCET in Apd1. (a) Least squares fits to the Henderson-Hasselbalch equation (solid lines) or the average absorbance difference for H255C/H259C. (b) pH dependence of the redox midpoint potential for wild type Apd1 by dye-mediated EPR redox titrations (fit for pK_{ox} values from (a) and $E_{m,\ low\ pH}$ = −161±5 mV). The inset shows a scheme with different states of the cluster (… indicates histidine-bound).

nounced as in MitoNEET or for the Rieske protein.

Oxidized Apd1 shows different Mössbauer signatures of all three protonation states of the cluster histidine ligands at 77 K (Figure 5). Measurement of Mössbauer spectra at 5 K and an applied magnetic field of 5 T ascertained the diamagnetic nature of oxidized Apd1 in all protonation states (Figure S19). From the pH values of the samples and the pK values (Figure 4) the proportion of the various forms were calculated (Figure 5d). For the diprotonated form parameters were determined directly from the pH 6.0 spectrum, neglecting the calculated 1 % monoprotonated form. Iterative rounds of simulation of the pH 8.5 (19 % di-, 76 % mono-, 5 % deprotonated), pH 9.0 (6 % di-, 78 % mono-, 16% deprotonated) and pH 10.5 (14 % mono-, 86 % deprotonated) Mössbauer spectra progressively extracted isomer shifts, quadrupole splittings and linewidth parameters. The isomer shift of subspectrum I was almost pH independent (0.23-0.24 mm/s) at 5 and 77 K, whereas only a slight decrease of the quadrupole splitting was seen upon successive deprotonation of the histidine ligands (0.57, 0.54 and 0.51 mm/s at 5 K, Table 1, Figure S19). For the *T. thermophilus* Rieske protein a similar trend for the all sulfur coordinated ferric ion was observed upon deprotonation.[41] A significant decrease of the isomer shift (0.36, 0.35, 0.33 mm/s) and quadrupole splitting (1.11, 1.05, 0.94 mm/s at 5 K) of the Apd1 subspectrum II occurred upon histidine deprotonation. In the *T. thermophilus* Rieske protein the changes of the Mössbauer parameters of the bis-histidinyl coordinated ferric ion are larger, but show the same tendency (δ=0.34, 0.29, 0.29 mm/s, ΔE_Q=1.05, 0.78, 0.71 mm/s).[41] These findings corroborate the assignment of subspectra I and II. The effects of ligand protonation on the two ferric ions support the choice of nesting of quadrupole doublets, i.e. which isomer shift is associated with which quadrupole splitting. An assignment by the minimization of ferric ion isomer shifts for the Rieske protein[6, 41] and for Apd1 holds for all protonation states.

With the Mössbauer data on the protonation states of Apd1, its monohistidinyl coordinated variants and data from literature (Table S5) we can construct a sufficiently densely populated truth diagram with isomer shifts along the x-axis and quadrupole splittings along the y-axis (Figure 5e). If data were available only for 77 K, isomer shifts were corrected to 4.2 K by +0.01 mm/s for a second order Doppler shift and quadrupole splittings were assumed temperature independent. Many all sulfur coordinated $[2Fe\text{-}2S]^{2+}$ clusters exhibit two almost identical quadrupole doublets for the ferric ions and enter the truth diagram as a single point or as two closely spaced points (4xCys, 4S, δ=0.28±0.02 mm/s, range 0.25-0.33, ΔE_Q=0.59±0.11 mm/s, range 0.39-0.87, n=84). For MitoNEET, Grx3-Fra2, IscR, RsrR, IscU and Apd1 monohistidinyl variants (3xCys, 4S, δ=0.27±0.02 mm/s, range 0.24-0.30 mm/s, ΔE_Q=0.52±0.08 mm/s, range 0.43-0.66, n=9), Rieske proteins and Apd1 in various protonation states (2xCys, 4S, δ=0.24±0.01 mm/s, range 0.24-0.26, ΔE_Q=0.52±0.07 mm/s, range 0.44-0.70, n=12) the Mössbauer parameters are not strongly affected by histidinyl coordination of the other ferric ion. The cloud for the all sulfur coordinated ferric ions in the lower left range of the truth diagram is separated from the mono- and bis-histidinyl coordinated ferric ions in the central part and top right part of the diagram, with exception of the pH 10 data of the *T. thermophilus* Rieske protein.[42] For the *T. thermophilus* Rieske protein[41] and Apd1 (Figure 5a-c) protonation of histidine ligands shifts the position in the diagram progressively to the top right. More emphasis on defined protonation states in future Mössbauer studies, including monohistidinyl coordinated clusters, will expand the application of this truth diagram for identification of the number of histidine ligands and their protonation state. It will be of equal importance to collect Mössbauer data on aspartate,[43] serine,[44] and water[45] coordinated [2Fe-2S] clusters.

Relevance of the redox potential and C-terminal tryptophan of Apd1 *in vivo*. We next tested the impact of alteration of the redox properties of the $[2Fe\text{-}2S]^{2+/1+}$ cluster on cell growth in the presence of 50 µM gallobenzophenone (Figure 6a). Clearly, single or double substitution of H255/H259 by cysteine, which drastically lowers the redox midpoint potential, has the same consequence as replacement of cluster coordinating ligands by alanine. Our results indicate that the native cluster coordination of Apd1 is of crucial importance for the *in vivo* protection against the redox potentiator gallobenzophenone.

The amino acid tryptophan occurs at 1.4 % of all human and 1.7 % of all yeast proteins as C-terminal residue.[46] Of 35 human and yeast cytosolic and nuclear iron sulfur proteins[47] seven (20 %) have a C-terminal tryptophan residue: Nar1[14], the polymerase catalytic subunits Pol3 and Rev3[15], viperin[16], isopropylmalate isomerase, glutamine phosphoribosylpyrophosphate amidotransferase and Apd1. This is unlikely to be coincidental and therefore suggests a functional relevance. For the human radical SAM protein viperin the C-terminal tryptophan residue is essential for *in vivo* [4Fe-4S] cluster insertion by the CIA machinery.[16] If [2Fe-2S] cluster insertion into Apd1 by the CIA machinery equally requires a C-terminal tryptophan, then the deletion of this amino acid should lead to gallobenzophenone sensitivity. Indeed, Δ*apd1* cells expressing Apd1 lacking its C-terminal tryptophan exhibit a very pronounced growth defect (Figure 6). These experiments highlight the importance of the C-terminal tryptophan for physiological function, most likely as signal for CIA machinery recruitment.

EPR detection of Apd1 in yeast cell extract. *E. coli* can incorporate an erroneous cluster type in recombinantly expres-

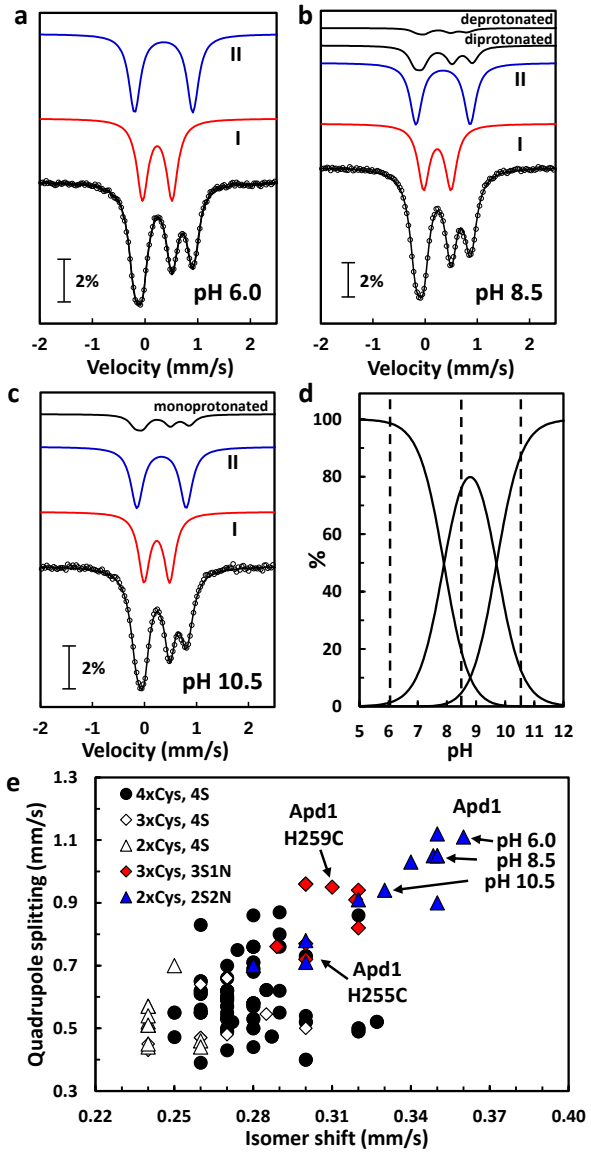

Figure 5. Mössbauer spectroscopy of the different protonation states of Apd1 (a-c). T= 77 K, no applied field. The sum of the simulations (black line) of component I, II (red and blue lines) and contributions of minor species (black lines, top) are superimposed on the experimental spectra (parameters are in Table 1). (d) Abundance of di-, mono- and deprotonated forms (pK_1=7.9, pK_2=9.7). Dashed lines correspond to the samples in (a-c). (e) Mössbauer truth diagram for biological $[2Fe\text{-}2S]^{2+}$ clusters. Values and references are in Table S5.

sed proteins.[48] Therefore we aimed to detect Apd1 *in vivo*. Since the abundance of Apd1 (~2.6×10^3 molecules/cell[49]) is too low for EPR detection we used Δ*apd1* yeast cells harboring a multicopy plasmid expressing Apd1 from the promoter for fructose 1,6-bisphosphate aldolase (Fba1, ~8.5×10^5 molecules/cell[49]). In Δ*apd1* yeast cell extract only a weak g=1.94 EPR signal and a slightly saturated g=2.01 signal are observed at conditions optimal for detection of recombinant Apd1 (Figure 6b). The former signal derives from the abundant endogenous [2Fe-2S]-containing protein succinate dehydrogenase, which is (partially) reduced in yeast cells.[50] The latter signal is from organic radicals of flavoenzymes and ubisemiquinone.[50] Due to the g-anisotropy the Rieske EPR signal is not detectable. In the difference spectrum an EPR signal with g_z=2.01, g_y=1.91 and

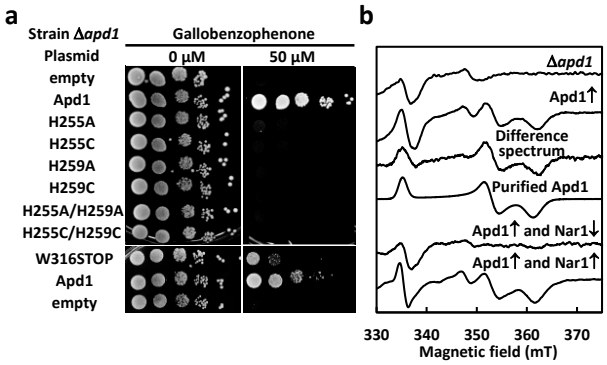

Figure 6. Bis-histidinyl [2Fe-2S] cluster coordination and the C-terminal tryptophan of Apd1 *in vivo*. (a) Gallobenzophenone growth sensitivity of Δ*apd1* yeast cells with empty plasmid or plasmids expressing Apd1 and indicated variants. See Figure 1 for conditions. (b) EPR spectroscopy of extracts of Δ*apd1*, Δ*apd1* overexpressing Apd1 (↑Apd1) or Δ*apd1*/Gal-Nar1 yeast cells (grown on glucose for 40 h) after reduction with 2 mM sodium dithionite for 2 min. T=77 K, 9.42 GHz, power 20 mW, modulation 1.5 mT.

g_x=1.86 is seen, which matches the g-values of purified recombinant Apd1 (Figure 6b). These findings provide concluding evidence that *in vivo* Apd1 has the same cluster type and coordination as the protein produced in *E. coli*. The *bona fide* nature of the [2Fe-2S] cluster of Apd1 was further assessed by the dependence on the CIA machinery factor Nar1. After depletion of Nar1 by growth on glucose medium for 40 h the EPR signal of Apd1 disappeared beyond detection in dithionite reduced Δ*apd1*/Gal-Nar1 yeast cell extract. Our findings show that the [2Fe-2S] cluster in Apd1 is a genuine target of the CIA machinery. Moreover, these data corroborate the cytosolic localization of Apd1 (Figure S20).

Phylogenetic analysis of the Apd1/Aim32 protein family. BLASTP analysis revealed numerous Apd1/Aim32 homologues annotated as pfam06999 ("Suc_Fer-like").[51] Most members are eukaryotic and bacterial proteins of 280-440 residues with a C-terminal ~100 amino acid TLF domain. This annotation has been propagated from a single publication[52] on a potato cDNA clone encoding a 42 kDa Apd1/Aim32-like protein. It is unlikely that this protein is a sucrase, as polyclonal antibodies raised against a 57 kDa sucrase were used.[53] Moreover, the recombinant protein presented a very low sucrase activity (K_M= 0.2 M, $V_{max}=2\times10^{-4}$ s^{-1}). Therefore, we suggest to use the more appropriate name Homologs of Apd1/Aim32 Thioredoxin-Like Ferredoxins (HAA-TLF) family. From the 1377 Pfam06999 members a collection of 1334 full length protein sequences was extracted, aligned with Clustal Omega[54] and phylogenetically analysed with iTOL[55] (Figure 7a). The leaves of the tree are subsets of homologs in particular taxonomic divisions. Whereas all fungi and Chloroplastida (plants and algae) have at least two homologs, other eukaryotes (Protozoa, Excavata, Amoebozoa and straminopiles-alveolates-Rhizaria (SAR) only have a single homolog. Metazoa, including man, and Archaea lack HAA-TLFs. For Fungi, a clear separation between Apd1 and Aim32 proteins was seen. Since our cellular localization experiments in *S. cerevisiae* show that Apd1 is a cytosolic protein and that Aim32 is a soluble mitochondrial matrix protein (Figure S20), we correlate these fungal Apd1 and Aim32 branches with cytosolic and mitochondrial HAA-TLFs, respectively. This observation is supported by the presence of a C-terminal tryptophan residue in the fungal Apd1 branch. In all non-fungal organisms a C-terminal tryptophan is absent, therefore these sequences are denominated as Apd1/Aim32-like proteins. Among prokary-

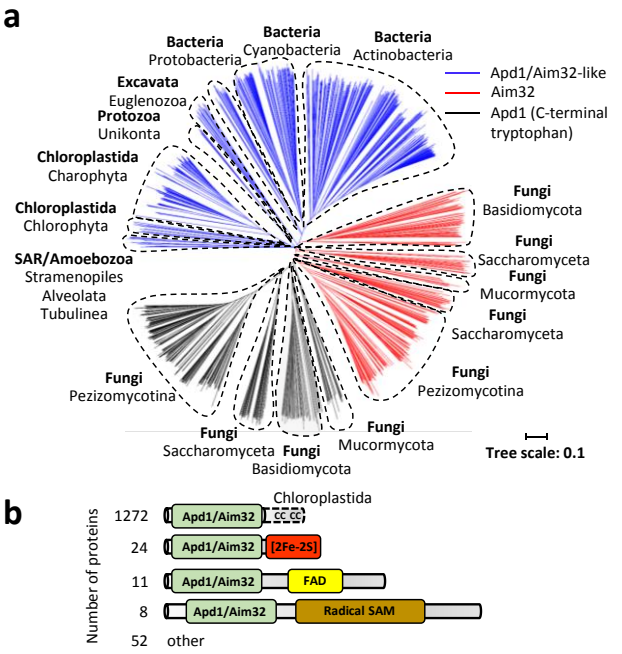

Figure 7. (a) Phylogenetic tree of Pfam06999[51] containing Apd1/Aim32 homologs. (b) Architectures of proteins with a Pfam06999 module and frequency of occurrence.

otes Apd1/Aim32-like proteins are found predominantly in Actinobacteria, Cyanobacteria, and to a lesser extent in Proteobacteria. The vast majority of the pfam06999 architectures (93 %) is formed solely by the Apd1/Aim32 module (Figure 7b). The three next most common architectures have an additional domain fused at their C-terminal end, which may be related the function of the Aim32/Apd1 metal center in these proteins: a [2Fe-2S] ferredoxin binding motif, an FAD-binding oxidoreductase domain or a radical SAM domain related to lipoyl synthase-like proteins (Figure 7b).

DISCUSSION

In this work we characterized a novel class of native bis-histidinyl coordinated [2Fe-2S] clusters in the yeast proteins Apd1 and Aim32. These proteins define a hitherto unrecognized family of redox-active metalloproteins (HAA-TLFs) found predominantly in fungi, plants and bacteria. We employed the synthetic lethality of yeast cells lacking Apd1 or Aim32/Sod2 upon treatment with the redox active compound gallobenzophenone or pyrogallol, respectively, to identify essential conditions and cluster ligands. EPR spectroscopy of yeast cell extracts showed that *in vivo* Apd1 binds a bis-histidinyl coordinated [2Fe-2S] cluster with properties identical to heterologously expressed protein isolated from *E. coli*. UV-Vis, EPR and Mössbauer spectroscopy of purified wild type Apd1 and three His to Cys variants demonstrated that Apd1 has two cysteine and two histidine ligands. In the $[2Fe\text{-}2S]^{2+}$ redox state the wild type Apd1 has pK_{ox} = 7.9 ± 0.1 and 9.7 ± 0.1, values similar to Rieske proteins of bc_1/b_6f complexes.[13] Contrarily, the redox midpoint potential of the cluster ($E_{m,7} \approx -164 \pm 5$ mV) is similar to the Rieske centers of dioxygenases. For the H255C and H259C variants only a single protonation/deprotonation of the remaining native histidine ligand of the $[2Fe\text{-}2S]^{2+}$ cluster was observed ($pK_{ox,\ H259}$= 9.8 ± 0.1 and $pK_{ox,\ H255}$ = 9.4 ± 0.1). The lack of pH dependence of the H255C/H259C variant demonstrates that changes are from (de)protonation of the non-coordinating imidazole nitrogen and not from amino acids in the vicinity of the cluster. At least the first protonation/deprotonation event of the oxidized form of wild type Apd1 (pK=7.9 ± 0.1) is close to physiological pH and could be employed for PCET function.

Modular architectures with Fe/S cluster binding domains, including TLFs, fused to redox enzymes occur in many biological systems. Examples are the electron transfer modules in complex I and [FeFe] hydrogenases,[56-58] which have tetracysteinyl-coordinated [2Fe-2S] TLF domains in the Nqo2 subunit of *T. thermophilus* complex I (amino acid 75-180) and in the HndA subunit of *Desulfovibrio fructosovorans* $NADP^+$-reducing [FeFe] hydrogenase, respectively. HAA-TLFs differ from such TLFs by coordination of the cluster by two cysteine and two histidine residues. Rieske proteins share the bis-histidinyl coordination, but have a completely divergent primary sequence and corresponding protein fold. The ligands of Rieske proteins are contained in the so-called Box I **C**X**H**XG<u>C</u> and Box II **C**X<u>C</u>**H**X(S/A/G)X(Y/F) motifs.[59] The [2Fe-2S] cluster is coordinated by the first cysteine (**C**) and the histidine of each motif. The additional cysteine residues in the motifs (<u>C</u>) form a disulfide bond in bc_1, b_6f complexes and arsenite oxidases, but not in the low potential Rieske dioxygenases.[60] HAA-TLFs have no further conserved cysteine residues in the TLF domain, which could form a disulfide bond. This differentiates Apd1/Aim32 from many Rieske proteins and *T. thermophilus* Nqo2, which have a disulfide bond in the cluster-binding domain. In [2Fe-2S] centers operating at a high potential a disulfide bond is a thermodynamically stable and useful feature to stabilize the tertiary structure. In systems operating at a low redox potential (Rieske dioxygenases and Apd1) a disulfide bond would be unstable and thus superfluous.

Previously, only substitution of a single histidine residue by cysteine could be achieved for MitoNEET[40] and, albeit leading to a very unstable cluster, for the *S. solfataricus* Rieske protein[39]. Based on a modelled structure for the C-terminal domain of Apd1 by Phyre2 (Figure S21a) the bis-histidinyl coordinated iron ion is at a surface exposed HVGGH loop of the $CX_8CX_{24\text{-}75}$HXGGH motif. The flexibility of the corresponding loop in *Clostridium pasteurianum* und *Aquifex aeolicus* TLFs allowed isolation of stable cysteine to serine variants.[44, 61] In *A. aeolicus* TLF structural changes from cysteine to serine substitution are accommodated by a translation of 0.4 Å of the loop in the C55S and C59S variants (Figure S21b). It appears that the loop in Apd1 has a similar flexibility, allowing characterization of stable His to Cys variants. Our results supply an unprecedented reference set of EPR and Mössbauer spectroscopic data for a [2Fe-2S] cluster with two histidine ligands, (two different) single histidine ligands or only cysteinyl ligands in the same protein fold. The compilation of average *g*-values for exclusively cysteinyl, monohistidinyl and bis-histidinyl coordinated clusters (g_{av}=1.962±0.011, n=152, g_{av}=1.940±0.007, n=19 and g_{av}=1.901±0.012, n=85, respectively, Figure 2e, Table S2-S4) facilitates assignment of cluster coordination. The difference of g_{av} between tetracysteinyl and monohistidinyl coordinated $[2Fe\text{-}2S]^{1+}$ is not large, especially if due to lack of EPR simulation or the presence of multiple species the accuracy of *g*-values is compromised. A single Gibson plot for all 256 systems with their three *g* values yields a too complicated diagram. Contrarily, a better resolved diagram with g_{av} as function of the z-axis rhombicity R_z $[300(g_y\text{-}g_x)/(2g_z\text{-}g_y\text{-}g_x)]$ (Figure 2e) adds the dimension required to resolve monohistidinyl from the tetracysteinyl $[2Fe\text{-}2S]^{1+}$ clusters. For $[2Fe\text{-}2S]^{2+}$ the Mössbauer truth diagram (Figure 5e) can reveal histidine coordination and highlight different protonation states. Differences from

the Rieske center could be caused by N_ε coordination of one or two of the histidine ligands in Apd1. Though structurally characterized Rieske and MitoNEET proteins have N_δ as ligand, $[4Fe\text{-}4S]^{2+/1+}$ clusters can either be coordinated by N_δ, as in nitrate reductase[62] and [NiFe] hydrogenase[63], or by N_ε, as in *Clostridium pasteurianum* [FeFe] hydrogenase[64] and center N5 of the respiratory complex I.[57] Pulsed EPR measurements with Apd1 (variants) with selectively ^{15}N-labelled histidine will have to reveal the mode of imidazole coordination.

A common trait of plants, algae, bacteria, and fungi, the phylogenetic core of the Apd1/Aim32 family, is production or degradation of allelochemicals, such as benzoquinones, coumarins, terpenoids, strigolactones, flavonoids and phenolic compounds[65]. One of the most common phenols in soils is gallic acid, which forms pyrogallol upon by decarboxylation. Here, we detected synthetic lethality in yeast cells lacking Sod2 and Aim32 in the presence of pyrogallol. Previously, an association between Sod2 and Aim32 was deduced from the increased resistance of cells lacking Sod2 against the antimalarial drug primaquine by overexpression of Aim32.[20] How can these observations be reconciled? If we assume that Apd1 and Aim32 are involved in the breakdown of pyrogallol-like substances, the detrimental reaction of these substances with O_2,[66] which leads to increased superoxide anion production in yeast cells, is only taking place to a limited extent. But if cells lack Apd1 or Aim32, then the pyrogallol-like substances persist and, especially in the absence of Sod2, lead to excessive oxidative stress and lethality. The efficacy of primaquine is dependent on the formation of mono-, di- and trihydroxylated aminoquinolines,[67] which are potentially toxic also in yeast cells. Thus, the resistance of *Δsod2* cells grown under strong aeration to primaquine by overexpression of Aim32[20] could be explained by degradation of these hydroxylated quinolines into less toxic products by Aim32 action. However, the precise role of Apd1 and Aim32 in conversions of the pyrogallol moiety remains to be determined. It is likely that the C-terminal TLF domain in HAA-TLFs is a low potential PCET module for a putative active site in the N-terminal part of the protein. The sequence of the N-terminal part is not related to mono- or dioxygenases, moreover no flavin, mononuclear or dinuclear iron centers were detected in Apd1. It is possible that electrons from the PCET module are directly shuttled to a pyrogallol moiety or an allelochemical bound to the N-terminal domain. A second possibility is that electrons are transferred to an interacting protein.

CONCLUSIONS

Apd1 and Aim32 are prototypes for a widely distributed class of Fe/S proteins which have a C-terminal TLF domain coordinating a [2Fe-2S] cluster by two cysteine and two histidine residues. Chemogenetic experiments show that the bis-histidinyl coordination is required under conditions at which Apd1 or Aim32 are necessary for survival of yeast cells. The histidine ligands (H255 and H259) in the native system enable PCET, which thusfar was only encountered for the [2Fe-2S] centers of MitoNEET and Rieske proteins. Apd1, Aim32 and their homologs present a remarkable example how bis-histidinyl coordination of [2Fe-2S] proteins convergently evolved in Nature.

MATERIAL AND METHODS

Yeast strains and cell growth. *Saccharomyces cerevisiae* W303-1A (*MAT**a**, ura3-1, ade2-1, trp1-1, his3-11,15* and *leu2-3,112*) was used as wild type strain. General methods for yeast genetics were as detailed previously.[15] Apd1 and Aim32 deletion strains were constructed by homologous recombination with a NAT cassette PCR amplified from pFA6a-natNT2.[68] Deletion of the *sod2* gene was achieved by replacement with a HIS cassette amplified from pFA-HISMX6. After transformation, cells were grown at 30 °C for 3-4 days on YP plates including 100 µg/ml nourseothricin (Δ*apd1*, Δ*aim32*) or on SC plates lacking histidine (Δ*sod2*). Media contained 2 % (m/v) glucose. Gene replacements were checked by PCR of genomic DNA. Solutions (0.05 M in EtOH) of gallobenzophenone (2,3,4-trihydroxybenzophenone), pyrogallol and harmaline, or hydroxyurea, were added at 65 °C before pouring agar containing SC medium supplemented with 2 % (m/v) glucose onto plates.

Plasmids and site-directed mutagenesis. For expression in *S. cerevisiae*, *apd1* or *aim32* were PCR amplified from *S. cerevisiae* genomic DNA and cloned into pRS416 (416), of which the promoter (*MET25*) was exchanged by the endogenous promoter region (500 nucleotides upstream of the start codon. For heterologous expression, Apd1 and Aim32 were cloned into pETDuet-1, supplying an N-terminal hexa-His tag. Mutagenesis was carried out according to Netz *et al*,[69] but with 8 instead of 4 cycles in the first step. Sequences of plasmids were confirmed by Sanger sequencing.

Protein production and purification. Aim32 and Apd1 were overexpressed in *E. coli* BL21 (DE3) cells transformed with pRK-ISC (harboring the *ISC* operon[70]). An overnight preculture was grown at 37 °C in LB medium supplemented 100 µg/mL ampicillin and 10 µg/mL tetracycline. The main culture was inoculated (2 %) in LB medium containing 0.4 mM ferric ammonium citrate and 1 mM cysteine-hydrochloride. After growth to OD600 of 0.5-0.6, the temperature was shifted to 18 °C, 0.5 mM IPTG was added and growth was continued for 16 h. Cells were collected, washed in lysis buffer (20 mM Tris, 300 mM NaCl, 10 mM imidazole; pH 9), harvested again and resuspended in lysis buffer with 1 mM PMSF. Cells were disrupted at 4 °C by one passage at 1000 psi through a French Press (SLM Aminco). After centrifugation (92,600g, 70 min, 4 °C), the supernatant was mixed with pre-equilibrated Ni-NTA agarose (Cube Biotech) and homogenized for 1 h at 4°C. The slurry was loaded on an empty PD-10 column and washed with 20 bed volumes of wash buffer (lysis buffer, but with 20 mM imidazole). After elution by the same buffer with 250 mM imidazole, the protein was desalted on Sephadex G-25 column (GE Healthcare) in a buffer containing 20 mM Tris, pH 9.0, 150 mM NaCl. The protein concentration (microbiuret TCA), non-heme iron and acid-labile sulfide concentrations were determined as described previously.[15]

EPR and Mössbauer spectroscopy. For EPR spectroscopy, Apd1 preparations were reduced with sodium dithionite (2 mM, final concentration) for 3 min in a Coy glove box. EPR spectra were recorded with a Bruker Elexsys E580 X band spectrometer, equipped with an Oxford Instruments ESR900 helium flow cryostat or Bruker ER 167FDS-Q liquid nitrogen finger dewar. For Mössbauer spectroscopy, Apd1 was expressed in LB medium with 100 µM ^{57}Fe-ammonium citrate. Mössbauer samples were frozen in the anaerobic chamber and stored in liquid nitrogen. Mössbauer samples were in 20 mM Tris/HCl, pH 9.0, 150 mM NaCl buffer (or adjusted with 300 mM MES, Tris, or CAPS to the desired pH value). For reduction a final concentration of 4 mM sodium dithionite (pH 9 buffer) was used. Mössbauer spectra were recorded in the constant acceleration mode with a conventional spectrometer from Wissel GmbH with a bath cryostat (Oxford Instruments). Isomer shifts are given relative to α-Fe at 25 °C. High field, low temperature spectra were measured with the same type of spectrometer in a

closed-cycle cryostat equipped with a superconducting magnet (CRYO Industries of America Inc.) operating with the applied field parallel to the γ rays. Magnetically split spectra were simulated with the spin Hamiltonian formalism[71] with the program Vinda.[72] Spectra were analyzed by least squared fits using Lorentzian line shapes.

pK determination and redox titrations. The pKs values of purified Apd1 ($Abs_{445\ nm}$ = 0.2-0.4) were measured by dilution into 200 mM buffer: from pH 5.0 to 6.5 MES, from pH 7.0 to 8.0 HEPES, from pH 8.5 to 9.0 TAPS and from pH 9.5 to 11.0 CAPS. The pH after dilution was determined with a microelectrode. UV-Vis spectra were scaled to an equal absorbance at pH 8.5 and fitted with an equation representing the sum of two Henderson-Hasselbalch equations as described before,[73] except that the absorbance difference between 445 nm and 465 nm was used. For redox titrations Apd1 (~13 µM) in 100 mM buffer (pH 7.0, HEPES; pH 7.3, MOPS; pH 7.5 and 8.0, HEPES; pH 7.8, 8.2, 8.5 and 9.0, TAPS; pH 9.5 and 10.0, CAPS) was mixed with mediators[74] in the anaerobic chamber. The solution potential was measured with an InLab ARGENTHAL (Mettler, Germany) microelectrode (+207 mV vs. SHE) and adjusted with sodium dithionite. Samples were frozen in liquid nitrogen for EPR measurements. Redox midpoint potentials were determined by non-linear least-squared fits to the Nernst equation (n = 1, 298 K) of the g_y amplitude.

ASSOCIATED CONTENT

Supporting Information.
The Supporting Information is available free of charge on the ACS Publications website at DOI: xx/jacs.xxx.
Sequence alignments, growth rates, drop tests, SDS-PAGE, visible, EPR and Mössbauer spectra, data on (pH) stability (of variants), pH dependence of visible and EPR spectra, EPR titration data, cellular localization, modelling and distances, EPR simulation parameters and compilation of EPR and Mössbauer spectroscopic data on biological [2Fe-2S] centers (PDF).

AUTHOR INFORMATION

Corresponding Author
*pierik@chemie.uni-kl.de
ORCID
Daili J. A. Netz: 0000-0001-9535-6963
Volker Schünemann: 0000-0002-3162-1032
Antonio J. Pierik: 0000-0002-1509-6370
Notes
The authors declare no competing financial interest.

Author Contributions

The manuscript was written through contributions of all authors. All authors have given approval to the final version of the manuscript. ‡These authors contributed equally.

Funding Sources

This work was supported by SCHU 1251/17-1 (VS) and PI 610/2-1 (AJP) from the DFG (SPP1927). The authors thank COST Action CA15133, supported by COST (European Cooperation in Science and Technology) for valuable interactions with other scientists.

ACKNOWLEDGMENTS

We thank Dr. Edward Reijerse of the MPI (Mülheim, Germany) for initial Q band ENDOR measurements.

REFERENCES

(1) Johnson, D. C.; Dean, D. R.; Smith, A. D.; Johnson, M. K., *Annu. Rev. Biochem.* **2005,** *74*, 247-281.
(2) Liu, J.; Chakraborty, S.; Hosseinzadeh, P.; Yu, Y.; Tian, S.; Petrik, I.; Bhagi, A.; Lu, Y., *Chem. Rev.* **2014,** *114*, 4366-469.
(3) Meyer, J.; Andrade, S. L. A.; Einsle, O., Thioredoxin-like [2Fe-2S] ferredoxin. In *Encyclopedia of inorganic and bioinorganic chemistry*, John Wiley & Sons: New York, 2011.
(4) Couturier, J.; Przybyla-Toscano, J.; Roret, T.; Didierjean, C.; Rouhier, N., *Biochim. Biophys. Acta.* **2015,** *1853*, 1513-1527.
(5) Cosper, M. M.; Jameson, G. N.; Hernandez, H. L.; Krebs, C.; Huynh, B. H.; Johnson, M. K., *Biochemistry* **2004,** *43*, 2007-2021.
(6) Fee, J. A.; Findling, K. L.; Yoshida, T.; Hille, R.; Tarr, G. E.; Hearshen, D. O.; Dunham, W. R.; Day, E. P.; Kent, T. A.; Münck, E., *J. Biol. Chem.* **1984,** *259*, 124-133.
(7) Iwata, S.; Saynovits, M.; Link, T. A.; Michel, H., *Structure* **1996,** *4*, 567-579.
(8) Link, T. A., The structures of Rieske and Rieske-type proteins. In *Advances in Inorganic Chemistry 47*, Sykes, A. G.; Cammack, R., Eds. Academic Press: San Diego, 1999; Vol. 47, pp 83-157.
(9) Bak, D. W.; Elliott, S. J., *Curr. Opin. Chem. Biol.* **2014,** *19*, 50-58.
(10) Tamir, S.; Paddock, M. L.; Darash-Yahana-Baram, M.; Holt, S. H.; Sohn, Y. S.; Agranat, L.; Michaeli, D.; Stofleth, J. T.; Lipper, C. H.; Morcos, F.; Cabantchik, I. Z.; Onuchic, J. N.; Jennings, P. A.; Mittler, R.; Nechushtai, R., *Biochim. Biophys. Acta* **2015,** *1853*, 1294-1315.
(11) Fleischhacker, A. S.; Stubna, A.; Hsueh, K. L.; Guo, Y.; Teter, S. J.; Rose, J. C.; Brunold, T. C.; Markley, J. L.; Munck, E.; Kiley, P. J., *Biochemistry* **2012,** *51*, 4453-4462.
(12) Dlouhy, A. C.; Li, H.; Albetel, A. N.; Zhang, B.; Mapolelo, D. T.; Randeniya, S.; Holland, A. A.; Johnson, M. K.; Outten, C. E., *Biochemistry* **2016,** *55*, 6869-6879.
(13) Zu, Y.; Couture, M. M.; Kolling, D. R.; Crofts, A. R.; Eltis, L. D.; Fee, J. A.; Hirst, J., *Biochemistry* **2003,** *42*, 12400-12408.
(14) Balk, J.; Pierik, A. J.; Netz, D. J. A.; Mühlenhoff, U.; Lill, R., *Biochem. Soc.Trans.* **2005,** *33*, 86-89.
(15) Netz, D. J. A.; Stith, C. M.; Stümpfig, M.; Köpf, G.; Vogel, D.; Genau, H. M.; Stodola, J. L.; Lill, R.; Burgers, P. M.; Pierik, A. J., *Nat. Chem. Biol.* **2012,** *8*, 125-132.
(16) Upadhyay, A. S.; Vonderstein, K.; Pichlmair, A.; Stehling, O.; Bennett, K. L.; Dobler, G.; Guo, J. T.; Superti-Furga, G.; Lill, R.; Overby, A. K.; Weber, F., *Cell Microbiol.* **2014,** *16*, 834-848.
(17) Entian, K. D.; Schuster, T.; Hegemann, J. H.; Becher, D.; Feldmann, H.; Guldener, U.; Gotz, R.; Hansen, M.; Hollenberg, C. P.; Jansen, G.; Kramer, W.; Klein, S.; Kotter, P.; Kricke, J.; Launhardt, H.; Mannhaupt, G.; Maierl, A.; Meyer, P.; Mewes, W.; Munder, T.; Niedenthal, R. K.; Ramezani Rad, M.; Rohmer, A.; Romer, A.; Hinnen, A.; et al., *Mol. Gen. Genet.* **1999,** *262*, 683-702.
(18) Tang, H. M.; Pan, K.; Kong, K. Y.; Hu, L.; Chan, L. C.; Siu, K. L.; Sun, H.; Wong, C. M.; Jin, D. Y., *Sci. Rep.* **2015,** *5*, 7897.
(19) Hess, D. C.; Myers, C. L.; Huttenhower, C.; Hibbs, M. A.; Hayes, A. P.; Paw, J.; Clore, J. J.; Mendoza, R. M.; Luis, B. S.; Nislow, C.; Giaever, G.; Costanzo, M.; Troyanskaya, O. G.; Caudy, A. A., *PLoS Genet.* **2009,** *5*, e1000407.
(20) Lalève, A.; Vallières, C.; Golinelli-Cohen, M. P.; Bouton, C.; Song, Z.; Pawlik, G.; Tindall, S. M.; Avery, S. V.; Clain, J.; Meunier, B., *Redox Biol.* **2016,** *7*, 21-29.
(21) Lee, A. Y.; St Onge, R. P.; Proctor, M. J.; Wallace, I. M.; Nile, A. H.; Spagnuolo, P. A.; Jitkova, Y.; Gronda, M.; Wu, Y.; Kim, M. K.; Cheung-Ong, K.; Torres, N. P.; Spear, E. D.; Han, M. K.; Schlecht, U.; Suresh, S.; Duby, G.; Heisler, L. E.; Surendra, A.; Fung, E.; Urbanus, M. L.; Gebbia, M.; Lissina, E.; Miranda, M.; Chiang, J. H.; Aparicio, A. M.; Zeghouf, M.; Davis, R. W.; Cherfils, J.; Boutry, M.; Kaiser, C. A.; Cummins, C. L.; Trimble, W. S.; Brown, G. W.; Schimmer, A. D.; Bankaitis, V. A.; Nislow, C.; Bader, G. D.; Giaever, G., *Science* **2014,** *344*, 208-211.
(22) Meyer, J.; Andrade, S. L. A.; Einsle, O., Thioredoxin-like [2Fe-2S] ferredoxin. In *Handbook of metalloproteins*, Messerschmidt, A., Ed. John Wiley & Sons: New York, 2008; pp 1-16.
(23) Sheftel, A. D.; Stehling, O.; Pierik, A. J.; Elsässer, H. P.; Mühlenhoff, U.; Webert, H.; Hobler, A.; Hannemann, F.; Bernhardt, R.; Lill, R., *Proc. Natl. Acad. Sci. U. S. A.* **2010,** *107*, 11775-11780.
(24) Kounosu, A.; Iwasaki, T.; Baba, S.; Hayashi-Iwasaki, Y.; Oshima, T.; Kumasaka, T., *Acta Crystallogr. Sect. F Struct. Biol. Cryst. Commun.* **2008,** *64*, 1146-1148.
(25) Iwasaki, T.; Isogai, Y.; Iizuka, T.; Oshima, T., *J. Bacteriol.* **1995,** *177*, 2576-2582.
(26) Haldar, S.; Paul, S.; Joshi, N.; Dasgupta, A.; Chattopadhyay, K., *PLoS One* **2012,** *7*, e31797.
(27) Orme-Johnson, W. H.; Orme-Johnson, N. R., *Methods Enzymol.* **1978,** *53*, 259-268.

(28) Pikus, J. D.; Studts, J. M.; Achim, C.; Kauffmann, K. E.; Münck, E.; Steffan, R. J.; McClay, K.; Fox, B. G., *Biochemistry* **1996,** *35*, 9106-9119.
(29) Cutsail, G. E., 3rd; Doan, P. E.; Hoffman, B. M.; Meyer, J.; Telser, J., *J. Biol. Inorg. Chem.* **2012,** *17*, 1137-1150.
(30) Dicus, M. M.; Conlan, A.; Nechushtai, R.; Jennings, P. A.; Paddock, M. L.; Britt, R. D.; Stoll, S., *J. Am. Chem. Soc.* **2010,** *132*, 2037-2049.
(31) Chatelet, C.; Gaillard, J.; Pétillot, Y.; Louwagie, M.; Meyer, J., *Biochem. Biophys. Res. Commun.* **1999,** *261*, 885-889.
(32) Wolfe, M. D.; Altier, D. J.; Stubna, A.; Popescu, C. V.; Münck, E.; Lipscomb, J. D., *Biochemistry* **2002,** *41*, 9611-9626.
(33) Lloyd, S. G.; Franco, R.; Moura, J. J. G.; Moura, I.; Ferreira, G. C.; Huynh, B. H., *J. Am. Chem. Soc.* **1996,** *118*, 9892-9900.
(34) Ferecatu, I.; Goncalves, S.; Golinelli-Cohen, M. P.; Clemancey, M.; Martelli, A.; Riquier, S.; Guittet, E.; Latour, J. M.; Puccio, H.; Drapier, J. C.; Lescop, E.; Bouton, C., *J. Biol. Chem.* **2014,** *289*, 28070-28086.
(35) Meyer, J.; Clay, M. D.; Johnson, M. K.; Stubna, A.; Münck, E.; Higgins, C.; Wittung-Stafshede, P., *Biochemistry* **2002,** *41*, 3096-3108.
(36) Werber, M. M.; Bauminger, E. R.; Cohen, S. G.; Ofer, S., *Biophys. Struct. Mech.* **1978,** *4*, 169-177.
(37) Clark, W. M., *Oxidation-reduction potentials of organic systems*. Williams & Wilkins: Baltimore, USA, 1960; p 1-584.
(38) Link, T. A.; Hagen, W. R.; Pierik, A. J.; Assmann, C.; Von Jagow, G., *Eur. J. Biochem.* **1992,** *208*, 685-691.
(39) Kounosu, A.; Li, Z.; Cosper, N. J.; Shokes, J. E.; Scott, R. A.; Imai, T.; Urushiyama, A.; Iwasaki, T., *J. Biol. Chem.* **2004,** *279*, 12519-12528.
(40) Zuris, J. A.; Halim, D. A.; Conlan, A. R.; Abresch, E. C.; Nechushtai, R.; Paddock, M. L.; Jennings, P. A., *J. Am. Chem. Soc.* **2010,** *132*, 13120-13122.
(41) Müller, C. S.; Auerbach, H.; Stegmaier, K.; Wolny, J. A.; Schünemann, V.; Pierik, A. J., *Hyperfine Interact.* **2017,** *238*, 102.
(42) Kuila, D.; Fee, J. A., *J. Biol. Chem.* **1986,** *261*, 2768-2771.
(43) Yankovskaya, V.; Horsefield, R.; Tornroth, S.; Luna-Chavez, C.; Miyoshi, H.; Leger, C.; Byrne, B.; Cecchini, G.; Iwata, S., *Science* **2003,** *299*, 700-704.
(44) Yeh, A. P.; Ambroggio, X. I.; Andrade, S. L.; Einsle, O.; Chatelet, C.; Meyer, J.; Rees, D. C., *J. Biol. Chem.* **2002,** *277*, 34499-34507.
(45) Rahman, M. M.; Andberg, M.; Thangaraj, S. K.; Parkkinen, T.; Penttila, M.; Janis, J.; Koivula, A.; Rouvinen, J.; Hakulinen, N., *ACS Chem. Biol.* **2017,** *12*, 1919-1927.
(46) Gatto, G. J.; Berg, J. M., *Genome Res.* **2003,** *13*, 617-623.
(47) Netz, D. J. A.; Mascarenhas, J.; Stehling, O.; Pierik, A. J.; Lill, R., *Trends Cell. Biol.* **2014,** *24*, 303-312.
(48) Pierik, A. J.; Netz, D. J.; Lill, R., *Nat. Protoc.* **2009,** *4*, 753-766.
(49) Kulak, N. A.; Pichler, G.; Paron, I.; Nagaraj, N.; Mann, M., *Nat. Methods* **2014,** *11*, 319-324.
(50) Hudder, B. N.; Morales, J. G.; Stubna, A.; Münck, E.; Hendrich, M. P.; Lindahl, P. A., *J. Biol. Inorg. Chem.* **2007,** *12*, 1029-1053.
(51) Finn, R. D.; Coggill, P.; Eberhardt, R. Y.; Eddy, S. R.; Mistry, J.; Mitchell, A. L.; Potter, S. C.; Punta, M.; Qureshi, M.; Sangrador-Vegas, A.; Salazar, G. A.; Tate, J.; Bateman, A., *Nucleic Acids Res.* **2016,** *44*, D279-285.
(52) Machray, G. C.; Burch, L.; Hedley, P. E.; Davies, H. V.; Waugh, R., *FEBS Lett.* **1994,** *354*, 123-127.
(53) Burch, L. R.; Davies, H. V.; Cuthbert, E. M.; Machray, G. C.; Hedley, P.; Waugh, R., *Phytochemistry* **1986,** *31*, 1901-1904.
(54) Sievers, F.; Wilm, A.; Dineen, D.; Gibson, T. J.; Karplus, K.; Li, W.; Lopez, R.; McWilliam, H.; Remmert, M.; Soding, J.; Thompson, J. D.; Higgins, D. G., *Mol. Syst. Biol.* **2011,** *7*, 539.
(55) Letunic, I.; Bork, P., *Nucleic Acids Res.* **2016,** *44*, W242-245.
(56) Nouailler, M.; Morelli, X.; Bornet, O.; Chetrit, B.; Dermoun, Z.; Guerlesquin, F., *Protein Sci.* **2006,** *15*, 1369-1378.
(57) Sazanov, L. A.; Hinchliffe, P., *Science* **2006,** *311*, 1430-1436.
(58) Artz, J. H.; Mulder, D. W.; Ratzloff, M. W.; Lubner, C. E.; Zadvornyy, O. A.; LeVan, A. X.; Williams, S. G.; Adams, M. W. W.; Jones, A. K.; King, P. W.; Peters, J. W., *J. Am. Chem. Soc.* **2017,** *139*, 9544-9550.
(59) Schneider, D.; Schmidt, C. L., *Biochim. Biophys. Acta* **2005,** *1710*, 1-12.
(60) Ferraro, D. J.; Gakhar, L.; Ramaswamy, S., *Biochem. Biophys. Res. Commun.* **2005,** *338*, 175-190.
(61) Subramanian, S.; Duin, E. C.; Fawcett, S. E.; Armstrong, F. A.; Meyer, J.; Johnson, M. K., *J. Am. Chem. Soc.* **2015,** *137*, 4567-4580.
(62) Bertero, M. G.; Rothery, R. A.; Palak, M.; Hou, C.; Lim, D.; Blasco, F.; Weiner, J. H.; Strynadka, N. C., *Nat. Struct. Biol.* **2003,** *10*, 681-687.
(63) Volbeda, A.; Charon, M. H.; Piras, C.; Hatchikian, E. C.; Frey, M.; Fontecilla-Camps, J. C., *Nature* **1995,** *373*, 580-587.
(64) Peters, J. W.; Lanzilotta, W. N.; Lemon, B. J.; Seefeldt, L. C., *Science* **1998,** *282*, 1853-1858.
(65) Kocacaliskan, I.; Talan, I.; Terzi, I., *Z. Naturforsch. C* **2006,** *61*, 639-642.
(66) Marklund, S.; Marklund, G., *Eur. J. Biochem.* **1974,** *47*, 469-474.
(67) Fasinu, P. S.; Tekwani, B. L.; Nanayakkara, N. P.; Avula, B.; Herath, H. M.; Wang, Y. H.; Adelli, V. R.; Elsohly, M. A.; Khan, S. I.; Khan, I. A.; Pybus, B. S.; Marcsisin, S. R.; Reichard, G. A.; McChesney, J. D.; Walker, L. A., *Malar. J.* **2014,** *13*, 507.
(68) Janke, C.; Magiera, M. M.; Rathfelder, N.; Taxis, C.; Reber, S.; Maekawa, H.; Moreno-Borchart, A.; Doenges, G.; Schwob, E.; Schiebel, E.; Knop, M., *Yeast* **2004,** *21*, 947-962.
(69) Netz, D. J. A.; Pierik, A. J.; Stümpfig, M.; Bill, E.; Sharma, A. K.; Pallesen, L. J.; Walden, W. E.; Lill, R., *J. Biol. Chem.* **2012,** *287*, 12365-12378.
(70) Nakamura, M.; Saeki, K.; Takahashi, Y., *J. Biochem.* **1999,** *126*, 10-18.
(71) Trautwein, A. X.; Bill, E.; Bominaar, E. L.; Winkler, H., *Structure and Bonding* **1991,** *78*, 1-95.
(72) Gunnlaugsson, H. P., *Hyperfine Interact.* **2016,** *237*, 79.
(73) Konkle, M. E.; Muellner, S. K.; Schwander, A. L.; Dicus, M. M.; Pokhrel, R.; Britt, R. D.; Taylor, A. B.; Hunsicker-Wang, L. M., *Biochemistry* **2009,** *48*, 9848-9857.
(74) Pierik, A. J.; Wassink, H.; Haaker, H.; Hagen, W. R., *Eur. J. Biochem.* **1993,** *212*, 51-61.

Table of Contents Artwork

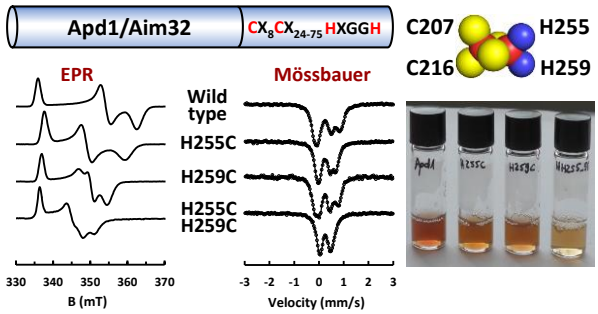

Supplementary Information

Apd1 and Aim32 are prototypes of bis-histidinyl-coordinated non-Rieske [2Fe-2S] proteins

Kathrin Stegmaier[§‡], Catharina M. Blinn[§‡], Dominique F. Bechtel[§], Carina Greth[§], Hendrik Auerbach[†], Christina S. Müller[†], Valentin Jakob[§], Daili J.A. Netz[§], Volker Schünemann[†] & Antonio J. Pierik[§*]

Technische Universität Kaiserslautern, [§]Fachbereich Chemie and [†]Fachbereich Physik, Erwin-Schrödinger-Str. 54/56, D67663 Kaiserslautern, Germany

*To whom correspondence should be addressed. Email: pierik@chemie.uni-kl.de

Figures S1-S21

Tables S1-S6

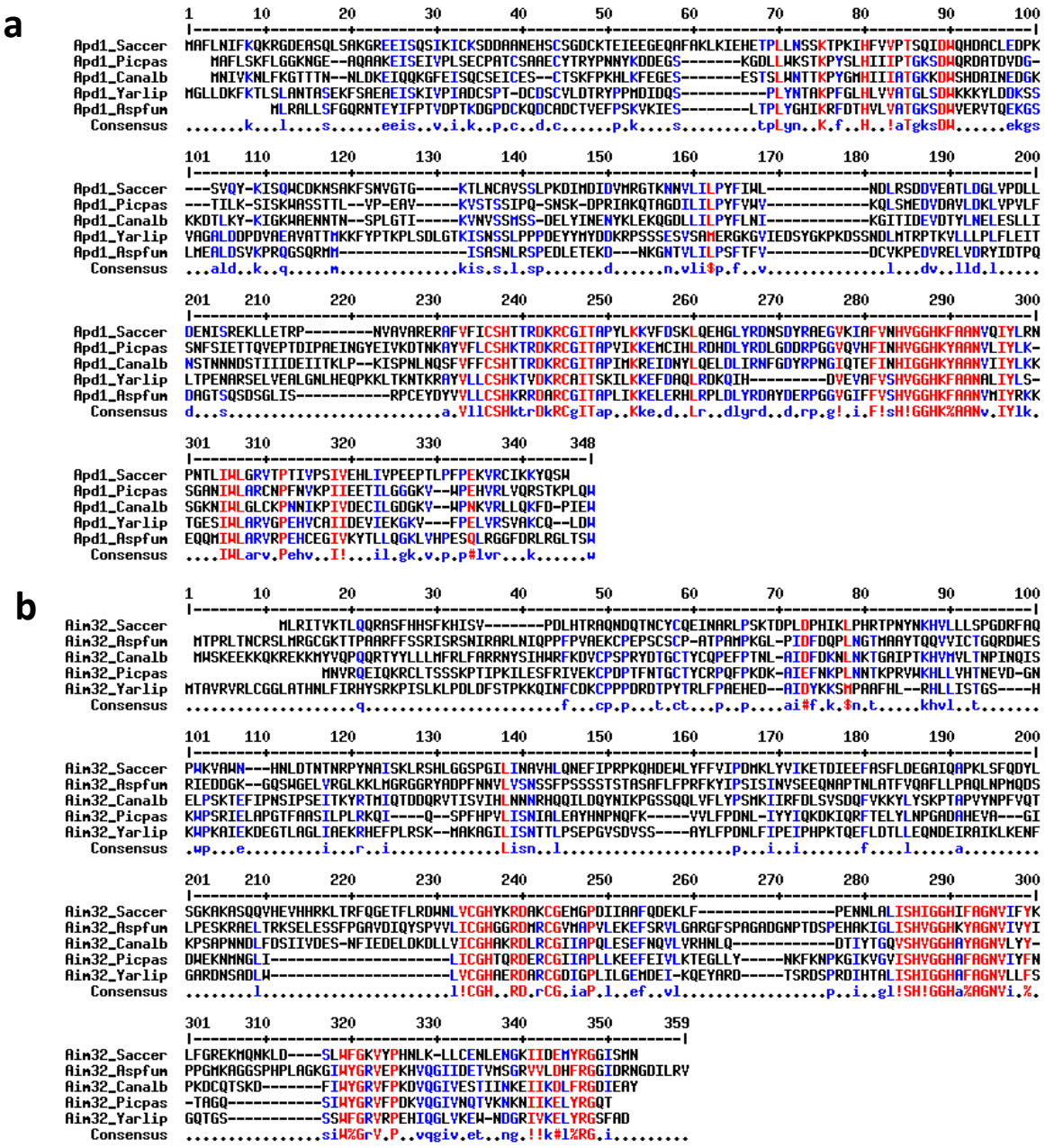

Figure S1. Multiple amino acid sequence alignment of five fungal Apd1 (a) and five fungal Aim32 homologs (b). Alignments were made with Multalin with default settings.[1] Consensus levels are indicated below the alignment: high=90% (uppercase amino acids), low=50% (lowercase amino acids). Further consensus symbols are: !, IV; $, LM; %, FY; #, NDQE. Abbreviations for organisms: Saccer, *Saccharomyces cerevisiae*; Picpas, *Pichia pastoris*; Canalb, *Candida albicans*; Yarlip, *Yarrowia lipolytica*; Aspfum, *Aspergillus fumigatus*.

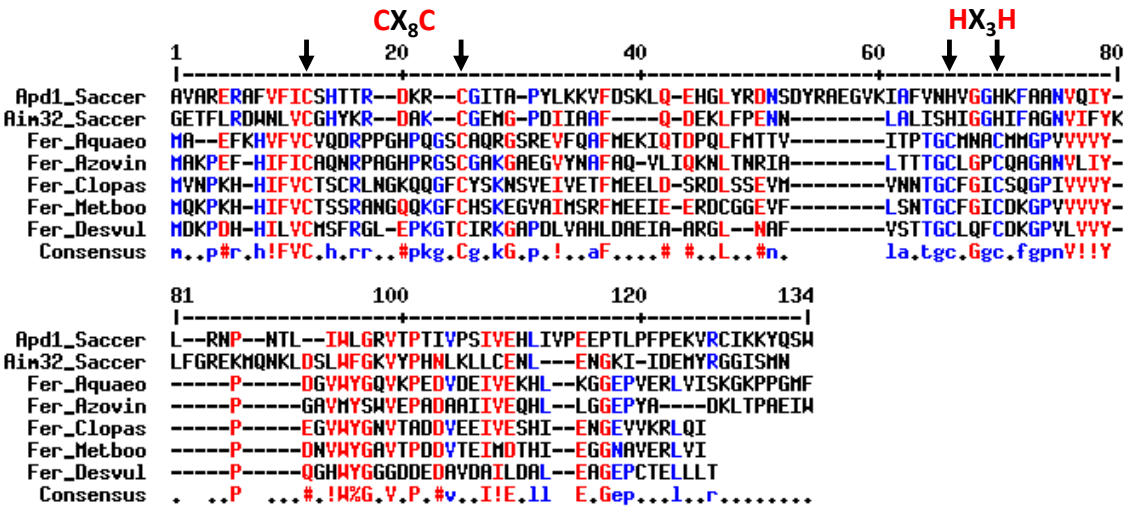

Figure S2. Multiple amino acid sequence alignment of the C-terminal part of yeast Apd1 and Aim32 with TLF proteins. Alignments were made as in Figure S1, but with a gap opening penalty of 4, and consensus levels of high=60% and low=40%. Abbreviations: Saccer for *Saccharomyces cerevisiae*, Fer_Aquae, *Aquifex aeolicus* ferredoxin (PDB 1F37), Fer_Azovin, *Azotobacter vinelandii* ferredoxin (PDB 1F37), Fer_Clopas, *Clostridium pasteurianum* ferredoxin, Fer_Metboo, *Methanoregula boonei* ferredoxin, Fer_desvul, *Desulfovibrio vulgaris* ferredoxin.

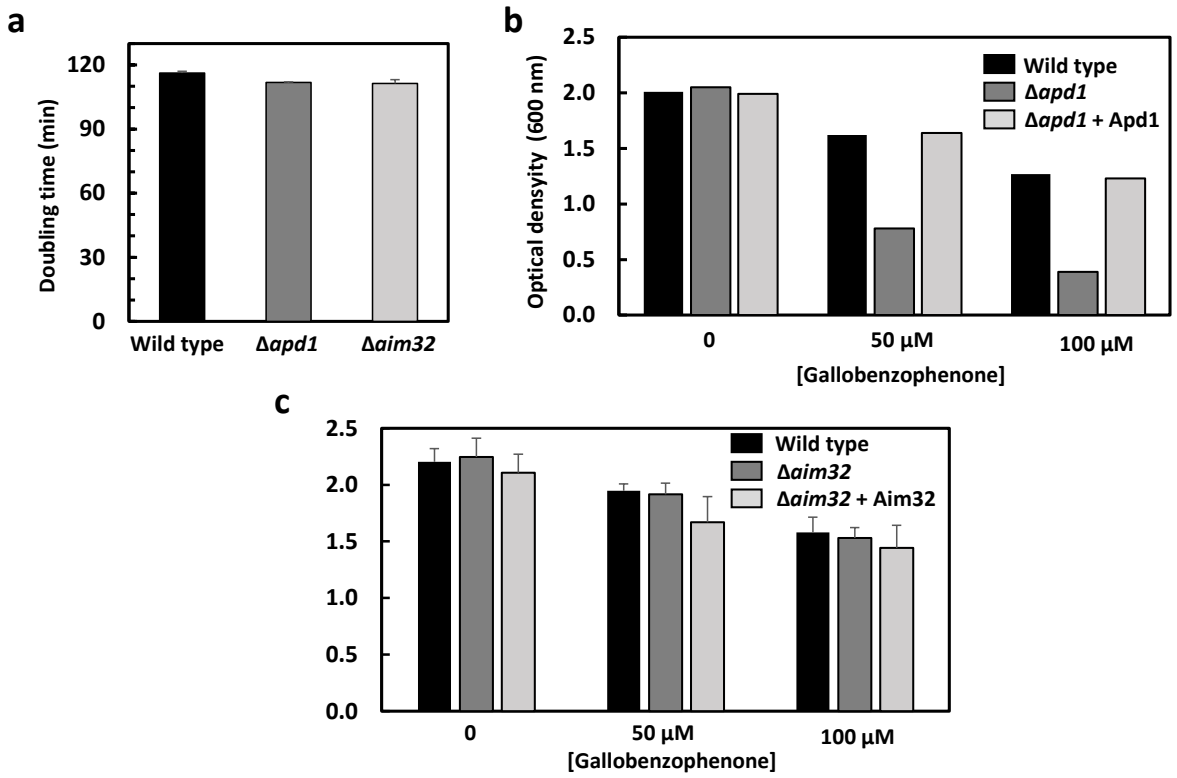

Figure S3. Growth of Δ*apd1* and Δ*aim32* cells in liquid media. (a) Wild type, Δ*apd1* or Δ*aim32* cells were inoculated into liquid SC medium with 2 % (m/v) glucose. Cell growth at 30 °C was followed by measuring the optical density at 600 nm. Doubling times were calculated for the exponential growth phase for two independent cultures. (b) Effect of gallobenzophenone on Δ*apd1* cells. Wild type yeast cells, Δ*apd1* and Δ*apd1* transformed with Apd1 encoded from a plasmid were grown in liquid SC medium with 2 % (m/v) glucose. Gallobenzophenone was added as indicated. Optical density of the cells were determined after 16 h of incubation at 30 °C (single experiment). (c) Effect of gallobenzophenone on Δ*aim32* cells. Wild type yeast cells, Δ*aim32* and Δ*aim32* transformed with Aim32 encoded from a plasmid were grown on liquid SC medium with 2 % (m/v) glucose. Gallobenzophenone was added as indicated. Optical densities of the cells were determined after 16 h of incubation at 30 °C (n=3).

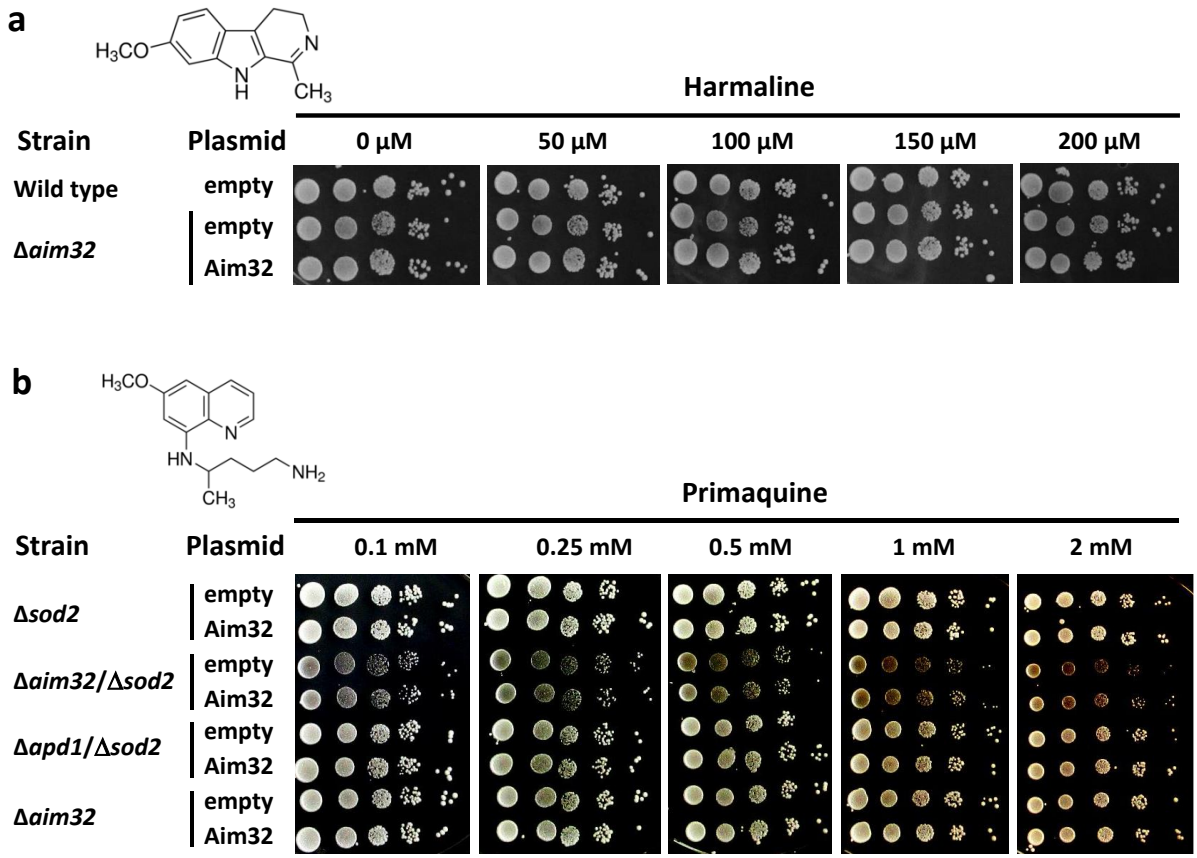

Figure S4. Lack of effect of harmaline and primaquine on yeast cells grown on solid medium. (a) Yeast cells (wild type, Δ*aim32* and Δ*aim32*, transformed with an empty 416 or a 416NP-Aim32 plasmid) were inoculated into liquid SC medium supplemented with 2% (m/v) glucose and grown for 24 h. After adjusting the optical density to 0.5 at 600 nm, 10-fold serial dilutions were spotted onto agar plates containing the indicated concentration of harmaline. After 2 days of incubation at 30 °C, the plates were photographed. (b) As in (a) but for primaquine and with Δ*sod2*, Δ*aim32*/Δ*sod2*, Δ*apd1*/Δ*sod2* and Δ*aim32* cells (transformed with an empty 416 or 416NP-Aim32 plasmid, as indicated).

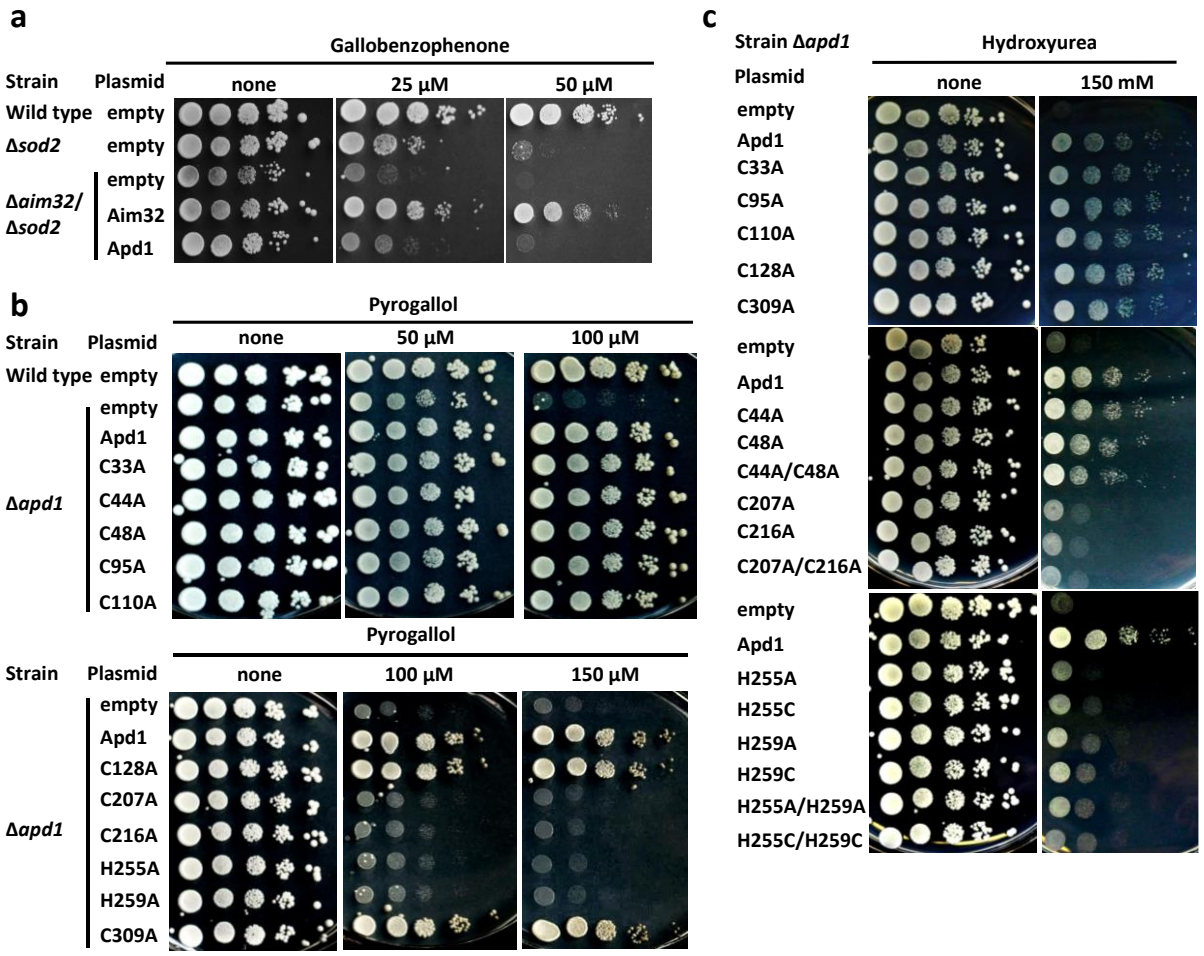

Figure S5. Effect of chemical compounds on Δ*sod2*, Δ*aim32*/Δ*sod2* and Δ*apd1* cells. Wild type, Δ*sod2* or Δ*aim32*/Δ*sod2* cells, transformed with an empty 416, 416NP-Aim32, 416NP-Apd1 plasmid or 416NP-Apd1 plasmids encoding indicated Apd1 variants were inoculated into liquid SC medium supplemented with 2% (m/v) glucose and grown for 24 h. After adjusting the optical density at 600 nm to 0.5, 10-fold serial dilutions were spotted onto agar plates containing gallobenzophenone, pyrogallol or hydroxyurea at indicated concentrations. After 2 days of incubation at 30 °C the plates were photographed.

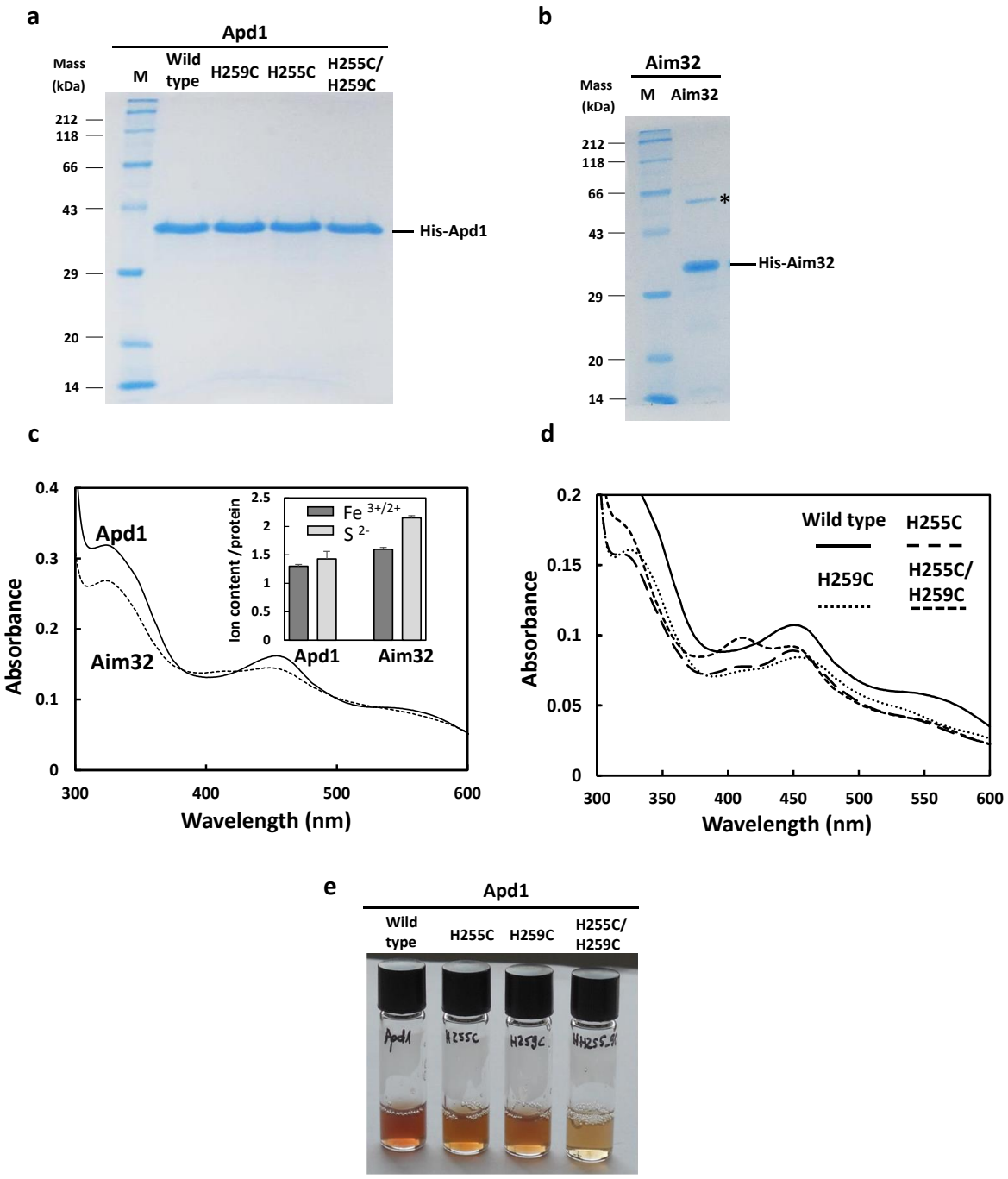

Figure S6. Purified recombinant Apd1 and Aim32. (a) SDS-PAGE of purified yeast Apd1 protein and indicated variants (~4 µg protein/lane) obtained by Ni-NTA affinity chromatography after expression in *E. coli*. M, molecular mass marker. (b) as in (a) but for Aim32 (*, GroEL contamination). (c) UV-Vis spectroscopy of purified Apd1 and Aim32. Wild type proteins. Inset: non-heme iron and sulfide ion contents. (d) UV-Vis spectroscopy of purified Apd1 and indicated variants. (e) Photographs of solutions of purified Apd1 and variants thereof.

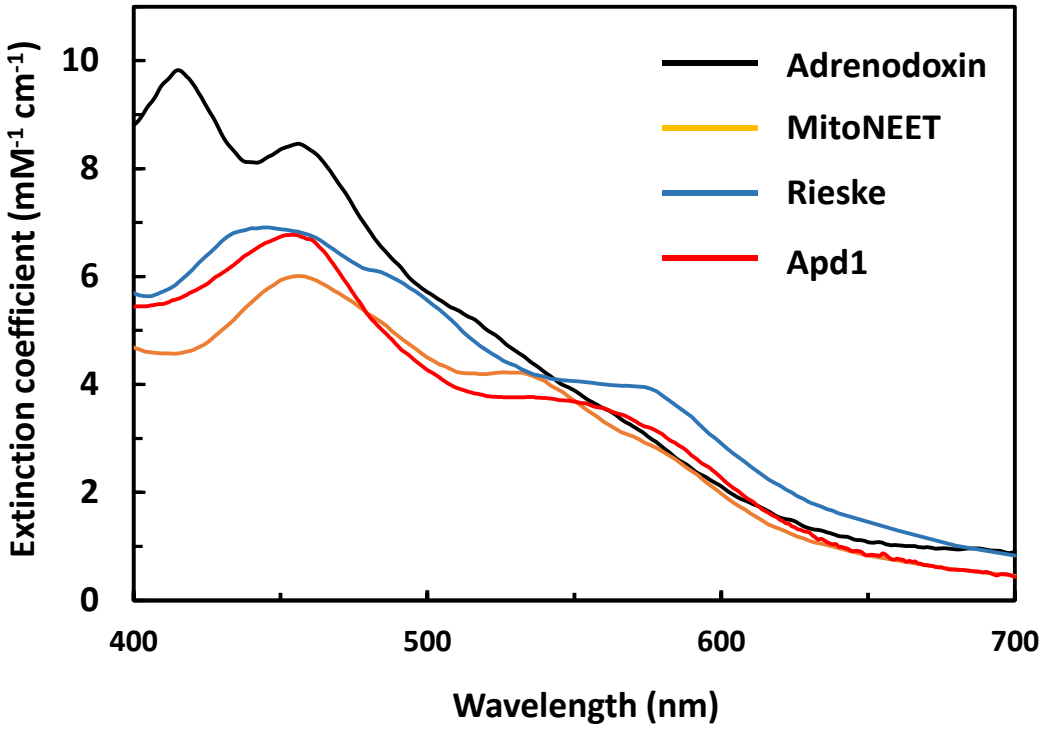

Figure S7. Comparison of visible spectra of Apd1 and indicated [2Fe-2S] cluster-containing proteins. Original data on human adrenodoxin are from Figure 1b in Sheftel et al.[3] The spectrum of MitoNEET[2] and the *Sulfolobus sp*. Rieske protein[4] was digitalized from published spectra.

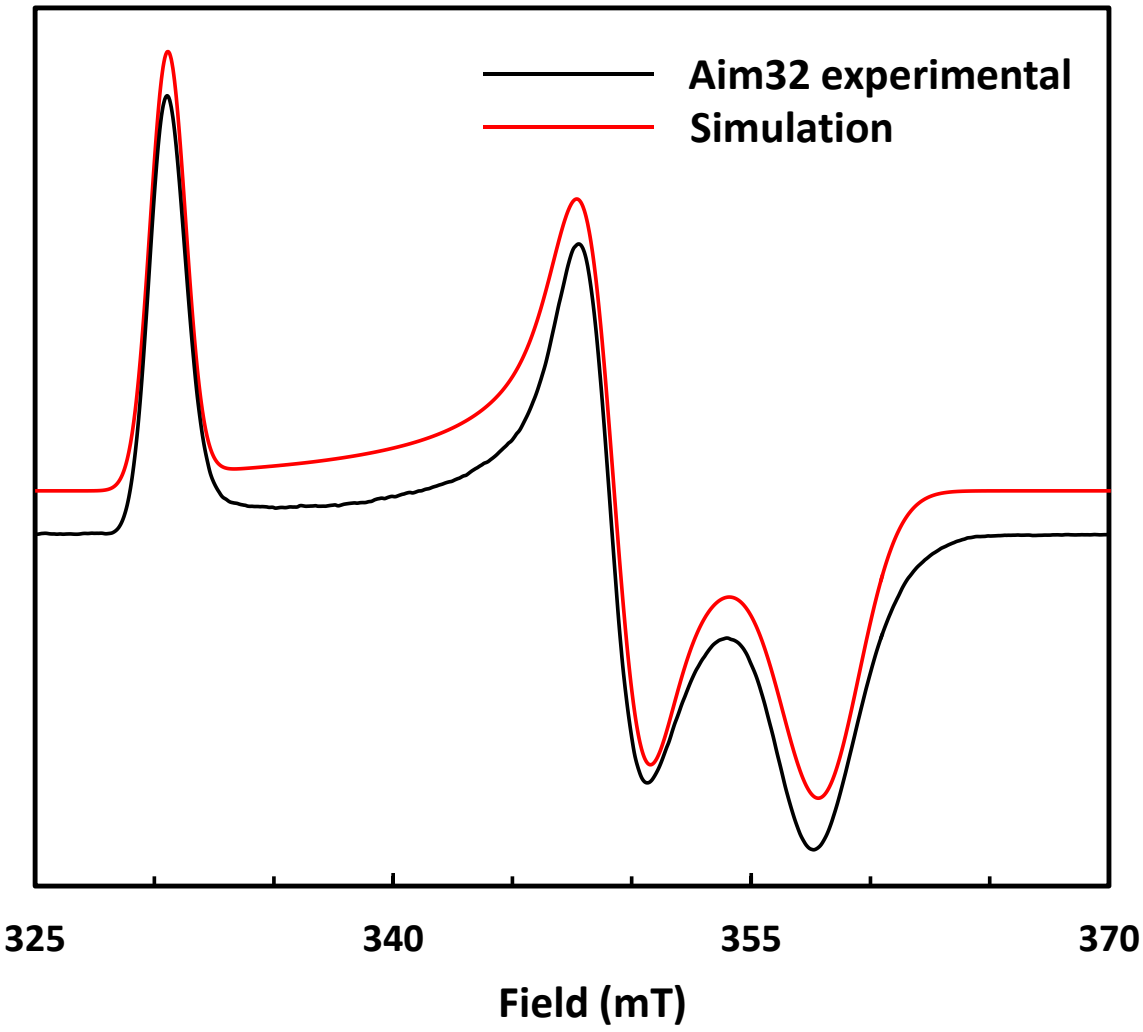

Figure S8. X-band EPR spectrum of dithionite-reduced wild type Aim32 and simulation. EPR conditions: 9.304 GHz, 20 K and 2 mW microwave power. Simulation parameters are in Table S1.

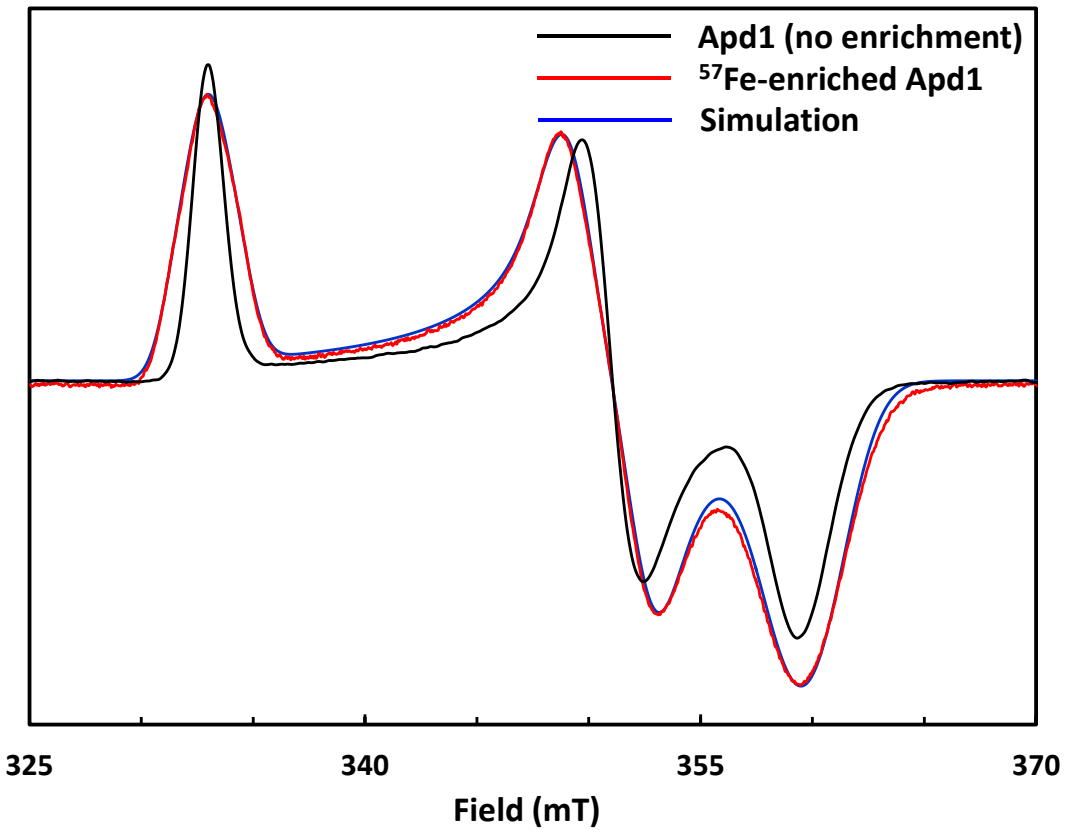

Figure S9. X-band EPR spectrum of dithionite-reduced unenriched wild type Apd1 (as in Figure 2a) and ~85% ^{57}Fe enriched Apd1. Simulation parameters for *g*-values and linewidths as in Table S1, but with two isotropic hyperfine parameters: $|\boldsymbol{A}|(^{57}Fe^{3+})$=50±10 MHz and $|\boldsymbol{A}|(^{57}Fe^{2+})$=20±5 MHz. EPR conditions (^{57}Fe-enriched): 9.36 GHz (field corrected to 9.456 GHz), 20 K and 0.02 mW microwave power.

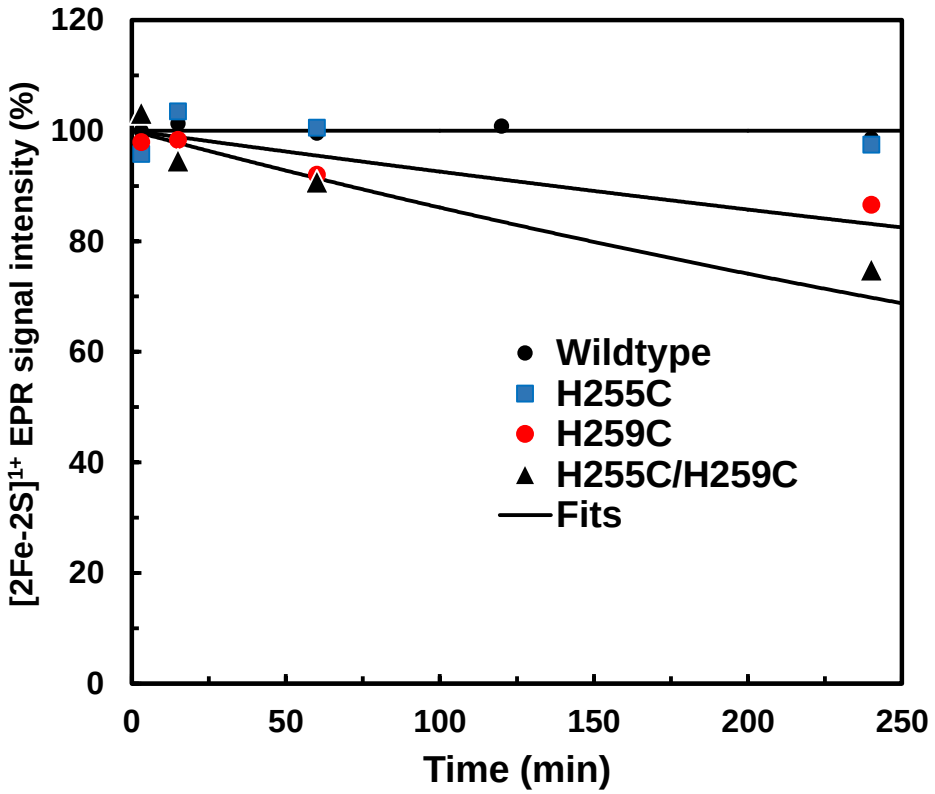

Figure S10. Stability of the reduced [2Fe-2S] cluster of Apd1 and its variants by EPR spectroscopy. At t=0 sodium dithionite (2 mM final concentration) in 100 mM Tris/Cl pH 9 was added to Apd1 or its variants (50-80 µM) in 20 mM Tris/HCl, pH 9.0, 150 mM NaCl. After incubation at 25 °C for 3, 15, 60 (wild type only), 120 and 240 min the samples were frozen in EPR tubes. EPR spectra were recorded at 20 mW microwave power, 1 mT modulation amplitude, 100 kHz modulation frequency, 9.42 GHz microwave frequency, 77 K. The disappearance of the double integrated EPR intensity was simulated with a single exponential decay with a halftime of 8 h and 15 h for the H259C and H255C/H259C variant, respectively.

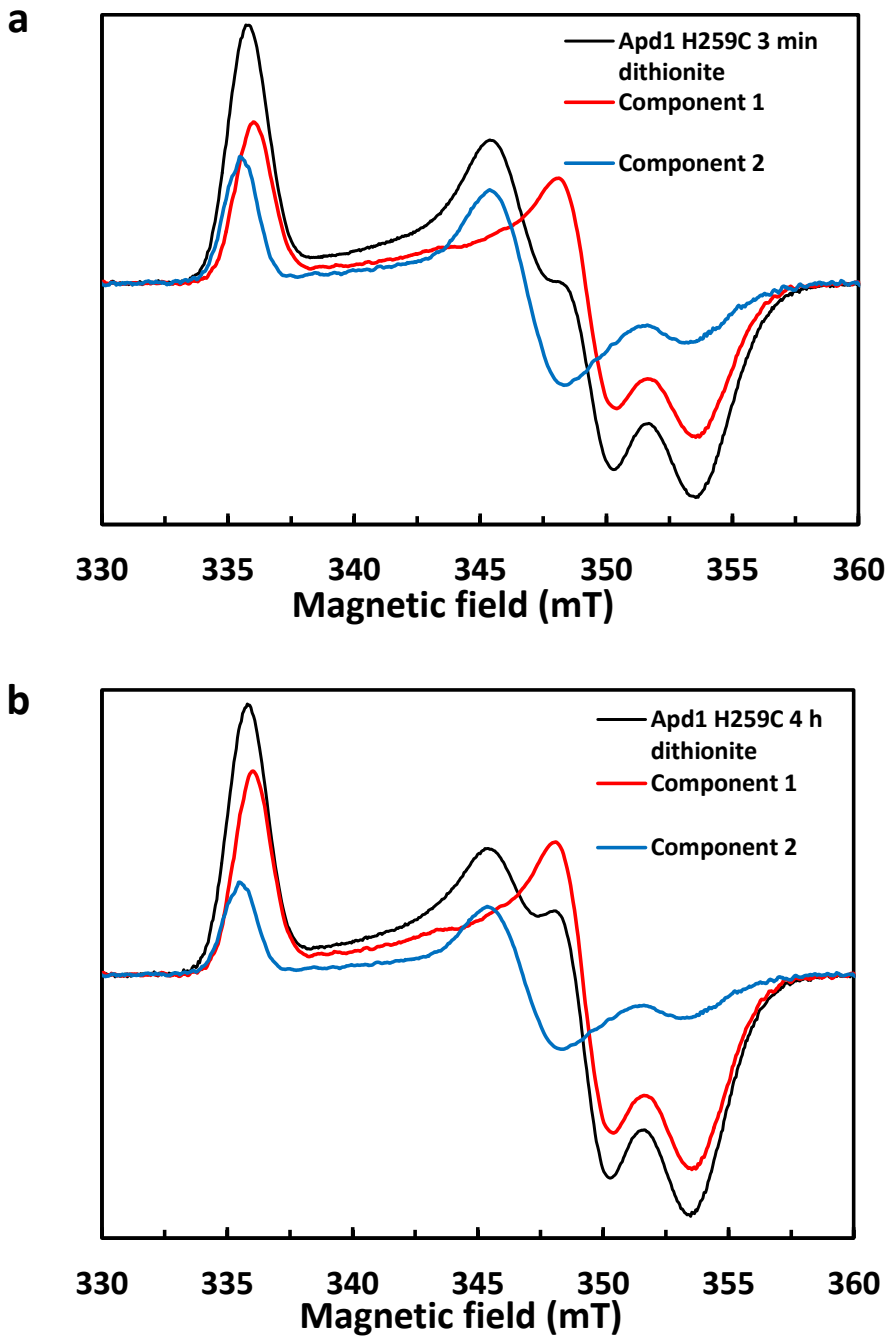

Figure S11. The relative proportion of component 1 and 2 in the EPR spectrum of the dithionite reduced Apd1 H259C variant changes after incubation. (a) 3 min, (b) 4 h. Experimental conditions as in Figure S10. EPR spectra of component 1 and 2 were obtained from difference spectra. The relative (double integrated) intensity of component 1 increased from 60 % (a) to 71 % (b).

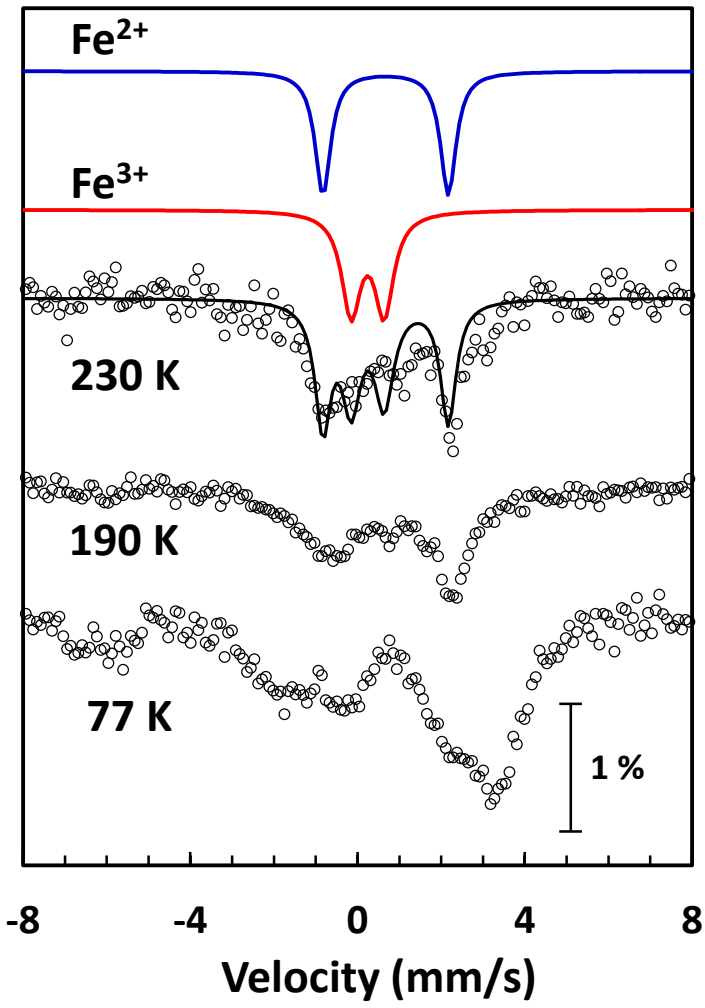

Figure S12. Mössbauer spectra of dithionite-reduced Apd1 at pH 9. Spectra were recorded in absence of a magnetic field at indicated temperatures. Simulations (for 230 K) highlight the still not well resolved quadrupole doublets of the ferric (δ=0.24 mm/s, ΔE_Q=0.79 mm/s, Γ=0.55 mm/s) and ferrous (δ=0.67 mm/s, ΔE_Q=3.00 mm/s, Γ=0.45 mm/s) subspectra with equal integrated intensities.

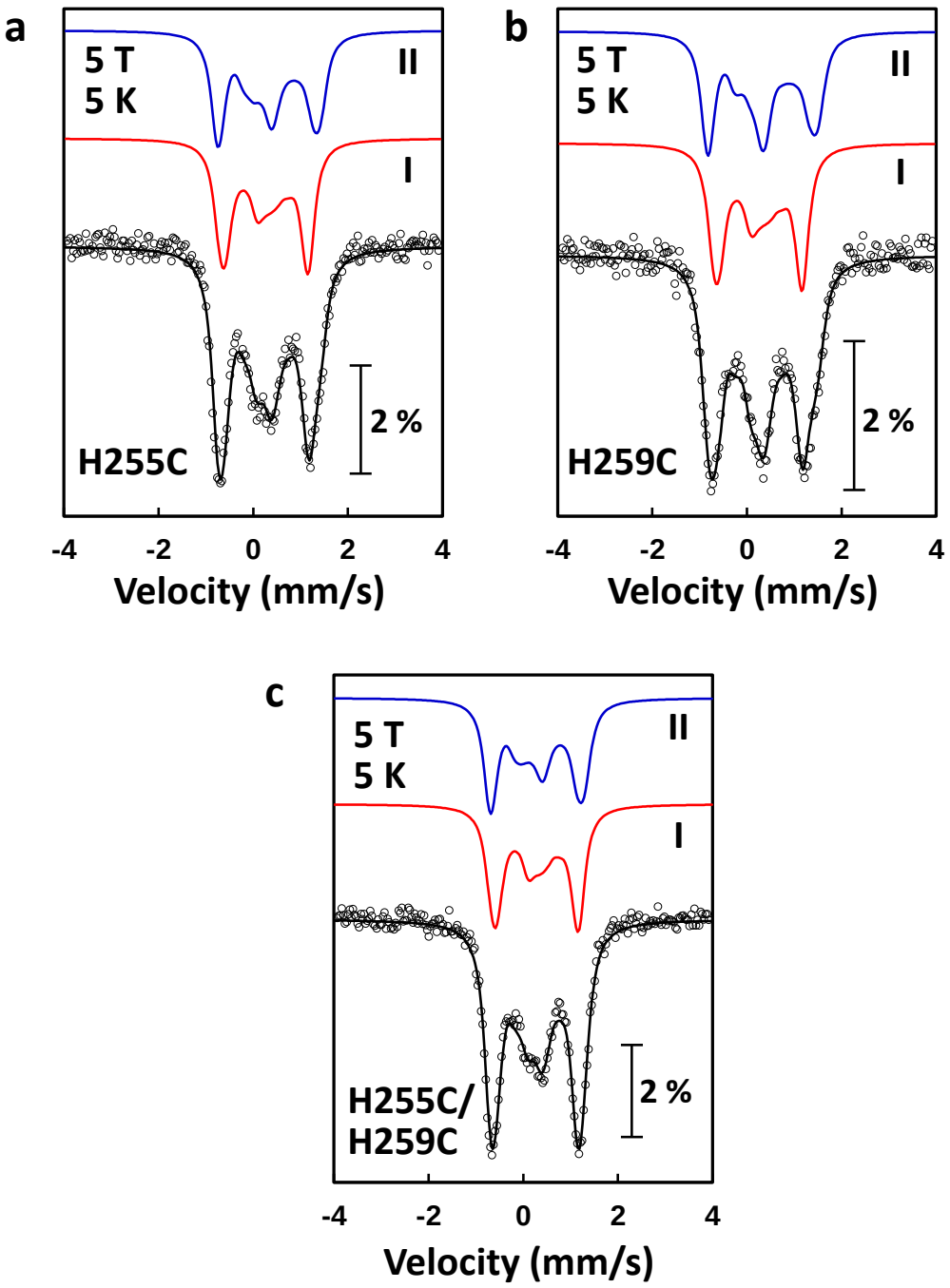

Figure S13. Low temperature and high-field Mössbauer spectra of oxidized Apd1 variants at pH 9.0. (a) H255C, (b) H259C and (c) H255C/H259C. Temperature, 5 K; applied magnetic field (parallel to γ beam), 5 T. Simulation parameters (components with equal integrated intensity) are in Table 1.

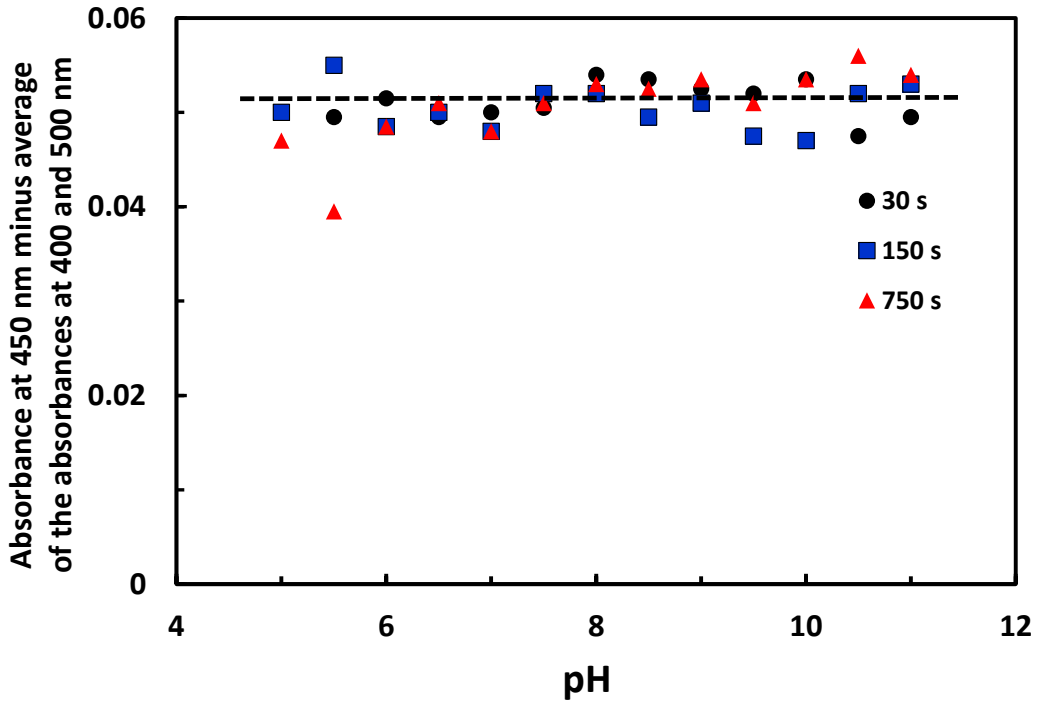

Figure S14. pH-stability of purified Apd1. Apd1 (14 µM) in 5 mM Tris/HCl, pH 9.0, 150 mM NaCl was mixed with 75 mM buffer at defined pH-values and, after mixing, incubated for 30, 150 or 750 s. Then the pH was readjusted to pH ~9.0 by addition of an excess of 150 mM Tris/HCl, pH 9.0, 150 mM NaCl. At this point aliquots were pipetted into a microtiter plate and spectra were recorded between 300 and 800 nm. pH-values of the samples were verified with a microelectrode. The stability of the visible [2Fe-2S] chromophore was estimated from $Abs_{450nm}-(Abs_{400nm}+Abs_{500nm})/2$.

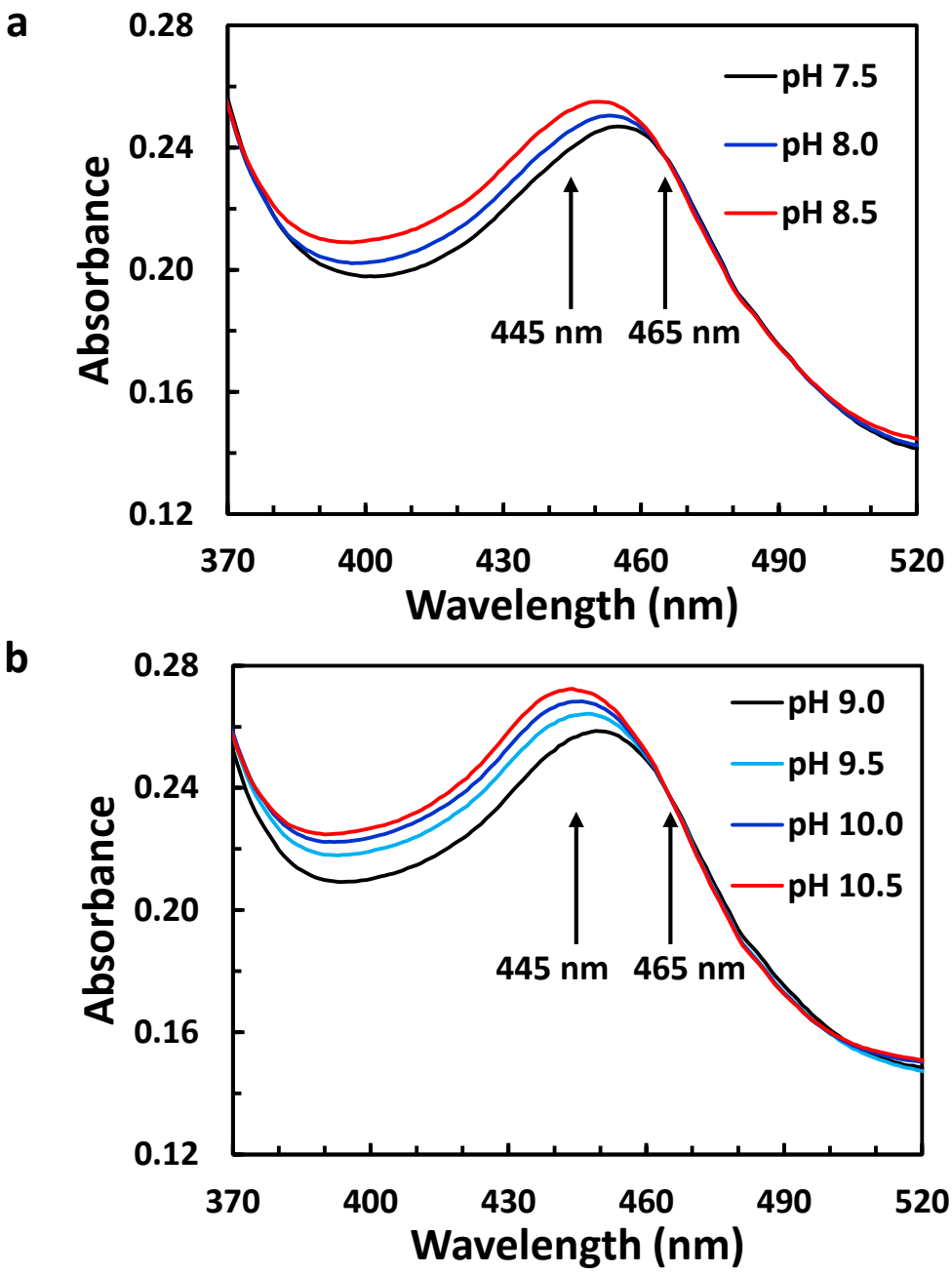

Figure S15. Visible spectra of Apd1 at different pH values. Apd1 (36 µM) in 5 mM Tris/HCl, pH 9.0, 150 mM NaCl was mixed with 75 mM buffer at defined pH-values. Spectra were recorded directly after mixing. Wavelengths used for the pK determination of oxidized Apd1 are indicated. The pH range around pK_{ox1}=7.9 (a) and around pK_{ox2}=9.7 (b) is shown.

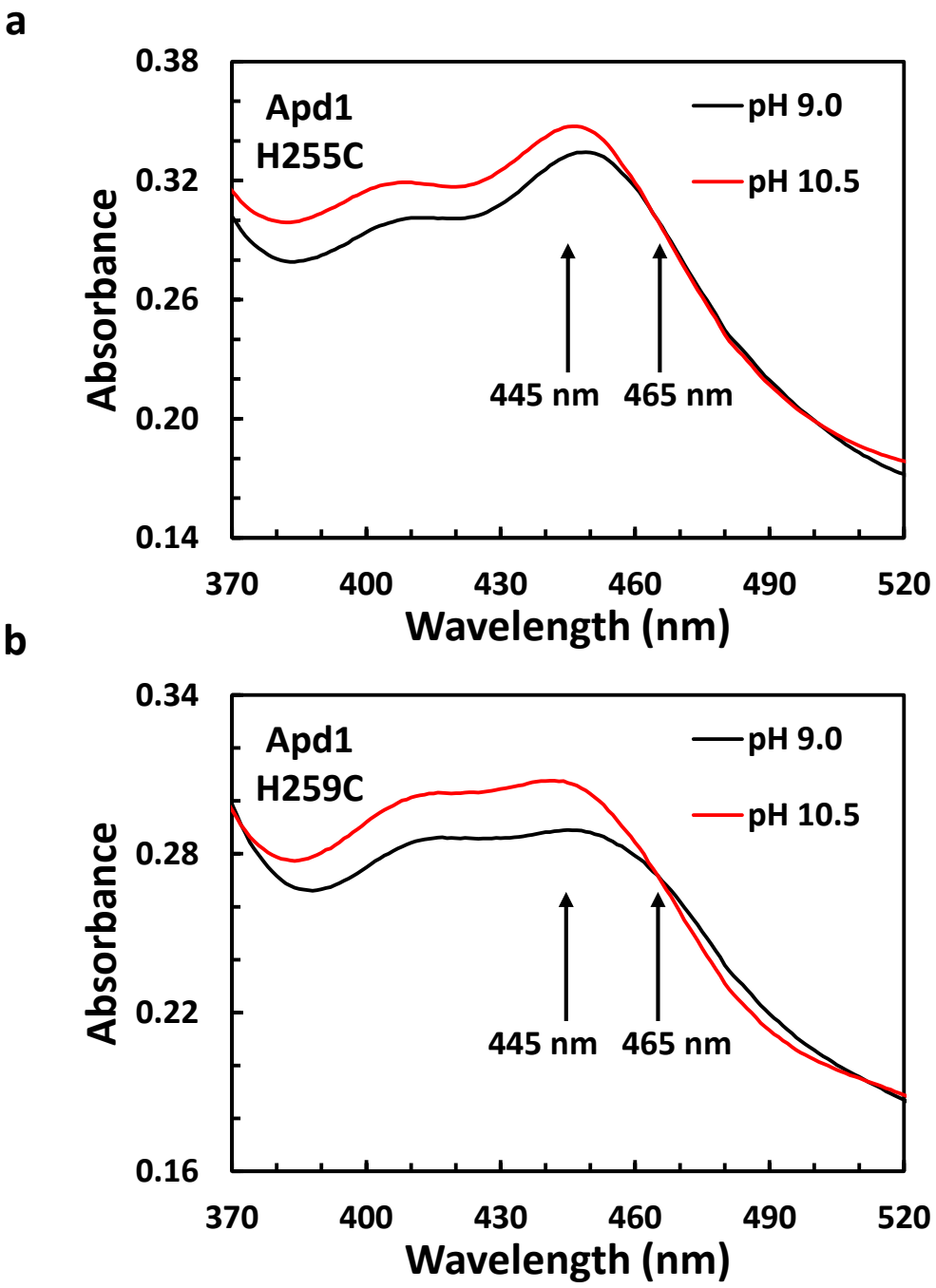

Figure S16. Visible spectra of Apd1 variants at different pH values. The Apd1 variants H255C (a) and H259C (b) (~45µM) in 5 mM Tris/HCl, pH 9.0, 150 mM NaCl were mixed with 75 mM buffer at defined pH-values. Spectra were recorded directly after mixing. Wavelengths used for the pK determination of the oxidized Apd1 variants are indicated. Spectra for pH 9.0 (H259 or H255 protonated in the H255C and H259C variants, respectively) and 10.5 (H259 or H255 deprotonated in the H255C and H259C variants, respectively) are shown.

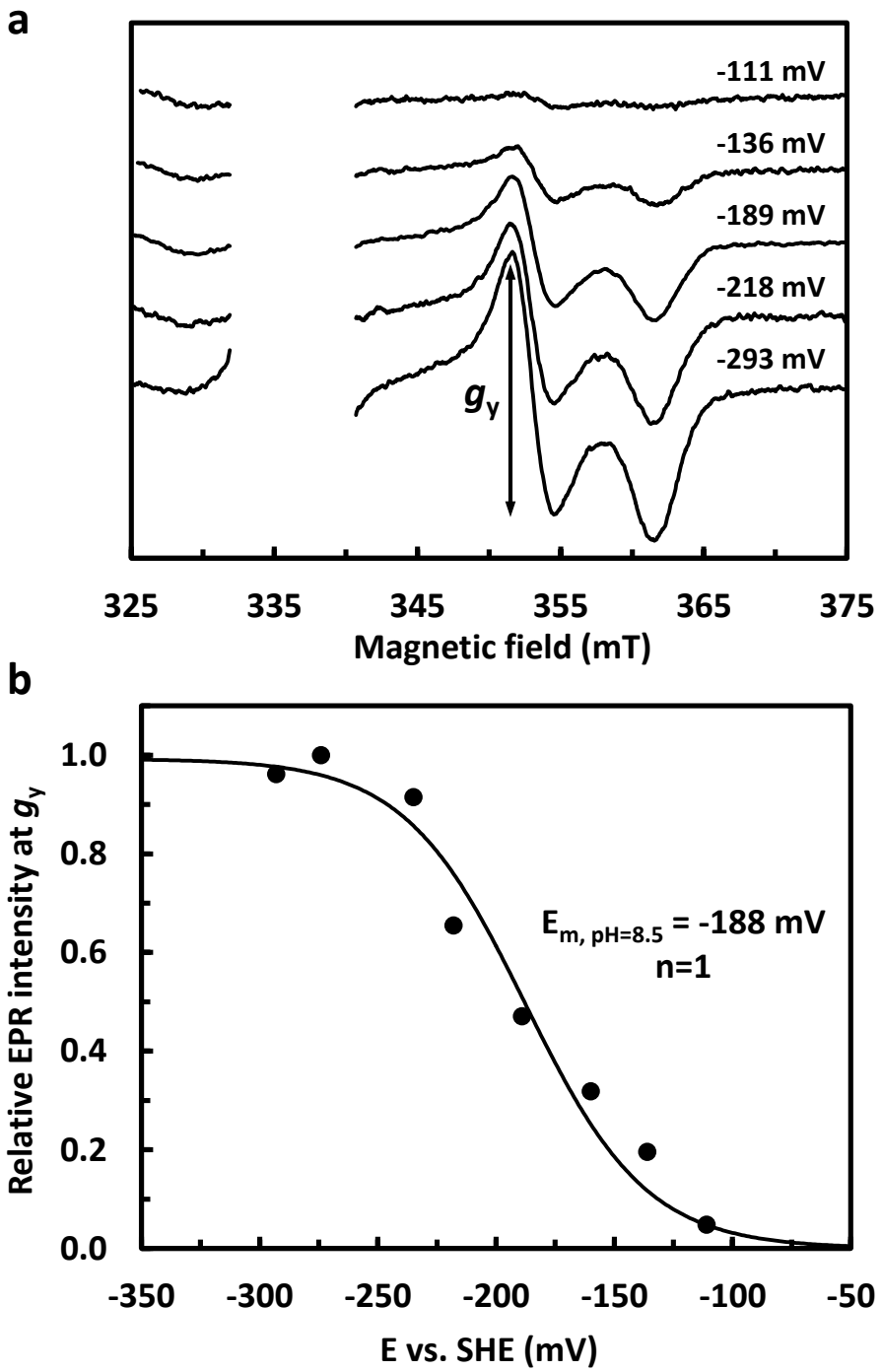

Figure S17. EPR-monitored redox titration of Apd1. (a) Excerpts from EPR spectra of Apd1 in 100 mM TAPS/NaOH pH 8.5 at various redox potentials. EPR conditions as in Figure S10. The amplitude of the g_y peak used for the titration is indicated. (b) The normalized amplitudes of the g_y peak were plotted against the measured redox potential. A fit to the Nernst equation (n=1) with E_m= –188 mV vs. H_2/H^+ is shown.

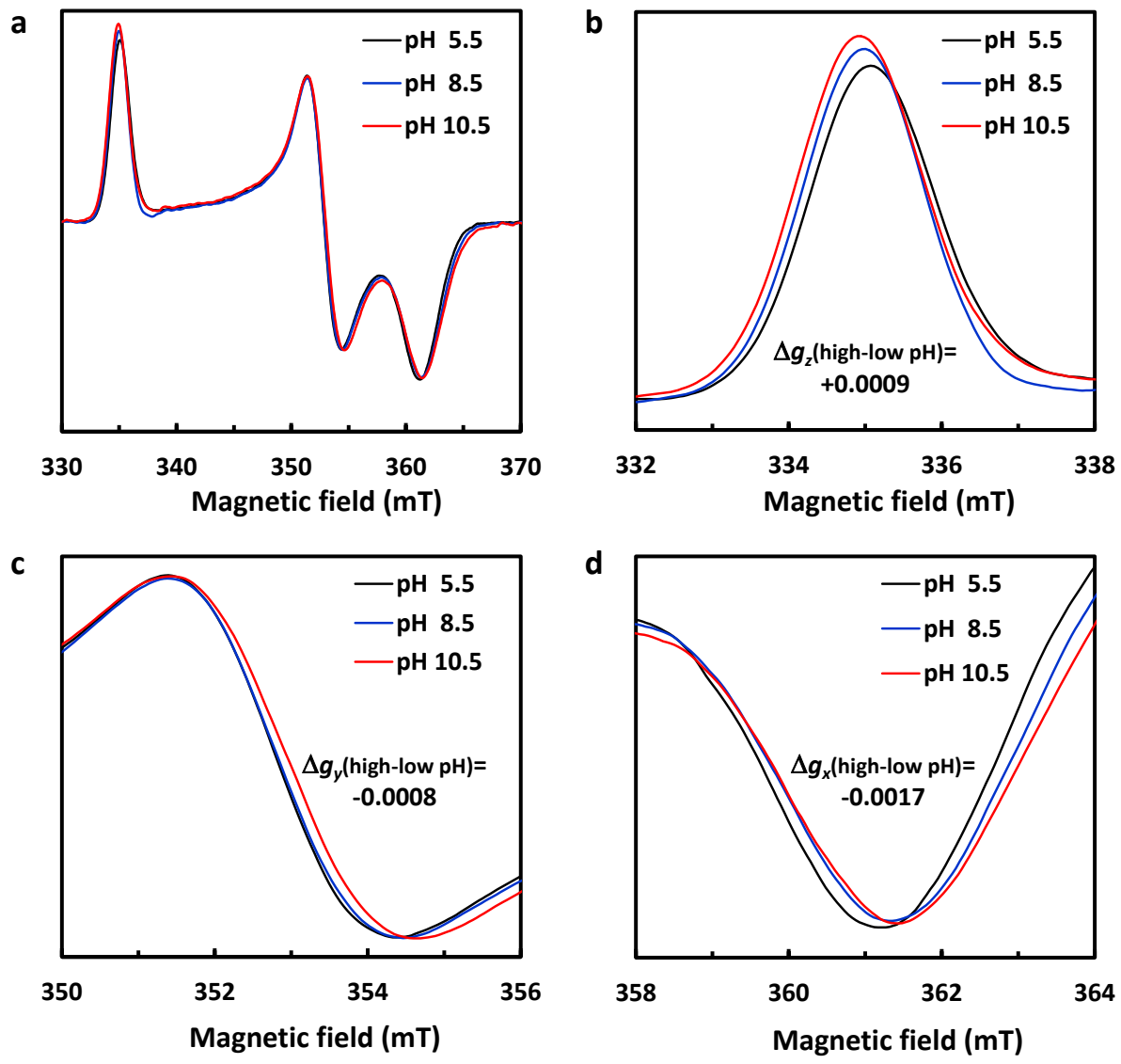

Figure S18. pH dependence of the EPR spectrum of Apd1. Apd1 (45 µM, 0.05 ml) in 50 mM Tris/HCl, pH 9.0, 150 mM NaCl was mixed with 0.25 ml 300 mM MES pH 5.5, 300 mM Tris pH 8.5 or 300 mM CAPS pH 10.5. Sodium dithionite (2 mM final concentration) was added. After 3 min of incubation at 23 °C samples were transferred to EPR tubes and frozen in liquid nitrogen. Experimental conditions as in Figure S10. Spectra are moving averages of 9 datapoints (0.4 mT).

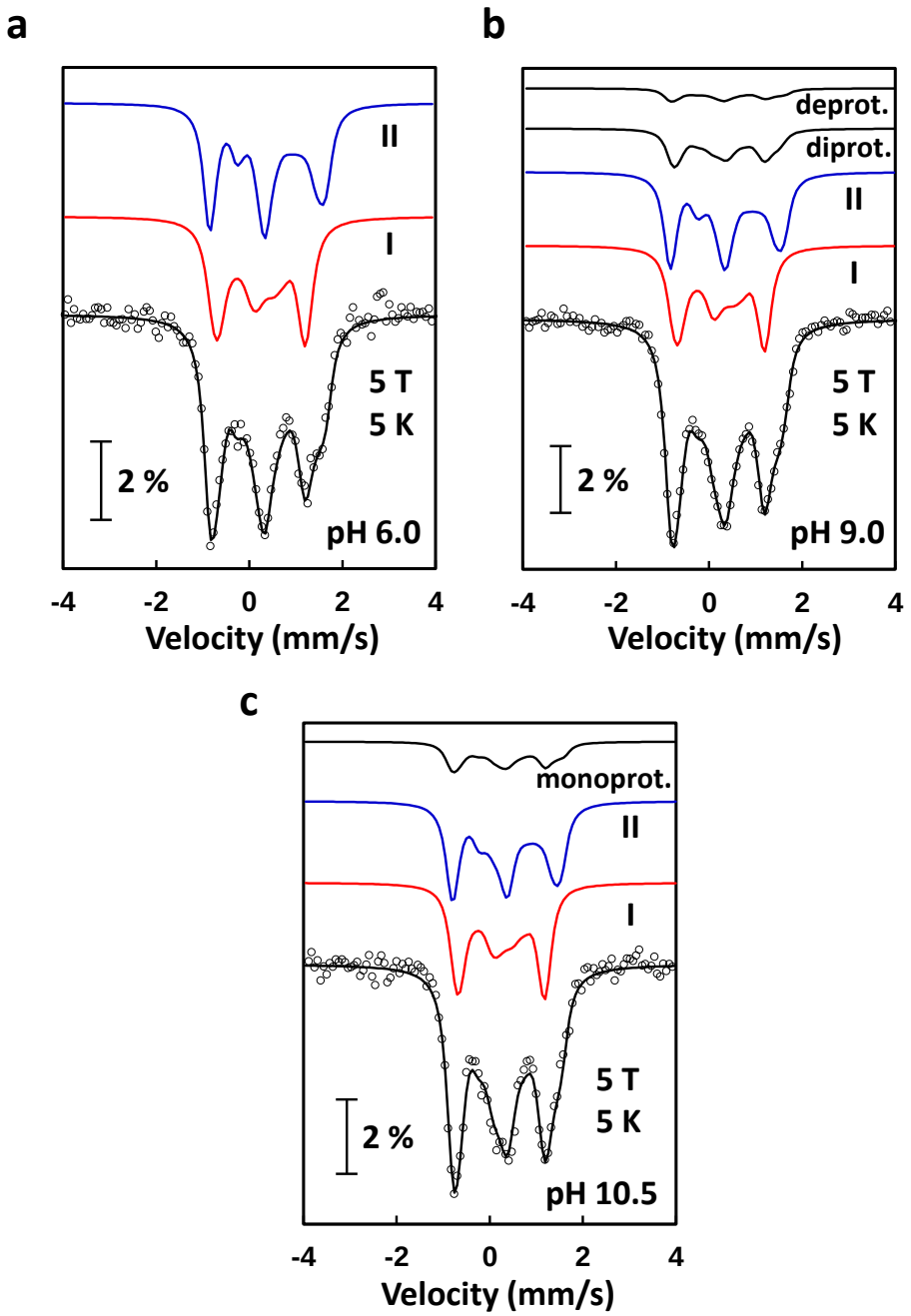

Figure S19. Low temperature and high-field Mössbauer spectra of oxidized Apd1 at pH 6 (a), pH 9.0 (b) and pH 10.5 (c). Temperature, 5 K; applied magnetic field (parallel to γ beam), 5 T. Parameters for the deprotonated form were derived directly from simulation of pH 6.0 data. From the pH 9.0 and pH 10.5 spectra parameters for subspectrum I and II of the mono- and deprotonated forms, respectively, were estimated. Iterative simulation taking into account the diprotonated:monoprotonated:deprotonated contents of 6:78:16 (pH 9.0) and 0:14:86 (pH 10.5) yielded the parameters for the monoprotonated and deprotonated forms (see Table 1).

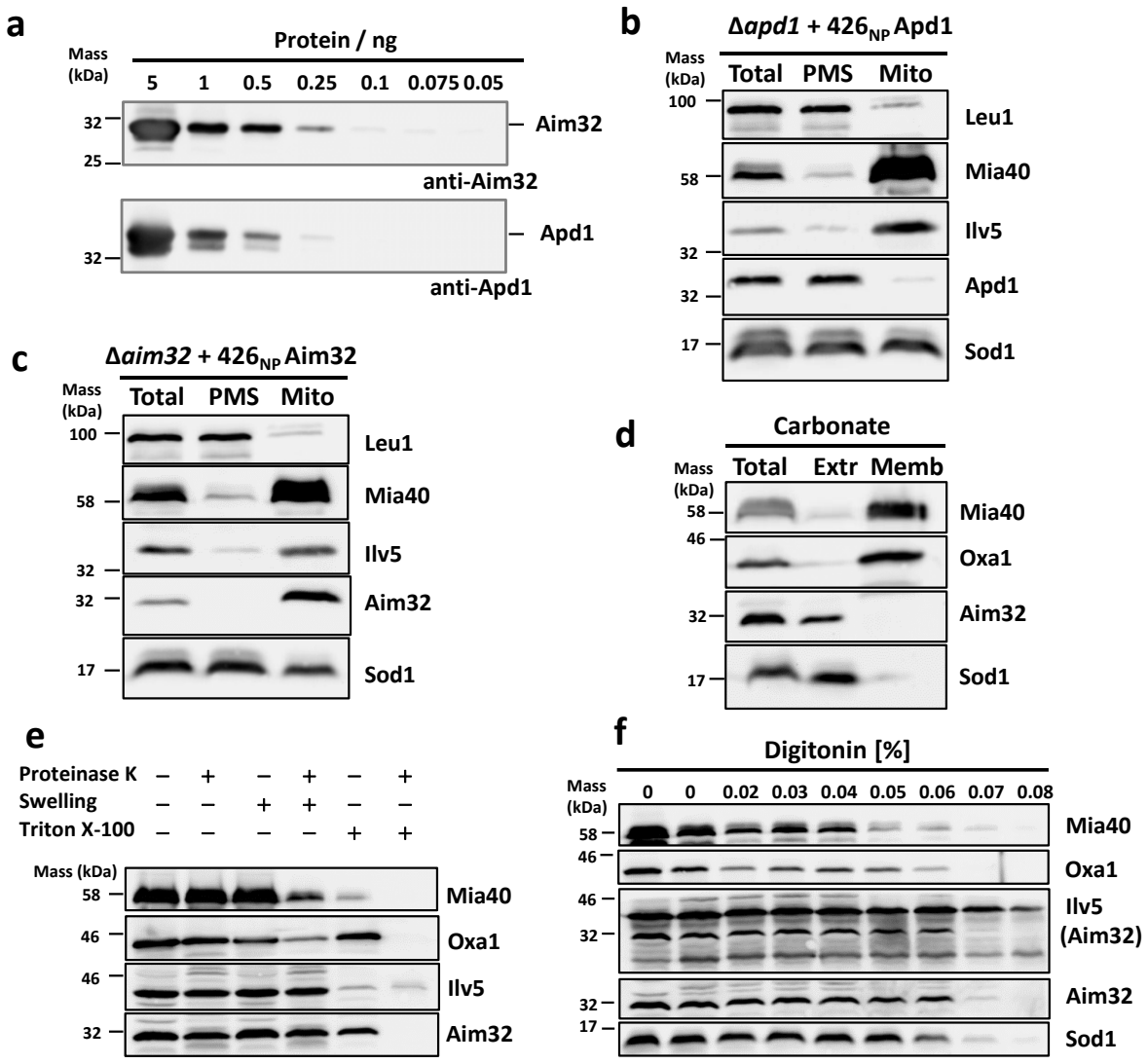

Figure S20. Sub-localization of Apd1 and Aim32. (a) Purified recombinant Aim32 and Apd1 can be detected in Western blots at the ng level. 426_{NP}Aim32 (b) and 426_{NP}Apd1 (c) were transformed into Δ*aim32* and Δ*apd1* yeast cells, respectively. Cells were fractionated by differential centrifugation and 100 µg of each fraction (T, total cell extract, PMS, post mitochondrial supernatant and M, crude mitochondria) were precipitated with TCA (25 %, final concentration), for 10 min on ice. After washing twice with acetone, the pellets were dissolved in Laemli buffer and subjected to SDS-PAGE. After Western blotting, the proteins of interest were detected with specific antibodies. For (d) to (f), mitochondria were prepared from cells described in (b). For sodium carbonate extraction (d) crude mitochondria (100 µg protein) were incubated in 0.1 M Na_2CO_3 with 2 mM PMSF. After centrifugation, the supernatant was removed and the pellet was washed with 0.1 M Na_2CO_3. In (e) mitochondria (50 µg protein) were incubated in the presence (+) or absence (-) of 200 µg/ml proteinase K or Triton X-100 under isosmotic (swelling -) or hypotonic (+) conditions. In (f**)**, crude mitochondria (50 µg protein) were incubated at different digitonin concentrations for 3 min on ice, followed by incubation with proteinase K (200 µg/ml) for 20 min. The digestion was stopped by adding 2 mM PMSF.

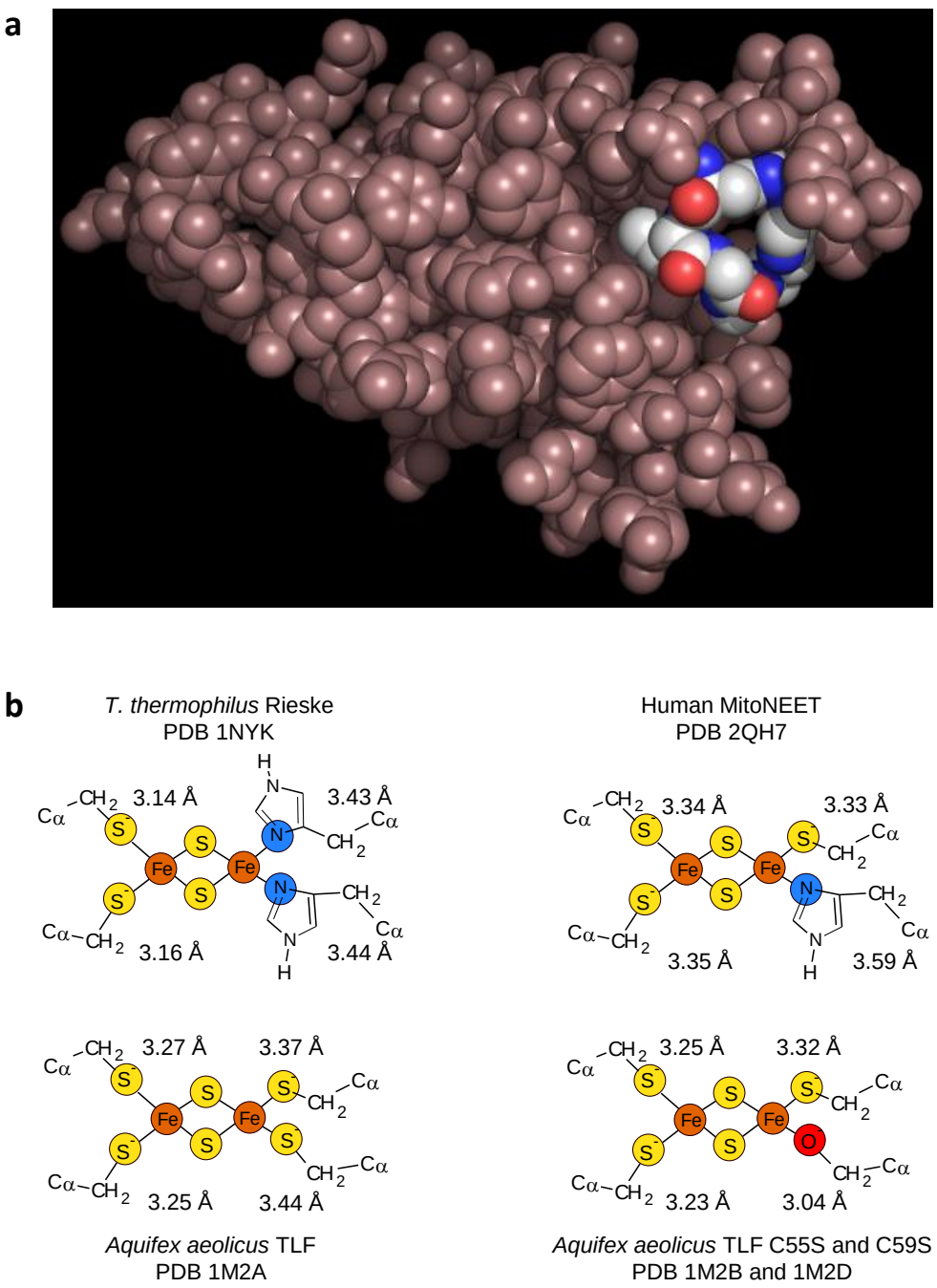

Figure S21. Surface exposure of the HVGGH loop in the C-terminal TLF domain of yeast Apd1 and distance constraints regarding ligand substitution. (a) Predicted structure based on *Azotobacter vinelandii* TLF (PDB 5ABR) modelled with Phyre2,[5] rendered in Pymol. (b) Distances of the Cβ atom of the ligands to the iron ions in the indicated [2Fe-2S] proteins. Values are averages in case there are two molecules in the unit cell.

Table S1. EPR simulation parameters for the $[2Fe\text{-}2S]^{1+}$ cluster of Apd1, its variants and Aim32.

Protein	Com-ponent	$g_{average}$	g_z	g_y	g_x	Linewidth (mT)	Δg_z	Δg_y	Δg_x	Intensity (%)
Apd1 wild type		1.9252	2.0090	1.9057	1.8608	1.5120	0.0000	0.0095	0.0136	100
Apd1 H255C		1.9371	1.9990	1.9341	1.8781	1.6101	0.0013	0.0109	0.0203	100
Apd1 H259C	1	1.9436	2.0034	1.9269	1.9006	1.2346	0.0000	0.0040	0.0201	60
	2	1.9490	2.0035	1.9398	1.9037	1.7979	0.0002	0.0040	0.0000	40
Apd1 H255C/	1	1.9602	2.0040	1.9450	1.9317	1.1996	0.0086	0.0145	0.0495	68
H259C	2	1.9617	2.0065	1.9587	1.9200	0.8163	0.0004	0.0080	0.0116	32
Aim32		1.9236	2.0108	1.9032	1.8567	1.4738	0.0000	0.0119	0.0177	100

Table S2. Bis-histidinyl coordinated biological [2Fe-2S] clusters: *g*-values and references

Entries no. 1-41 have been compiled by Link.[6] Abbreviations: B, bc_1 and b_6f complexes and Rieske proteins thereof; FO, Rieske type ferredoxin of oxygenase systems; O, Rieske type centre of oxygenase systems; T, thioredoxin-like ferredoxin. For entry 42 the *g*-values were corrected due to the erroneous use of 0.7 in stead of 0.714484 for calculation.

No.	Protein	Organism	Type	$\Sigma g/3$	R_z	g_z	g_y	g_x	Ref.
1	Rieske	*Bos taurus*	B	1.895	101	2.029	1.896	1.761	[7]
2	Rieske	*Saccharomyces cerevisiae*	B	1.898	108	2.030	1.903	1.760	[6]
3	Rieske	*Paracoccus denitrificans*	B	1.901	99	2.033	1.901	1.770	[6]
4	Rieske	*Paracoccus denitrificans*	B	1.890	101	2.021	1.890	1.758	[8]
5	Rieske	*Neurospora crassa*	B	1.894	108	2.031	1.900	1.752	[9]
6	Rieske	*Spinacea oleracea*	B	1.890	114	2.030	1.900	1.740	[10]
7	Rieske pH 6.1	*Thermus thermophilus*	B	1.916	86	2.033	1.908	1.807	[11]
8	Rieske (complex)	*Thermus thermophilus*	B	1.903	105	2.023	1.906	1.780	[12]
9	Rieske SoxL	*Sulfolobus acidocaldarius*	B	1.899	94	2.035	1.895	1.768	[13]
10	Rieske SoxF	*Sulfolobus acidocaldarius*	B	1.907	82	2.042	1.895	1.785	[14]
11	Rieske	*Nostoc sp.* PCC 7906	B	1.887	105	2.030	1.890	1.740	[15]
12	bc_1 ascorbate	*Bos taurus*	B	1.905	75	2.019	1.891	1.805	[16]
13	bc_1 dithionite	*Bos taurus*	B	1.898	95	2.024	1.895	1.775	[16]
14	bc_1 QH_2	*Bos taurus*	B	1.894	109	2.023	1.900	1.760	[17]
15	bc_1	*Bos taurus*	B	1.906	90	2.017	1.900	1.800	[17]
16	bc_1 ascorbate	*Saccharomyces cerevisiae*	B	1.908	69	2.025	1.890	1.810	[18]
17	bc_1 dithionite	*Saccharomyces cerevisiae*	B	1.902	81	2.026	1.890	1.790	[18]
18	bc_1 dithionite	*Saccharomyces cerevisiae*	B	1.897	108	2.028	1.902	1.760	[6]
19	bc_1 ascorbate	*Paracoccus denitrificans*	B	1.902	76	2.021	1.888	1.797	[8]
20	bc_1 dithionite	*Paracoccus denitrificans*	B	1.896	103	2.030	1.898	1.760	[19]
21	bc_1	*Rhodobacter capsulatus*	B	1.891	103	2.019	1.893	1.762	[9]
22	bc_1 ascorbate	*Rhodobacter sphaeroides*	B	1.913	77	2.030	1.900	1.810	[20]
23	bc_1 dithionite	*Rhodobacter sphaeroides*	B	1.896	106	2.029	1.900	1.760	[20]
24	*bc* ascorbate	*Heliobacterium chlorum*	B	1.912	65	2.035	1.890	1.810	[21]
25	*bc* ascorbate	*Bacillus firmus*	B	1.920	63	2.028	1.900	1.832	[22]
26	*bc* dithionite	*Bacillus firmus*	B	1.918	69	2.030	1.900	1.823	[22]
27	b_6f dithionite	*Spinacea oleracea*	B	1.893	110	2.030	1.900	1.750	[23]
28	Ferredoxin benzene dioxygenase	*Pseudomonas putida*	FO	1.917	51	2.026	1.890	1.834	[24]
29	Ferredoxin toluene-4-monooxygenase	*Pseudomonas mendocina*	FO	1.895	138	2.009	1.917	1.760	[25]
30	Ferredoxin biphenyl 2,3-dioxygenase (BphF)	*Burkholderia xenovorans* LB400	FO	1.920	100	2.020	1.920	1.820	[26]
31	Pyrazon dioxygenase	*Phenylobacterium immobile*	O	1.907	106	2.020	1.910	1.790	[27]

32	4-Methoxybenzoate monooxygenase (putidamonoxin)	*Pseudomonas putida*	O	1.880	151	2.008	1.913	1.720	[28]
33	Benzene dioxygenase	*Pseudomonas putida*	O	1.896	134	2.018	1.917	1.754	[24]
34	Phthalate dioxygenase	*Burkholderia cepacea*	O	1.898	128	2.016	1.914	1.763	[12]
35	Naphthalene dioxygenase	*Pseudomonas putida*	O	1.907	106	2.010	1.910	1.800	[29]
36	2-Halobenzoate-1,2-dioxygenase	*Burkholderia cepacea*	O	1.908	103	2.025	1.910	1.790	[30]
37	2-Oxo-1,2-dihydroquinolinate monooxygenase	*Pseudomonas putida*	B	1.893	129	2.010	1.910	1.760	[31]
38	Trichlorophenoxyacetate monooxygenase	*Burkholderia cepacea* AC1100	B	1.893	129	2.010	1.910	1.760	[32]
39	CMP-N-acetylneuraminic acid hydroxylase	*Sus scrofa*	X	1.900	118	2.010	1.910	1.780	[33]
40	Alkene monooxygenase ferredoxin	*Xanthobacter autotrophicus* PY2	FO	1.903	126	2.016	1.918	1.776	[34]
41	Choline monoxygenase	*Spinacea oleracea*	O	1.886	147	2.008	1.915	1.736	[35]
42	Ferredoxin (toluene dioxygenase)	*Pseudomonas putida* F1	FO	1.933	43	2.052	1.899	1.848	[36]
43	Isolated Rieske pH 10.2	*Thermus thermophilus*	B	1.916	88	2.030	1.909	1.809	[11]
44	4-Chlorophenylacetate 3,4-dioxygenase	*Pseudomonas sp*. CBS3	O	1.893	145	2.021	1.922	1.737	[37]
45	bc_1 ascorbate/UHDBT	*Rhodobacter sphaeroides*	B	1.902	65	2.026	1.880	1.800	[20]
46	bc_1 ascorbate/ stigmatellin	*Rhodobacter sphaeroides*	B	1.897	74	2.032	1.880	1.780	[20]
47	bc_1 dithionite	*Rhodobacter sphaeroides*	B	1.896	106	2.029	1.900	1.760	[20]
48	bc_1	*Rhodospirillum rubrum*	B	1.897	105	2.020	1.900	1.770	[38]
49	bc_1 (Stigmatellin)	*Rhodospirillum rubrum*	B	1.900	83	2.020	1.890	1.790	[38]
50	Arsenite oxidase	*Alcaligenes faecalis*	O	1.893	95	2.030	1.890	1.760	[39]
51	*bc* (+44 mV)	*Bacillus sp.* BS3	B	1.920	64	2.030	1.900	1.830	[40]
52	Ferredoxin (o-haloben-zoate 1,2-dioxygenase)	*Pseudomonas aeruginosa* 142	FO	1.915	81	2.020	1.905	1.820	[41]
53	2-Halobenzoate 1,2-dioxygenase	*Pseudomonas cepacea* 2CBS	O	1.908	106	2.025	1.912	1.788	[31]
54	2-Oxo-1,2-dihydroqui-noline 8-monooxygenase	*Pseudomonas putida* 86	O	1.893	129	2.010	1.910	1.760	[31]
55	Biphenyl 2,3-dioxygenase	*Burkholderia xenovorans* LB400	O	1.890	150	2.010	1.920	1.740	[42]
56	Phthalate dioxygenase	*Burkholderia cepacea*	O	1.873	154	2.010	1.910	1.700	[43]
57	Trichlorophenoxyacetate monooxygenase aged	*Burkholderia cepacea* AC1100	O	1.877	135	2.010	1.900	1.720	[44]
58	4-Sulfobenzoate dioxygenase	*Comamonas testosteroni* T-2	O	1.897	138	2.025	1.921	1.745	[45]
59	4-Toluenesulfonate methyl-monooxygenase	*Comamonas testosteroni* T-2	O	1.909	116	2.019	1.918	1.790	[46]
60	*bc* hydroquinone	*Sulfolobus metallicus*	B	1.889	115	2.028	1.900	1.740	[47]
61	Rieske	*Pyrobaculum aerophilum*	B	1.904	74	2.030	1.888	1.795	[48]
62	Toluene dioxygenase	*Pseudomonas putida* F1	O	1.893	129	2.010	1.910	1.760	[49]
63	Anthranilate 1,2-dioxygenase	*Acinetobacter sp.* ADP1	O	1.913	134	2.010	1.930	1.800	[50]
64	Benzoate 1,2-dioxygenase	*Pseudomonas putida*	O	1.897	124	2.010	1.910	1.770	[51]
65	Rieske ferredoxin	*Sulfolobus tokodaii*	B	1.903	114	2.008	1.910	1.790	[52]
66	Rieske ferredoxin	*Sulfolobus sulfataricus*	B	1.910	82	2.020	1.900	1.810	[53]
67	Maturation NiFe hydrogenase	*Acidianus ambivalens*	O	1.893	110	2.030	1.900	1.750	[54]
68	Dicamba *O*-demethylase	*Pseudomonas maltophila*	O	1.900	121	2.008	1.911	1.78	[55]
69	Rieske PetA1	*Rubrivivax gelatinosus*	B	1.881	114	2.011	1.890	1.742	[56]
70	Rieske PetA2	*Rubrivivax gelatinosus*	B	1.874	120	2.006	1.887	1.728	[56]

71	Ferredoxin (nitrotoluene dioxygenase)	*Acidovorax sp.* JS42	O	1.910	82	2.020	1.900	1.810	[57]
72	Nitrotoluene dioxygenase	*Acidovorax sp.* JS42	O	1.900	118	2.010	1.910	1.780	[57]
73	Nitrobenzene dioxygenase	*Comamonas sp.* JS765	O	1.893	126	2.020	1.910	1.750	[57]
74	Naphthalene dioxygenase	*Sphingomonas sp.* CHY-1	O	1.883	154	2.020	1.920	1.710	[58]
75	Ferredoxin (biphenyl 2,3-dioxygenase)	*Sphingobium yanoikuyae* B1	O	1.913	75	2.020	1.900	1.820	[59]
76	Biphenyl 2,3-dioxygenase	*Sphingobium yanoikuyae* B1	O	1.883	142	2.010	1.910	1.730	[59]
77	HcaC	*Escherichia coli*	O	1.920	73	2.022	1.906	1.831	[60]
78	YeaW	*Escherichia coli*	X	1.907	114	2.010	1.914	1.797	[60]
79	bc_1 ascorbate	*Halorhodospira halophila*	B	1.902	105	2.030	1.905	1.770	[61]
80	Arsenite oxidase	*Rhizobium sp*. NT-26	O	1.892	82	2.027	1.880	1.770	[62]
81	Arsenite oxidase	*Ralstonia sp*. 22	O	1.892	82	2.027	1.880	1.770	[62]
82	GrxS14-BolA1	*Arabidopsis thaliana*	X	1.877	216	2.020	1.960	1.650	[63]
83	Rieske (PetC)	*Chlorobaculum tepidum*	B	1.913	77	2.030	1.900	1.810	[64]
84	Apd1	*Saccharomyces cerevisiae*	T	1.925	54	2.009	1.906	1.861	This work
85	Aim32	*Saccharomyces cerevisiae*	T	1.924	53	2.011	1.903	1.857	This work

Table S3. Mono-histidinyl coordinated biological [2Fe-2S] clusters: *g*-values and references.

These values have not been compiled for Gibson plots before. Abbreviations: M, MitoNEET family; D, diverse; T, thioredoxin-like ferredoxin.

No.	Protein	Organism	Type	$\Sigma g/3$	R_z	g_z	g_y	g_x	Ref.
1	Outer membrane MitoNEET	*Rattus norvegicus*	M	1.945	73	2.008	1.937	1.891	[65]
2	IscR	*Escherichia coli*	D	1.937	113	1.990	1.940	1.880	[66]
3	Rieske ferredoxin H64C	*Sulfolobus sulfataricus*	D	1.947	0	2.000	1.920	1.920	[53]
4	MitoNEET	*Rattus norvegicus*	M	1.946	71	2.005	1.937	1.895	[67]
5	Grx3-Fra2 heterodimer	*Saccharomyces cerevisiae*	D	1.933	65	2.010	1.920	1.870	[68]
6	MitoNEET	*Homo sapiens*	M	1.947	67	2.007	1.937	1.897	[69]
7	Glrx3-A-BolA2 heterodimer	*Homo sapiens*	D	1.933	39	2.010	1.910	1.880	[70]
8	Glrx3-B-BolA2 heterodimer	*Homo sapiens*	D	1.933	39	2.010	1.910	1.880	[70]
9	Glrx3-BolA2 heterodimer	*Homo sapiens*	D	1.933	39	2.010	1.910	1.880	[70]
10	AirS	*Staphylococcus aureus*	D	1.936	52	2.023	1.915	1.870	[71]
11	RsrR	*Streptomyces venezuelae*	D	1.928	75	1.997	1.919	1.867	[72]
12	Grx4-IbaG heterodimer	*Escherichia coli*	D	1.933	65	2.010	1.920	1.870	[73]
13	MitoNEET	*Homo sapiens*	M	1.950	67	2.010	1.940	1.900	[74]
14	Miner1	*Homo sapiens*	M	1.950	67	2.010	1.940	1.900	[74]
15	Miner2 cluster 1	*Homo sapiens*	M	1.940	33	2.000	1.920	1.900	[74]
16	Miner2 cluster 2	*Homo sapiens*	M	1.947	79	2.010	1.940	1.890	[74]
17	Apd1 H255C	*Saccharomyces cerevisiae*	T	1.937	90	1.999	1.934	1.878	This work
18	Apd1 H259C main species	*Saccharomyces cerevisiae*	T	1.944	44	2.003	1.927	1.901	This work
19	Apd1 H259C minor species	*Saccharomyces cerevisiae*	T	1.949	67	2.003	1.940	1.904	This work

Table S4. All cysteinyl coordinated biological [2Fe-2S] clusters: *g*-values and references.

Entries 1-18 correspond to Table 1 in Bertrand and Gayda[75], entry 19-23 are from references added by Bertrand *et al*.[76], entry 24-26 are from references added by Guigliarelli and Bertrand.[77] Abbreviations: A, adrenodoxin type; T, thioredoxin-like ferredoxin; I and II xanthine dehydrogenase family type I and II [2Fe-2S]; FC, ferrochelatase; D, diverse.

No.	Protein	Organism	Type	$\Sigma g/3$	R_z	g_z	g_y	g_x	Ref.
1	Putidaredoxin	*Pseudomonas putida*	A	1.963	0	2.020	1.934	1.934	[78]
2	Adrenodoxin	*Sus scrofa*	A	1.962	9	2.020	1.935	1.930	[79]
3	Ferredoxin TLF	*Clostridium pasteurianum*	T	1.959	63	2.005	1.951	1.923	[80]
4	Ferredoxin IA (Shethna I) TLF	*Azotobacter vinelandii*	T	1.956	45	2.009	1.941	1.917	[81]
5	Ferredoxin IB (Shethna I) TLF	*Azotobacter vinelandii*	T	1.957	48	2.009	1.943	1.918	[81]
6	Ferredoxin II	*Azotobacter vinelandii*	A	1.956	66	2.036	1.943	1.891	[81]
7	Ferredoxin denatured MeOH	*Spinacea oleracea*	A	1.962	63	2.042	1.947	1.897	[82]
8	Ferredoxin denatured urea	*Spinacea oleracea*	A	1.957	63	2.040	1.942	1.890	[83]
9	Ferredoxin denatured TCA	*Spinacea oleracea*	A	1.961	67	2.039	1.948	1.895	[84]
10	Ferredoxin	*Petroselinum crispum*	A	1.970	73	2.052	1.959	1.899	[85]
11	Ferredoxin	*Spirulina sp.*	A	1.960	80	2.042	1.952	1.887	[86]
12	Ferredoxin powder	*Spinacea oleracea*	A	1.958	76	2.045	1.947	1.881	[87]
13	Ferredoxin 1	*Spinacea oleracea*	A	1.967	84	2.050	1.960	1.890	[79]
14	Ferredoxin	*Microcystis flos-aquae*	A	1.968	82	2.053	1.960	1.890	[88]
15	Ferredoxin	*Spirulina maxima*	A	1.965	83	2.051	1.958	1.887	[75]
16	Ferredoxin	*Scenedesmus sp.*	A	1.967	87	2.052	1.961	1.887	[75]
17	Ferredoxin	*Spinacea oleracea*	A	1.958	84	2.048	1.951	1.875	[87]
18	Ferredoxin	*Synechococcus lividus*	A	1.963	92	2.050	1.960	1.880	[89]
19	NADH dehydrogenase N1b form A	*Paracoccus denitrificans*	A	1.961	27	2.029	1.937	1.918	[90]
20	NADH dehydrogenase N1b form B	*Paracoccus denitrificans*	A	1.963	22	2.019	1.941	1.929	[90]
21	Fumarate reductase	*Escherichia coli*	A	1.960	21	2.026	1.934	1.920	[91]
22	Succinate dehydrogenase	*Bos taurus*	A	1.958	34	2.026	1.935	1.912	[92]
23	Ferredoxin 2	*Spinacea oleracea*	A	1.962	100	2.049	1.962	1.875	[93]
24	Ferrochelatase	*Homo sapiens*	FC	1.950	46	2.002	1.936	1.912	[94]
25	Hydrogenase HndA	*Desulfovibrio fructosivorans*	T	1.955	78	2.000	1.950	1.915	[95]
26	Phthalate oxygenase reductase	*Burkholderia cepacea*	A	1.963	63	2.041	1.949	1.900	[96]
27	Dihydroorotate dehydrogenase	*Clostridium oroticum*	D	1.957	38	2.010	1.940	1.920	[97]
28	Sucinate dehydrogenase (succinate)	*Bos taurus*	A	1.954	28	2.027	1.928	1.908	[98]
29	Sucinate dehydrogenase (dithionite)	*Bos taurus*	A	1.958	18	2.030	1.928	1.915	[98]
30	Ferredoxin	*Porphyra umbilicalis*	A	1.963	92	2.050	1.960	1.880	[99]
31	Xanthine dehydrogenase I	*Meleagris gallopavo*	I	1.952	40	2.017	1.932	1.906	[100]
32	Xanthine dehydrogenase II	*Meleagris gallopavo*	II	2.000	100	2.080	2.000	1.920	[100]
33	Ferredoxin	*Halobacterium halobium*	A	1.980	82	2.066	1.972	1.901	[101]
34	Pyrazon dioxygenase	*Phenylobacterium immobile*	A	1.967	0	2.020	1.940	1.940	[27]
35	Succinate dehydrogenase	*Candida utilis*	A	1.957	29	2.024	1.933	1.914	[102]
36	MMO reductase	*Methylococcus capsulatus*	A	1.957	107	2.047	1.960	1.864	[103]
37	Reductase (4-methoxy-benzoate monooxygenase)	*Pseudomonas putida*	A	1.956	64	2.032	1.942	1.893	[28]

38	Ferredoxin	*Spinacea oleracea*	A	1.961	85	2.046	1.955	1.882	[104]
39	Aldehyde oxidoreductase I	*Oryctolagus cuniculus*	I	1.955	19	2.018	1.930	1.918	[105]
40	Aldehyde oxidoreductase II	*Oryctolagus cuniculus*	II	2.008	90	2.106	2.003	1.915	[105]
41	Milk xanthine oxidase I	*Bos taurus*	I	1.949	52	2.022	1.932	1.894	[106]
42	Milk xanthine oxidase II	*Bos taurus*	II	2.001	82	2.110	1.991	1.902	[106]
43	Methane monooxygenase reductase	*Methanobacterium sp.* CRL26	A	1.957	108	2.040	1.960	1.870	[107]
44	Reductase (4-chlorophenyl-acetate 3,4-dioxygenase)	*Pseudomonas sp.* CBS3	A	1.957	55	2.030	1.940	1.900	[108]
45	Hydrogenase	*Pyrococcus furiosus*	A	1.953	13	2.030	1.920	1.910	[109]
46	Xanthine dehydrogenase I	*Drosophila melanogaster*	I	1.952	44	2.022	1.933	1.902	[110]
47	Xanthine dehydrogenase II	*Drosophila melanogaster*	II	2.006	98	2.118	2.005	1.896	[110]
48	Ferredoxin (Isc operon)	*Escherichia coli*	A	1.967	0	2.020	1.940	1.940	[111]
49	Reductase (AcsD)	*Yersinia pseudotuberculosis*	D	1.960	100	2.043	1.960	1.877	[112]
50	Dehydrase (AscC)	*Yersinia pseudotuberculosis*	D	1.962	45	2.007	1.950	1.930	[113]
51	Methane monooxygenase reductase	*Methylosinus trichosporium*	A	1.957	107	2.050	1.960	1.860	[114]
52	Ferredoxin (TLF)	*Clostridium pasteurianum*	T	1.958	57	2.004	1.948	1.922	[115]
53	Ferredoxin WT	*Anabaena sp.* 7120	A	1.963	92	2.050	1.960	1.880	[116]
54	FeFe hydrogenase HydA	*Thermotoga maritima*	A	1.969	9	2.026	1.943	1.938	[117]
55	SoxR	*Escherichia coli*	D	1.944	30	2.007	1.922	1.903	[118]
56	Complex Nqo3 (non-TLF, N1b)	*Paracoccus denitrificans*	A	1.965	0	2.026	1.934	1.934	[119]
57	Reductase (2-HBD)	*Burkholderia cepacea*	A	1.967	84	2.050	1.960	1.890	[30]
58	Reductase (ODQ monooxygenase)	*Pseudomonas putida*	A	1.953	65	2.030	1.940	1.890	[31]
59	Reductase (2-halobenzoate 1,2-dioxygenase)	*Pseudomonas cepacea* 2CBS	A	1.962	74	2.043	1.951	1.891	[31]
60	Reductase (2-oxo-1,2-dihydroquinoline 8-monooxygenase)	*Pseudomonas putida* 86	A	1.953	65	2.030	1.940	1.890	[31]
61	Ferrochelatase	*Mus musculus*	FC	1.947	38	2.000	1.930	1.910	[120]
62	Ferredoxin (bacterioferritin)	*Escherichia coli*	D	1.967	0	2.020	1.940	1.940	[121]
63	Ferredoxin (bacterioferritin)	*Escherichia coli*	D	1.967	0	2.020	1.940	1.940	[122]
64	Nicotinate dehydrogenase I	*Eubacterium barkeri*	I	1.962	59	2.041	1.946	1.899	[123]
65	Nicotinate dehydrogenase II	*Eubacterium barkeri*	II	1.965	54	2.054	1.945	1.897	[123]
66	Complex I Nqo2 (TLF, N1a)	*Thermus thermophilus*	T	1.954	65	2.002	1.946	1.915	[124]
67	Complex I Nqo2 (TLF, N1a)	*Paracoccus denitrificans*	T	1.957	71	2.002	1.950	1.918	[124]
68	Quinoline 2-oxidoreductase I	*Pseudomonas putida*	I	1.961	70	2.035	1.950	1.898	[125]
69	Quinoline 2-oxidoreductase II	*Pseudomonas putida*	II	1.969	101	2.072	1.970	1.866	[125]
70	Isoquinoline 1-oxidoreductase I	*Pseudomonas diminuta*	I	1.958	50	2.010	1.945	1.919	[125]
71	Isoquinoline 1-oxidoreductase II	*Pseudomonas diminuta*	II	1.986	76	2.084	1.974	1.900	[125]
72	Quinaldine 4-oxidoreductase I	*Arthrobacter sp.* Rü61a	I	1.965	0	2.020	1.937	1.937	[125]
73	Quinaldine 4-oxidoreductase II	*Arthrobacter sp.* Rü61a	II	1.977	112	2.075	1.983	1.874	[125]
74	Aldehyde dehydrogenase I	*Comamonas testosteroni*	I	1.956	55	2.023	1.941	1.904	[126]
75	Aldehyde dehydrogenase II	*Comamonas testosteroni*	II	1.989	83	2.092	1.980	1.895	[126]

76	CO dehydrogenase I	*Hydrogenophaga pseudoflava*	I	1.958	65	2.023	1.947	1.905	[127]
77	CO dehydrogenase II	*Hydrogenophaga pseudoflava*	II	2.002	64	2.160	1.974	1.873	[127]
78	Ferrochelatase	*Xenopus laevis*	FC	1.950	65	2.003	1.941	1.907	[128]
79	Ferrochelatase	*Gallus gallus*	FC	1.948	73	2.003	1.941	1.901	[128]
80	FhuF	*Escherichia coli*	D	1.947	160	1.994	1.961	1.886	[129]
81	FeFe hydrogenase N-terminus	*Clostridium pasteurianum*	A	1.971	56	2.047	1.954	1.911	[130]
82	Alkene monooxygenase reductase	*Nocardia corallina* B-276	A	1.953	93	2.050	1.950	1.860	[131]
83	Ferredoxin 4 (TLF)	*Aquifex aeolicus*	T	1.958	67	2.006	1.950	1.918	[132]
84	NifU (stable 2Fe-2S)	*Azotobacter vinelandii*	A	1.946	48	2.019	1.927	1.892	[133]
85	NifU (stable 2Fe-2S)	*Helicobacter pylori*	A	1.950	42	2.017	1.930	1.902	[133]
86	Ferredoxin 3 dioxin dioxygenase	*Sphingomonas sp.* RW1	A	1.960	33	2.020	1.940	1.920	[134]
87	Ferredoxin	*Haloarcula japonica*	A	1.977	83	2.064	1.970	1.898	[135]
88	FeFe hydrogenase HydC (TLF)	*Thermotoga maritima*	T	1.954	77	2.000	1.949	1.914	[136]
89	Anthranilate 1,2-dioxygenase reductase	*Acinetobacter sp.* ADP1	A	1.967	87	2.070	1.960	1.870	[50]
90	Complex I 24 kDa (N1a)	*Escherichia coli*	T	1.957	61	2.001	1.948	1.921	[137]
91	Hydrogenase HndA (C-term.) TLF	*Desulfovibrio fructosovorans*	T	1.955	78	2.000	1.950	1.915	[138]
92	Hydrogenase HndD (N-term.)	*Desulfovibrio fructosovorans*	A	1.972	73	2.054	1.961	1.901	[138]
93	Succinate dehydrogenase (SdhC)	*Sulfolobus tokodaii*	A	1.955	55	2.028	1.938	1.898	[139]
94	Benzoate 1,2-dioxygenase reductase	*Pseudomonas putida*	A	1.960	78	2.050	1.950	1.880	[51]
95	Ferredoxin 1	*Aquifex aeolicus*	A	1.963	92	2.050	1.960	1.880	[140]
96	Ferredoxin 5	*Aquifex aeolicus*	A	1.959	8	2.021	1.931	1.926	[141]
97	Ferredoxin (ISC)	*Azotobacter vinelandii*	A	1.963	16	2.021	1.939	1.930	[141]
98	Ferredoxin (TLF)	*Thermotoga maritima*	T	1.956	74	2.000	1.950	1.917	[142]
99	Dihydroorotate dehydrogenase B	*Lactococcus lactis*	A	1.960	75	2.040	1.950	1.890	[143]
100	Complex 1 (NqrF)	*Vibrio cholerae*	A	1.962	0	2.018	1.934	1.934	[144]
101	NqrF (soluble)	*Vibrio cholerae*	A	1.965	0	2.020	1.938	1.938	[145]
102	Aldehyde oxidoreductase I	*Desulfovibrio gigas*	I	1.958	29	2.020	1.936	1.918	[146]
103	Aldehyde oxidoreductase II	*Desulfovibrio gigas*	II	1.975	84	2.061	1.969	1.896	[146]
104	Ferredoxin (dicamba *O*-demethylase)	*Pseudomonas maltophila*	A	1.961	0	2.017	1.933	1.933	[55]
105	Reductase (nitrotoluene dioxygenase)	*Acidovorax sp.* JS42	A	1.963	0	2.030	1.930	1.930	[57]
106	6-Hydroxynicotinate reductase	*Eubacterium barkeri*	A	1.949	85	2.046	1.942	1.860	[147]
107	Ferredoxin	*Haloferax mediterranei*	A	1.987	84	2.070	1.980	1.910	[148]
108	Ferredoxin (YfaE)	*Escherichia coli*	A	1.955	74	2.036	1.944	1.884	[149]
109	Complex I 24 kDa (N1a)	*Bos taurus*	T	1.955	58	2.004	1.945	1.917	[150]
110	Grx3 homodimer	*Saccharomyces cerevisiae*	D	1.970	0	2.030	1.940	1.940	[68]
111	Ferredoxin 1	*Sorangium cellulosum*	A	1.962	15	2.022	1.937	1.928	[151]
112	Ferredoxin 3 (TLF)	*Sorangium cellulosum*	T	1.959	103	2.000	1.960	1.918	[151]
113	Ferredoxin 5	*Sorangium cellulosum*	A	1.963	77	2.046	1.954	1.890	[151]
114	NiFe hydrogenase HoxU	*Synechocystis sp.* PCC6803	A	1.960	12	2.016	1.935	1.928	[152]
115	Activase	*Acetobacterium dehalogenans*	A	1.967	15	2.020	1.944	1.936	[153]
116	Ferredoxin	*Arthrospira platensis*	A	1.965	81	2.052	1.957	1.887	[154]

117	Fdx1 (adrenodoxin)	*Homo sapiens*	A	1.966	14	2.025	1.941	1.933	[3]
118	Fdx2 (ISC)	*Homo sapiens*	A	1.965	15	2.022	1.941	1.933	[3]
119	Complex I (N1b)	*Bos taurus*	A	1.963	20	2.023	1.939	1.927	[155]
120	Ferredoxin	*Mastigocladus laminosus*	A	1.964	86	2.050	1.958	1.884	[69]
121	MitoNEET H87C main species	*Homo sapiens*	D	1.965	145	2.005	1.974	1.916	[69]
122	MitoNEET H87C second species	*Homo sapiens*	D	1.950	156	1.993	1.962	1.895	[69]
123	Ferredoxin 2	*Arabidopsis thaliana*	A	1.963	69	2.050	1.950	1.890	[156]
124	Ferredoxin C1	*Arabidopsis thaliana*	A	1.957	55	2.030	1.940	1.900	[156]
125	Ferredoxin reductase (tetralin)	*Sphingomonas macrogolitabida*	A	1.960	75	2.040	1.950	1.890	[157]
126	Ferredoxin	*Rhodopseudomonas palustris*	A	1.963	0	2.023	1.933	1.933	[158]
127	Glrx3-A homodimer	*Homo sapiens*	A	1.967	0	2.020	1.940	1.940	[70]
128	Glrx3-B homodimer	*Homo sapiens*	D	1.967	115	2.010	1.970	1.920	[70]
129	Glrx3-AB homodimer	*Homo sapiens*	D	1.957	75	2.010	1.950	1.910	[70]
130	IscA (nif)	*Azotobacter vinelandii*	D	1.967	115	2.010	1.970	1.920	[159]
131	CsmI	*Chlorobaculum tepidum*	A	1.963	24	2.017	1.942	1.929	[160]
132	CsmJ	*Chlorobaculum tepidum*	A	1.962	4	2.019	1.935	1.933	[160]
133	CsmX	*Chlorobaculum tepidum*	A	1.958	7	2.011	1.933	1.929	[160]
134	Ciapin1 M1	*Homo sapiens*	D	1.960	100	2.000	1.960	1.920	[161]
135	NSP5	Rotavirus	D	1.953	136	1.990	1.960	1.910	[162]
136	Succinate dehydrogenase (ascorbate)	*Thermus thermophilus*	A	1.957	0	2.020	1.926	1.926	[163]
137	Succinate dehydrogenase (succinate)	*Thermus thermophilus*	A	1.955	21	2.027	1.927	1.912	[163]
138	SoxR	*Streptomyces coelicolor*	D	1.950	15	2.010	1.925	1.916	[164]
139	SoxR	*Pseudomonas aeruginosa*	D	1.948	41	2.011	1.930	1.904	[164]
140	Ciapin1 M2	*Homo sapiens*	D	1.940	71	2.010	1.930	1.880	[165]
141	PetF	*Synechocystis sp.* PCC6803	A	1.960	78	2.050	1.950	1.880	[166]
142	Dre2 M1 cluster	*Saccharomyces cerevisiae*	D	1.959	109	1.996	1.960	1.919	[167]
143	Grx4 homodimer	*Escherichia coli*	D	1.970	0	2.030	1.940	1.940	[73]
144	FeFe hydrogenase (HydC)	*Thermotoga maritima*	T	1.958	66	2.005	1.950	1.919	[168]
145	Opine dehydrogenase	*Bradyrhizobium japonicum*	D	1.964	45	2.006	1.952	1.933	[169]
146	Dde_3197	*Desulfovibrio desulfuricans* G20	D	1.957	69	2.000	1.950	1.920	[170]
147	ISCA1	*Mus musculus*	D	1.956	112	1.990	1.958	1.920	[171]
148	PqqE (AuxI)	*Methylobacterium extorquens*	D	1.956	107	2.005	1.958	1.906	[172]
149	Complex I (N1a)	*Escherichia coli*	T	1.958	61	1.999	1.950	1.925	[173]
150	Complex I (N1b)	*Escherichia coli*	A	1.969	0	2.028	1.940	1.940	[173]
151	Apd1 H255C/H259C main species	*Saccharomyces cerevisiae*	T	1.960	30	2.004	1.945	1.932	This work
152	Apd1 H255C/H259C minor species	*Saccharomyces cerevisiae*	T	1.962	88	2.006	1.959	1.920	This work

Table S5. Mössbauer parameters of biological $[2Fe\text{-}2S]^{2+}$ clusters

Data of Dunham *et al.* were referred to ^{57}Co diffused into platinum[174] and were corrected by addition of 0.34 mm/s.[175] Occupancy 100 % indicates identical parameters for the two ferric sites, 50% indicates two different ferric sites.

Proteins with all cysteinyl coordinated $[2Fe\text{-}2S]^{2+}$ clusters											
	Protein	Organism	T (K)	δ (mm/s)	ΔE_Q (mm/s)	η	δ (mm/s)	ΔE_Q (mm/s)	η	Occu-pancy (%)	Ref.
1	Putidaredoxin	*Pseudomonas putida*	4.2	0.27	0.596	n.r.	0.27	0.596	n.r.	100	[176]
			100	0.19	0.597	n.r.	0.19	0.597	n.r.	100	[176]
			200	0.18	0.594	n.r.	0.18	0.594	n.r.	100	[176]
			250	0.18	0.592	n.r.	0.18	0.592	n.r.	100	[176]
2	Spinach	*Spinacea oleracea*	4.2	0.26	0.65	0.5	0.26	0.65	0.5	100	[174]
3	Parsley	*Petroselinum crispum*	4.2	0.27	0.66	0.5	0.27	0.66	0.5	100	[174]
4	Adrenodoxin	*Sus scrofa domesticus*	4.2	0.285	0.622	n.r.	0.285	0.622	n.r.	100	[177]
			77	0.263	0.632	n.r.	0.263	0.632	n.r.	100	[177]
			197	0.222	0.614	n.r.	0.222	0.614	n.r.	100	[177]
5	Adrenodoxin	*Sus scrofa domesticus*	4.2	0.26	0.61	0.5	0.26	0.61	0.5	100	[174]
6	Ferredoxin (TLF)	*Clostridium pasteurianum*	4.2	0.27	0.62	0.5	0.27	0.62	0.5	100	[174]
7	Shethna I (TLF)	*Azotobacter vinelandii*	4.2	0.30	0.73	0.5	0.30	0.73	0.5	100	[174]
8	Shethna II (adr.)	*Azotobacter vinelandii*	4.2	0.28	0.71	0.5	0.28	0.71	0.5	100	[174]
9	Putidaredoxin	*Pseudomonas putida*	4.2	0.27	0.602	0.42	0.27	0.602	0.42	100	[178]
			150	0.18	0.595	n.r.	0.18	0.595	n.r.	100	[178]
10	Ferredoxin	*Synechococcus lividus*	4.2	0.26	0.55	n.r.	0.26	0.83	0.5	50	[89]
11	Ferredoxin	*Halobacterium sp.*	4.2	0.250	0.472	n.r.	0.290	0.87	n.r.	50	[179]
			82	0.232	0.480	n.r.	0.272	0.87	n.r.	50	[179]
			220	0.190	0.500	n.r.	0.225	0.90	n.r.	50	[179]
12	Aldehyde oxidoreductase	*Desulfovibrio gigas*	4.2	0.27	0.62	n.r.	0.27	0.62	n.r.	100	[180]
			180	0.25	0.70	n.r.	0.25	0.70	n.r.	100	[180]
13	Methane monooxygenase reductase	*Methylosinus trichosporium*	4.2	0.27	0.50	0.6	0.29	0.80	1.0	50	[114]
14	Ferrochelatase	*Mus musculus*	4.2	0.28	0.69	0.6	0.28	0.69	0.6	100	[120]
15	FNR	*Escherichia coli*	4.2	0.26	0.62	n.r.	0.28	0.58	n.r.	50	[181]

16	FhuF	*Escherichia coli*	4.2	0.287	0.474	n.r.	0.287	0.474	n.r.	100	[129]
			190	0.222	0.458	n.r.	0.222	0.458	n.r.	100	[129]
17	4-Hydroxyben-zoyl-CoA reductase	*Thauera aromatica*	4.2	0.29	0.61	0.5	0.29	0.61	0.5	100	[182]
18	IscA	*Azotobacter vinelandii*	4.2	0.26	0.55	n.r.	0.26	0.55	n.r.	100	[183]
19	Isa1	*Schizosaccharomyces pombe*	4.2	0.27	0.56	n.r.	0.27	0.56	n.r.	100	[184]
20	Benzoate dioxygenase reductase	*Pseudomonas putida*	4.2	0.27	0.55	n.r.	0.28	0.86	n.r.	50	[51]
21	Ferredoxin I (plant-type)	*Aquifex aeolicus*	4.2	0.26	0.62	0.7	0.28	0.76	0.7	50	[140]
22	Isc-Ferredoxin (Fd5)	*Aquifex aeolicus*	4.2	0.28	0.44	0.75	0.29	0.62	0.75	50	[141]
23	SufA	*Erwinia chrysanthemi*	4.2	0.27	0.59	n.r.	0.27	0.59	n.r.	100	[185]
24	IscA	*Synechocystis sp.* PCC 6803	80	0.27	0.57	n.r.	0.27	0.57	n.r.	100	[186]
25	NqrF	*Vibrio cholerae*	80	0.283	0.61	n.r.	0.283	0.61	n.r.	100	[187]
26	NifU (permanent)	*Azotobacter vinelandii*	4.2	0.27	0.59	n.r.	0.28	0.37	n.r.	50	[188]
27	Grx2 (mitochondrial)	*Homo sapiens*	4.2	0.27	0.61	0.6	0.27	0.61	0.6	100	[189]
			80	0.27	0.60	n.r.	0.27	0.60	n.r.	100	[189]
28	YfaE (4 Cys)	*Escherichia coli*	4.2	0.28	0.58	n.r.	0.28	0.58	n.r.	100	[149]
29	GrxS14	*Populus sp.*	4.2	0.26	0.56	n.r.	0.28	0.76	n.r.	50	[190]
30	GrxC1	*Populus sp.*	4.2	0.27	0.54	n.r.	0.28	0.76	n.r.	50	[190]
31	Grx3	*Saccharomyces cerevisiae*	4.2	0.29	0.55	n.r.	0.29	0.76	n.r.	50	[68]
32	SufA	*Escherichia coli*	4.2	0.28	0.53	n.r.	0.28	0.53	n.r.	100	[191]
33	Ferredoxin (C-term. domain)	*Schizosaccharomyces pombe*	100	0.33	0.59	n.d.	0.33	0.59	n.r.	100	[192]
34	APS reductase (breakdown)	*Mycobacterium tuberculosis*	4.2	0.25	0.55	n.r.	0.25	0.55	n.r.	100	[193]
35	IscA (Nif)	*Azotobacter vinelandii*	4.2	0.27	0.50	n.r.	0.28	0.68	n.r.	50	[159]
36	PAPS reductase (breakdown)	*Escherichia coli*	4.2	0.27	0.57	n.r.	0.27	0.57	n.r.	100	[194]
37	Grx2	*Danio rerio*	80	0.29	0.40	n.r.	0.29	0.40	n.r.	100	[195]

38	Nfu2	*Arabidopsis thaliana*	4.2	0.27	0.43	n.r.	0.27	0.70	n.r.	50	[196]
39	Ferredoxin VI	*Rhodobacter capsulatus*	4.2	0.272	0.52	n.r.	0.274	0.75	n.r.	50	[197]
40	TtcA (breakdown)	*Escherichia coli*	4.2	0.27	0.49	n.r.	0.27	0.49	n.r.	100	[198]
41	Endonuclease III (breakdown)	*Escherichia coli*	180	0.25	0.59	n.r.	0.25	0.59	n.r.	100	[199]
42	Yap5	*Saccharomyces cerevisiae*	80	0.31	0.50	n.r.	0.31	0.50	n.r.	67	[200]
43	HydC (TLF)	*Thermotoga maritima*	80	0.29	0.54	n.r.	0.31	0.86	n.r.	50	[168]
44	PqqE Radical SAM	*Methylobacterium extorquens*	4.2	0.32	0.49	n.r.	0.32	0.49	n.r.	100	[201]
45	RicAFT complex after O_2 exp.	*Bacillus subtilis*	4.2	0.30	0.52	n.r.	0.30	0.52	n.r.	100	[202]
46	ISCA1	*Mus musculus*	4.2	0.27	0.53	n.r.	0.27	0.53	n.r.	100	[171]
47	ISCA2	*Mus musculus*	4.2	0.28	0.50	n.r.	0.28	0.50	n.r.	100	[171]
48	PqqE Radical SAM (breakdown)	*Methylobacterium extorquens*	4.2	0.327	0.521	n.r.	0.327	0.521	n.r.	100	[172]
49	SkfB	*Bacillus subtilis*	4.2	0.29	0.55	n.r.	0.29	0.55	n.r.	100	[203]
50	SkfB (RS mutant)	*Bacillus subtilis*	4.2	0.28	0.58	n.r.	0.28	0.58	n.r.	100	[203]
51	Apd1 H255C/H259C	*Saccharomyces cerevisiae*	5	0.26	0.39	0.5	0.28	0.58	0.4	50	This work
Proteins with monohistidinyl coordinated $[2Fe\text{-}2S]^{2+}$ clusters											
	Protein	Organism	T (K)	δ (mm/s)	ΔE_Q (mm/s)	η	δ (mm/s)	ΔE_Q (mm/s)	η	Occupancy (%)	Ref.
1	IscU (fraction 2) pH 7.8	*Azotobacter vinelandii*	4.2	0.26	0.64	1.0	0.32	0.91	0.7	50	[204]
2	IscU (fraction 3) pH 7.8	*Azotobacter vinelandii*	4.2	0.27	0.66	1.0	0.32	0.94	0.7	50	[204]
3	IscU (breakdown) pH 7.4	*Azotobacter vinelandii*	4.2	0.27	0.56	n.r.	0.32	0.84	n.r.	50	[205]
4	NifU (IscU-like N-terminus)	*Azotobacter vinelandii*	4.2	0.29	0.73	n.r.	0.29	0.50	n.r.	50	[188]
5	NifU (IscU-like N-terminus D37A)	*Azotobacter vinelandii*	4.2	0.27	0.48	n.r.	0.28	0.68	n.r.	50	[188]
6	ISCU2	*Homo sapiens*	5	0.30	0.70	n.r.	0.30	0.70	n.r.	100	[206]

7	Grx3-Fra2 TRIS/MES pH 8.0	*Saccharomyces cerevisiae*	4.2	0.30	0.50	n.r.	0.32	0.82	n.r.	50	[68]
8	IscR Tris pH 7.4	*Escherichia coli*	4.2	0.27	0.48	0.5	0.30	0.72	0.5	50	[207]
9	MitoNEET (KPi, pH 8.0)	*Homo sapiens*	4.2	0.26	0.47	n.r.	0.30	0.96	n.r.	50	[208]
10	MitoNEET (KPi, pH 8.0)	*Homo sapiens*	4.2	0.26	0.47	n.r.	0.30	0.96	n.r.	50	[209]
11	RscR (pH 8.0)	*Streptomyces venezuelae*	6	0.285	0.545	n.r.	0.289	0.761	n.r.	50	[210]
12	Apd1 H255C pH 9.0	*Saccharomyces cerevisiae*	4.2	0.24	0.43	0.5	0.30	0.77	0.5	50	This work
13	Apd1 H259C pH 9.0	*Saccharomyces cerevisiae*	4.2	0.24	0.45	0.5	0.31	0.95	0.4	50	This work
Proteins with bis-histidinyl coordinated $[2Fe\text{-}2S]^{2+}$ clusters											
	Protein	Organism	T (K)	δ (mm/s)	ΔE_Q (mm/s)	η	δ (mm/s)	ΔE_Q (mm/s)	η	Occupancy (%)	Ref.
1	Rieske cytochrome b_6f	*Spinacea oleracea*	4.2	0.25	0.70	n.r.	0.35	0.90	n.r.	50	[211]
2	Rieske cytochrome b_6f	*Spinacea oleracea*	190	0.15	0.70	n.r.	0.25	0.90	n.r.	50	[211]
3	Rieske benzene dioxygenase	*Pseudomonas putida*	77	0.23	0.45	n.r.	0.33	1.03	n.r.	50	[212]
4	Rieske benzene dioxygenase	*Pseudomonas putida*	195	0.18	0.44	n.r.	0.29	1.03	n.r.	50	[212]
5	Rieske benzoate dioxygenase	*Pseudomonas putida*	4.2	0.24	0.51	n.r.	0.35	1.05	n.r.	50	[51]
6	Rieske Fd of toluene-4-monooxygenase	*Pseudomonas mendocina*	4.2	0.24	0.51	n.r.	0.35	1.12	n.r.	50	[25]
7	Rieske (diprot)	*Thermus thermophilus*	77	0.23	0.57	n.r.	0.34	1.05	n.r.	50	[213]
8	Rieske (monoprot)	*Thermus thermophilus*	77	0.25	0.46	n.r.	0.29	0.78	n.r.	50	[213]
9	Rieske (deprot)	*Thermus thermophilus*	77	0.25	0.44	n.r.	0.29	0.71	n.r.	50	[213]
10	Apd1 (diprot)	*Saccharomyces cerevisiae*	5	0.23	0.57	n.r.	0.36	1.11	n.r.	50	This work
11	Apd1 (monoprot)	*Saccharomyces cerevisiae*	5	0.24	0.54	n.r.	0.35	1.05	n.r.	50	This work
12	Apd1 (deprot)	*Saccharomyces cerevisiae*	5	0.24	0.51	n.r.	0.31	0.94	n.r.	50	This work
13	Rieske ox pH 7.8	*Thermus thermophilus*	4.2	0.24	0.52	n.r.	0.32	0.91	n.r.	50	[214]

14	Rieske ox pH 7.8	*Thermus thermophilus*	200	0.185	0.52	n.r.	0.265	0.91	n.r.	50	[214]
15	Rieske ox pH 10	*Thermus thermophilus*	4.2	0.24	0.44	n.r.	0.28	0.70	n.r.	50	[11]

Table S6. Mössbauer parameters of biological $[2Fe\text{-}2S]^{1+}$ clusters.

Data of Dunham *et al*. were referred to ^{57}Co diffused into platinum[174] and were corrected by addition of 0.34 mm/s.[175] Entry 6, values as listed by [214]. In entry 10, δ and η were swapped in Table 2 and assignment of parameters to individual $[2Fe\text{-}2S]^{1+}$ clusters not stated.[180]

Proteins with all cysteinyl coordinated $[2Fe\text{-}2S]^{1+}$ clusters								
	Protein	Organism	T (K)	δ (mm/s)	ΔE_Q (mm/s)	δ (mm/s)	ΔE_Q (mm/s)	Ref.
1	Spinach ferrredoxin	*Spinacea oleracea*	4.2	0.24	0.64	0.53	-3.00	[174]
			250	0.28	0.64	0.55	-2.63	[174]
2	Parsley ferredoxin	*Petroselinum crispum*	4.2	0.24	0.68	0.53	-3.00	[174]
			250	0.28	0.68	0.57	-2.77	[174]
3	Adrenodoxin	*Sus scrofa domestica*	250	0.27	0.81	0.53	2.72	[174]
4	Ferredoxin	*Scenedesmus sp.*	195	0.22	0.59	0.56	2.75	[215]
5	Spinach ferredoxin	*Spinacea oleracea*	195	0.22	0.59	0.56	2.75	[215]
6	Putidaredoxin	*Pseudomonas putida*	4.2	0.35	0.60	0.65	-2.70	[178]
7	Ferredoxin	*Halobacterium sp.*	200	0.30	0.60	0.55	2.64	[179]
8	Ferredoxin	*Synechococcus lividus*	200	0.25	n.r.	0.57	n.r.	[214]
9	Methane mono-oxygenase reductase	*Methylosinus trichosporium*	4.2	0.31	0.59	0.65	-3.00	[114]
10	Aldehyde oxido-reductase	*Desulfovibrio gigas*	4.2	0.30	1.00	0.62	-3.60	[180]
			85	n.r.	Indep.	n.r.	2.93	[180]
			85	n.r.	Indep.	n.r.	3.42	[180]
			180	0.24	0.42	0.57	2.69	[180]
			180	0.28	0.97	0.55	3.14	[180]
11	Ferrochelatase	*Mus musculus*	4.2	0.28	1.20	0.67	+3.3	[120]
12	FhuF	*Escherichia coli*	190	0.298	0.978	0.584	3.03	[129]
13	Benzoate dioxygenase reductase	*Pseudomonas putida*	4.2	0.30	0.80	0.65	-3.00	[51]
14	Ferredoxin I (plant-type)	*Aquifex aeolicus*	4.2	0.30	1.00	0.62	3.0	[140]
15	Isc-Ferredoxin (Fd5)	*Aquifex aeolicus*	4.2	0.32	0.80	0.65	2.9	[141]
			200	n.d.	n.d.	0.58	2.9	[141]
16	YfaE (4 Cys)	*Escherichia coli*	4.2	0.33	0.78	0.60	-3.13	[149]
			210	0.25	0.75	0.57	2.82	[149]
Proteins with monohistidinyl coordinated $[2Fe\text{-}2S]^{1+}$ clusters								
	Protein	Organism	T (K)	δ (mm/s)	ΔE_Q (mm/s)	δ (mm/s)	ΔE_Q (mm/s)	Ref.
1	IscR (pH 7.4)	*Escherichia coli*	4.2	0.33	1.09	0.70	-3.40	[207]
2	MitoNEET (pH 8.0)	*Homo sapiens*	4.2	0.32	1.07	0.68	3.15	[209]
Proteins with bis-histidinyl coordinated $[2Fe\text{-}2S]^{1+}$ clusters								
	Protein	Organism	T (K)	δ (mm/s)	ΔE_Q (mm/s)	δ (mm/s)	ΔE_Q (mm/s)	Ref.
1	Rieske cytochrome *b6f*	*Spinacea oleracea*	4.2	0.25	0.70	0.73	-2.95	[211]
			190	0.15	0.66	0.64	2.69	[211]
2	Rieske benzene dioxygenase	*Pseudomonas putida*	195	0.25	0.70	0.68	2.94	[212]

3	Rieske in 4-methoxybenzoate monoxygenase	*Pseudomonas putida*	150	0.25	0.70	0.70	3.04	[216]
4	Rieske	*Thermus thermophilus*	4.2	0.31	0.63	0.74	3.05	[214]
			195	n.r.	Indep.	n.r.	2.90	[214]
			230	0.22	0.61	0.65	2.81	[214]
5	Rieske benzoate dioxygenase	*Pseudomonas putida*	4.2	0.30	0.65	0.75	-3.20	[51]
			195	0.23	0.65	0.68	2.99	[51]
6	Rieske Fd of toluene-4-monooxygenase	*Pseudomonas mendocina*	4.2	0.30	0.71	0.72	-3.07	[25]
			200	0.25	0.68	n.r.	n.r.	[25]
7	Apd1	*Saccharomyces cerevisiae*	4.2	0.32	0.81	0.75	-3.16	This work
			230	0.24	0.79	0.67	3.00	This work

References

(1) Corpet, F., *Nucleic Acids Res.* **1988,** *16*, 10881-10890.

(2) Kounosu, A.; Iwasaki, T.; Baba, S.; Hayashi-Iwasaki, Y.; Oshima, T.; Kumasaka, T., *Acta Crystallogr. Sect. F Struct. Biol. Cryst. Commun.* **2008,** *64*, 1146-1148.

(3) Sheftel, A. D.; Stehling, O.; Pierik, A. J.; Elsässer, H. P.; Mühlenhoff, U.; Webert, H.; Hobler, A.; Hannemann, F.; Bernhardt, R.; Lill, R., *Proc. Natl. Acad. Sci. U. S. A.* **2010,** *107*, 11775-11780.

(4) Iwasaki, T.; Isogai, Y.; Iizuka, T.; Oshima, T., *J. Bacteriol.* **1995,** *177*, 2576-2582.

(5) Kelley, L. A.; Mezulis, S.; Yates, C. M.; Wass, M. N.; Sternberg, M. J., *Nat. Protoc.* **2015,** *10*, 845-858.

(6) Link, T. A., The structures of Rieske and Rieske-type proteins. In *Advances in Inorganic Chemistry 47*, Sykes, A. G.; Cammack, R., Eds. Academic Press: San Diego, 1999; Vol. 47, pp 83-157.

(7) Link, T. A.; Saynovits, M.; Assmann, C.; Iwata, S.; Ohnishi, T.; Von Jagow, G., *Eur. J. Biochem.* **1996,** *237*, 71-75.

(8) De Vries, S. P. J.; Cherepanov, A.; Berg, A.; Canters, G. W., *Inorg. Chim. Acta* **1998,** *275-276*, 493-499.

(9) Ding, H.; Robertson, D. E.; Daldal, F.; Dutton, P. L., *Biochemistry* **1992,** *31*, 3144-3158.

(10) Zhang, H.; Carrell, C. J.; Huang, D.; Sled, V.; Ohnishi, T.; Smith, J. L.; Cramer, W. A., *J. Biol. Chem.* **1996,** *271*, 31360-31366.

(11) Kuila, D.; Fee, J. A., *J. Biol. Chem.* **1986,** *261*, 2768-2771.

(12) Cline, J. F.; Hoffman, B. M.; Mims, W. B.; LaHaie, E.; Ballou, D. P.; Fee, J. A., *J. Biol. Chem.* **1985,** *260*, 3251-3254.

(13) Schmidt, C. L.; Anemüller, S.; Teixeira, M.; Schäfer, G., *FEBS Lett.* **1995,** *359*, 239-243.

(14) Schmidt, C. L.; Hatzfeld, O. M.; Petersen, A.; Link, T. A.; Schäfer, G., *Biochem. Biophys. Res. Commun.* **1997,** *234*, 283-287.

(15) Holton, B.; Wu, X.; Tsapin, A. I.; Kramer, D. M.; Malkin, R.; Kallas, T., *Biochemistry* **1996,** *35*, 15485-15493.

(16) De Vries, S.; Albracht, S. P. J.; Berden, J. A.; Marres, C. A.; Slater, E. C., *Biochim. Biophys. Acta* **1983,** *723*, 91-103.

(17) Ohnishi, T.; Meinhardt, S. W.; von Jagow, G.; Yagi, T.; Hatefi, Y., *FEBS Lett.* **1994,** *353*, 103-107.

(18) Siedow, J. N.; Power, S.; de la Rosa, F. F.; Palmer, G., *J. Biol. Chem.* **1978,** *253*, 2392-2399.

(19) Yang, X. H.; Trumpower, B. L., *J. Biol. Chem.* **1986,** *261*, 12282-12289.

(20) Andrews, K. M.; Crofts, A. R.; Gennis, R. B., *Biochemistry* **1990,** *29*, 2645-2651.

(21) Liedl, U.; Rutherford, A. W.; Nitschke, W., *FEBS Lett.* **1990,** *261*, 427-430.

(22) Riedel, A.; Kellner, E.; Grodzitzki, D.; Liebl, U.; Hauska, G.; Müller, A.; Rutherford, A. W.; Nitschke, W., *Biochim. Biophys. Acta* **1993,** *1183*, 263-268.

(23) Riedel, A.; Rutherford, A. W.; Hauska, G.; Müller, A.; Nitschke, W., *J. Biol. Chem.* **1991,** *266*, 17838-17844.

(24) Geary, P. J.; Saboowalla, F.; Patil, D.; Cammack, R., *Biochem. J.* **1984,** *217*, 667-673.

(25) Pikus, J. D.; Studts, J. M.; Achim, C.; Kauffmann, K. E.; Münck, E.; Steffan, R. J.; McClay, K.; Fox, B. G., *Biochemistry* **1996,** *35*, 9106-9119.

(26) Haddock, J. D.; Pelletier, D. A.; Gibson, D. T., *J. Ind. Microbiol. Biotechnol.* **1997,** *19*, 355-359.

(27) Sauber, K.; Fröhner, C.; Rosenberg, G.; Eberspächer, J.; Lingens, F., *Eur. J. Biochem.* **1977,** *74*, 89-97.

(28) Twilfer, H.; Bernhardt, F. H.; Gersonde, K., *Eur. J. Biochem.* **1981,** *119*, 595-602.

(29) Suen, W.-C.; Gibson, D. T., *J. Bacteriol.* **1985,** *175*, 5877-5881.

(30) Riedel, A.; Fetzner, S.; Rampp, M.; Lingens, F.; Liebl, U.; Zimmermann, J. L.; Nitschke, W., *J. Biol. Chem.* **1995,** *270*, 30869-30873.
(31) Rosche, B.; Fetzner, S.; Lingens, F.; Nitschke, W.; Riedel, A., *Biochim. Biophys. Acta* **1995,** *1252*, 177-179.
(32) Dikanov, S. A.; Xun, L.; Karpiel, A. B.; Tyryshkin, A. M.; Bowman, M. K., *J. Am. Chem. Soc.* **1986,** *118*, 8408-8416.
(33) Schlenzska, W.; Shaw, L.; Kelm, S.; Schmidt, C. L.; Bill, E.; Trautwein, A. X.; Lottspeich, F.; Schauer, R., *FEBS Lett.* **1986,** *385*, 197-200.
(34) Small, F. J.; Ensign, S. A., *J. Biol. Chem.* **1997,** *272*, 24913-24920.
(35) Rathinasabapathi, B.; Burnet, M.; Russell, B. L.; Gage, D. A.; Liao, P. C.; Nye, G. J.; Scott, P.; Golbeck, J. H.; Hanson, A. D., *Proc. Natl. Acad. Sci. U. S. A.* **1997,** *94*, 3454-3458.
(36) Subramanian, V.; Liu, T. N.; Yeh, W. K.; Serdar, C. M.; Wackett, L. P.; Gibson, D. T., *J. Biol. Chem.* **1985,** *260*, 2355-2363.
(37) Seez, M. Elektronenspinresonanz und immunologische Untersuchungen an der Chlorphenylessigsäure-Dioxygenase aus *Pseudomonas* species CBS3. PhD, University of Hohenheim, Hohenheim, 1989.
(38) Güner, S.; Robertson, D. E.; Yu, L.; Qiu, Z. H.; Yu, C. A.; Knaff, D. B., *Biochim. Biophys. Acta* **1991,** *1058*, 269-279.
(39) Anderson, G. L.; Williams, J.; Hille, R., *J. Biol. Chem.* **1992,** *267*, 23674-23682.
(40) Liebl, U.; Pezennec, S.; Riedel, A.; Kellner, E.; Nitschke, W., *J. Biol. Chem.* **1992,** *267*, 14068-14072.
(41) Romanov, V.; Hausinger, R. P., *J Bacteriol* **1994,** *176*, 3368-3374.
(42) Haddock, J. D.; Gibson, D. T., *J. Bacteriol.* **1995,** *177*, 5834-5839.
(43) Gurbiel, R. J.; Doan, P. E.; Gassner, G. T.; Macke, T. J.; Case, D. A.; Ohnishi, T.; Fee, J. A.; Ballou, D. P.; Hoffman, B. M., *Biochemistry* **1996,** *35*, 7834-7845.
(44) Dikanov, S. A.; Davydov, R. M.; Xun, L.; Bowman, M. K., *J. Magn. Reson. B* **1996,** *112*, 289-294.
(45) Junker, F.; Saller, E.; Schläfli Oppenberg, H. R.; Kroneck, P. M. H.; Leisinger, T.; Cook, A. M., *Microbiology* **1996,** *142*, 2419-2427.
(46) Junker, F.; Kiewitz, R.; Cook, A. M., *J. Bacteriol.* **1997,** *179*, 919-927.
(47) Gomes, C. M.; Huber, H.; Stetter, K. O.; Teixeira, M., *FEBS Lett.* **1998,** *432*, 99-102.
(48) Henninger, T.; Anemüller, S.; Fitz-Gibbon, S.; Miller, J. H.; Schäfer, G.; Schmidt, C. L., *J. Bioenerg. Biomembr.* **1999,** *31*, 119-128.
(49) Jiang, H.; Parales, R. E.; Gibson, D. T., *Appl. Environ. Microbiol.* **1999,** *65*, 315-318.
(50) Eby, D. M.; Beharry, Z. M.; Coulter, E. D.; Kurtz, D. M., Jr.; Neidle, E. L., *J. Bacteriol.* **2001,** *183*, 109-118.
(51) Wolfe, M. D.; Altier, D. J.; Stubna, A.; Popescu, C. V.; Münck, E.; Lipscomb, J. D., *Biochemistry* **2002,** *41*, 9611-9626.
(52) Iwasaki, T.; Kounosu, A.; Uzawa, T.; Samoilova, R. I.; Dikanov, S. A., *J. Am. Chem. Soc.* **2004,** *126*, 13902-13903.
(53) Kounosu, A.; Li, Z.; Cosper, N. J.; Shokes, J. E.; Scott, R. A.; Imai, T.; Urushiyama, A.; Iwasaki, T., *J. Biol. Chem.* **2004,** *279*, 12519-12528.
(54) Kletzin, A.; Ferreira, A. S.; Hechler, T.; Bandeiras, T. M.; Teixeira, M.; Gomes, C. M., *FEBS Lett.* **2005,** *579*, 1020-1026.
(55) Chakraborty, S.; Behrens, M.; Herman, P. L.; Arendsen, A. F.; Hagen, W. R.; Carlson, D. L.; Wang, X. Z.; Weeks, D. P., *Arch. Biochem. Biophys.* **2005,** *437*, 20-28.
(56) Ouchane, S.; Nitschke, W.; Bianco, P.; Vermeglio, A.; Astier, C., *Mol. Microbiol.* **2005,** *57*, 261-275.
(57) Parales, R. E.; Huang, R.; Yu, C. L.; Parales, J. V.; Lee, F. K.; Lessner, D. J.; Ivkovic-Jensen, M. M.; Liu, W.; Friemann, R.; Ramaswamy, S.; Gibson, D. T., *Appl. Environ. Microbiol.* **2005,** *71*, 3806-3814.
(58) Jouanneau, Y.; Meyer, C.; Jakoncic, J.; Stojanoff, V.; Gaillard, J., *Biochemistry* **2006,** *45*, 12380-12391.
(59) Yu, C. L.; Liu, W.; Ferraro, D. J.; Brown, E. N.; Parales, J. V.; Ramaswamy, S.; Zylstra, G. J.; Gibson, D. T.; Parales, R. E., *J. Ind. Microbiol. Biotechnol.* **2007,** *34*, 311-324.
(60) Boxhammer, S.; Glaser, S.; Kühl, A.; Wagner, A. K.; Schmidt, C. L., *Biometals* **2008,** *21*, 459-467.
(61) Schoepp-Cothenet, B.; Lieutaud, C.; Baymann, F.; Vermeglio, A.; Friedrich, T.; Kramer, D. M.; Nitschke, W., *Proc. Natl. Acad. Sci. U. S. A.* **2009,** *106*, 8549-8554.
(62) Duval, S.; Santini, J. M.; Nitschke, W.; Hille, R.; Schoepp-Cothenet, B., *J. Biol. Chem.* **2010,** *285*, 20442-20451.
(63) Roret, T.; Tsan, P.; Couturier, J.; Zhang, B.; Johnson, M. K.; Rouhier, N.; Didierjean, C., *J. Biol. Chem.* **2014,** *289*, 24588-24598.
(64) Nagashima, H.; Kishimoto, H.; Mutoh, R.; Terashima, N.; Oh-Oka, H.; Kurisu, G.; Mino, H., *J. Phys. Chem. B* **2017,** *121*, 2543-2553.
(65) Bäckström, D.; Hoffström, I.; Gustafsson, I.; Ehrenberg, A., *Biochem. Biophys. Res. Commun.* **1973,** *53*, 596-602.

(66) Schwartz, C. J.; Giel, J. L.; Patschkowski, T.; Luther, C.; Ruzicka, F. J.; Beinert, H.; Kiley, P. J., *Proc. Natl. Acad. Sci. U. S. A.* **2001,** *98*, 14895-14900.
(67) Iwasaki, T.; Samoilova, R. I.; Kounosu, A.; Ohmori, D.; Dikanov, S. A., *J. Am. Chem. Soc.* **2009,** *131*, 13659-13667.
(68) Li, H.; Mapolelo, D. T.; Dingra, N. N.; Naik, S. G.; Lees, N. S.; Hoffman, B. M.; Riggs-Gelasco, P. J.; Huynh, B. H.; Johnson, M. K.; Outten, C. E., *Biochemistry* **2009,** *48*, 9569-9581.
(69) Dicus, M. M.; Conlan, A.; Nechushtai, R.; Jennings, P. A.; Paddock, M. L.; Britt, R. D.; Stoll, S., *J. Am. Chem. Soc.* **2010,** *132*, 2037-2049.
(70) Li, H.; Mapolelo, D. T.; Randeniya, S.; Johnson, M. K.; Outten, C. E., *Biochemistry* **2012,** *51*, 1687-1696.
(71) Sun, F.; Ji, Q.; Jones, M. B.; Deng, X.; Liang, H.; Frank, B.; Telser, J.; Peterson, S. N.; Bae, T.; He, C., *J. Am. Chem. Soc.* **2012,** *134*, 305-314.
(72) Munnoch, J. T.; Martinez, M. T.; Svistunenko, D. A.; Crack, J. C.; Le Brun, N. E.; Hutchings, M. I., *Sci Rep.* **2016,** *6*, 31597.
(73) Dlouhy, A. C.; Li, H.; Albetel, A. N.; Zhang, B.; Mapolelo, D. T.; Randeniya, S.; Holland, A. A.; Johnson, M. K.; Outten, C. E., *Biochemistry* **2016,** *55*, 6869-6879.
(74) Cheng, Z.; Landry, A. P.; Wang, Y.; Ding, H., *J. Biol. Chem.* **2017,** *292*, 3146-3153.
(75) Bertrand, P.; Gayda, J. P., *Biochim. Biophys. Acta* **1979,** *579*, 107-121.
(76) Bertrand, P.; Guigliarelli, B.; More, C., *New J. Chem.* **1981,** *15*, 445-454.
(77) Guigliarelli, B.; Bertrand, P., Application of EPR spectroscopy to the structural and functional study of iron-sulfur proteins. In *Advances in Inorganic Chemistry 47*, Sykes, A. G.; Cammack, R., Eds. Academic Press: San Diego, 1999; Vol. 47, pp 421-497.
(78) Orme-Johnson, W. H.; Hansen, R. E.; Beinert, H.; Tsibris, J. C. M.; Bartholomaus, R. C.; Gunsalus, I. C., *Proc. Natl. Acad. Sci. U. S. A.* **1968,** *60*, 368-372.
(79) Fritz, J.; Anderson, R.; Fee, J.; Palmer, G.; Sands, R. H.; Tsibris, J. C.; Gunsalus, I. C.; Orme-Johnson, W. H.; Beinert, H., *Biochim. Biophys. Acta* **1971,** *253*, 110-133.
(80) Chatelet, C.; Meyer, J., *J. Biol. Inorg. Chem.* **1999,** *4*, 311-317.
(81) DerVartanian, D. V.; Shethna, Y. I.; Beinert, H., *Biochim. Biophys. Acta* **1969,** *194*, 548-563.
(82) Coffman, R. E.; Stavens, B. W., *Biochem. Biophys. Res. Commun.* **1970,** *41*, 163-169.
(83) Petering, D. H.; Palmer, G., *Arch. Biochem. Biophys.* **1970,** *141*, 456-464.
(84) Cammack, R.; Rao, K. K.; Hall, D. O., *Biochem. Biophys. Res. Commun.* **1971,** *44*, 8-14.
(85) Fee, J. A.; Palmer, G., *Biochim. Biophys. Acta* **1971,** *245*, 175-195.
(86) Hall, D. O.; Cammack, R.; Rao, K. K., *Pure Appl. Chem* **1973,** *34*, 553-577.
(87) Mukai, K.; Kimura, T.; Helbert, J.; Kevan, L., *Biochim. Biophys. Acta* **1973,** *295*, 49-56.
(88) Rao, K. K.; Smith, R. V.; Cammack, R.; Evans, M. C. W.; Hall, D. O., *Biochem. J.* **1972,** *129*, 1159-1162.
(89) Anderson, R. E.; Dunham, W. R.; Sands, R. H.; Bearden, A. J.; Crespi, H. L., *Biochim. Biophys. Acta* **1975,** *408*, 306-318.
(90) Meinhardt, S. W.; Kula, T.; Yagi, T.; Lillich, T.; Ohnishi, T., *J. Biol. Chem.* **1987,** *262*, 9147-9153.
(91) Johnson, M. K.; Morningstar, J. E.; Cecchini, G.; Ackrell, B. A., *Biochem. Biophys. Res. Commun.* **1985,** *131*, 653-658.
(92) Johnson, M. K.; Morningstar, J. E.; Kearney, E. B.; Cecchini, G.; Ackrell, B. A. C., The iron-sulfur clusters in succinate dehydrogenase. In *Cytochrome systems: molecular biology and bioenergetics*, Papa, S.; Chance, B.; Ernster, L., Eds. Plenum Press: New York, 1987; pp 473-484.
(93) Ohmori, D.; Hasumi, H.; Yamakura, F.; Murakami, M.; Fujisawa, K.; Taneoka, Y.; Yamamura, T., *Biochim. Biophys. Acta* **1989,** *996*, 16-172.
(94) Crouse, B. R.; Sellers, V. M.; Finnegan, M. G.; Dailey, H. A.; Johnson, M. K., *Biochemistry* **1996,** *35*, 16222-16229.
(95) De Luca, G.; Asso, M.; Belaich, J. P.; Dermoun, Z., *Biochemistry* **1998,** *37*, 2660-2665.
(96) Batie, C. J.; LaHaie, E.; Ballou, D. P., *J. Biol. Chem.* **1987,** *262*, 1510-1518.
(97) Aleman, V.; Handler, P.; Palmer, G.; Beinert, H., *J. Biol. Chem.* **1968,** *243*, 2560-2568.
(98) Beinert, H.; Ackrell, B. A.; Kearney, E. B.; Singer, T. P., *Eur. J. Biochem.* **1975,** *54*, 185-194.
(99) Andrew, P. W.; Rogers, L. J.; Boulter, D.; Haslett, B. G., *Eur. J. Biochem.* **1976,** *69*, 243-248.
(100) Barber, M. J.; Bray, R. C.; Lowe, D. J.; Coughlan, M. P., *Biochem. J.* **1976,** *153*, 297-307.
(101) Kerscher, L.; Oesterhelt, D.; Cammack, R.; Hall, D. O., *Eur. J. Biochem.* **1976,** *71*, 101-107.
(102) Albracht, S. P. J.; Subramanian, J., *Biochim. Biophys. Acta* **1977,** *462*, 36-48.
(103) Colby, J.; Dalton, H., *Biochem. J.* **1979,** *177*, 903-908.
(104) Hagen, W. R.; Albracht, S. P. J., *Biochim. Biophys. Acta* **1982,** *702*, 61-71.
(105) Barber, M. J.; Coughlan, M. P.; Rajagopalan, K. V.; Siegel, L. M., *Biochemistry* **1982,** *21*, 3561-3568.

(106) Hille, R.; Hagen, W. R.; Dunham, W. R., *J. Biol. Chem.* **1985,** *260*, 10569-10575.
(107) Patel, R. C.; Prince, R. N., *FEBS Lett.* **1986,** *206*, 127-130.
(108) Schweizer, D.; Markus, A.; Seez, M.; Ruf, H. H.; Lingens, F., *J. Biol. Chem.* **1987,** *262*, 9340-9346.
(109) Bryant, F. O.; Adams, M. W. W., *J. Biol. Chem.* **1989,** *264*, 5070-5079.
(110) Hughes, R. K.; Bennett, B.; Bray, R. C., *Biochemistry* **1992,** *31*, 3073-3083.
(111) Ta, D. T.; Vickery, L. E., *J. Biol. Chem.* **1992,** *267*, 11120-11125.
(112) Miller, V. P.; Thorson, J. S.; Ploux, O.; Lo, S. F.; Liu, H. W., *Biochemistry* **1993,** *32*, 11934-11942.
(113) Thorson, J. S.; Liu, H.-W., *J. Am. Chem. Soc.* **1993,** *115*, 7539-40.
(114) Fox, B. G.; Hendrich, M. P.; Surerus, K. K.; Andersson, K. K.; Froland, W. A.; Lipscomb, J. D.; Münck, E., *J. Am. Chem. Soc.* **1993,** *113*, 3688-3701.
(115) Meyer, J.; Fujinaga, J.; Gaillard, J.; Lutz, M., *Biochemistry* **1994,** *33*, 13642-13650.
(116) Cheng, H.; Xia, B.; Reed, G. H.; Markley, J. L., *Biochemistry* **1994,** *33*, 3155-3164.
(117) Smith, E. T.; Adams, M. W. W., *Biochim. Biophys. Acta* **1994,** *1206*, 105-112.
(118) Wu, J.; Dunham, W. R.; Weiss, B., *J. Biol. Chem.* **1995,** *270*, 10323-10327.
(119) Yano, T.; Yagi, T.; Sled, V. D.; Ohnishi, T., *J. Biol. Chem.* **1995,** *270*, 18264-18270.
(120) Lloyd, S. G.; Franco, R.; Moura, J. J. G.; Moura, I.; Ferreira, G. C.; Huynh, B. H., *J. Am. Chem. Soc.* **1996,** *118*, 9892-9900.
(121) Garg, R. P.; Vargo, C. J.; Cui, X.; Kurtz, D. M., Jr., *Biochemistry* **1996,** *35*, 6297-6301.
(122) Quail, M. A.; Jordan, P.; Grogan, J. M.; Butt, J. N.; Lutz, M.; Thomson, A. J.; Andrews, S. C.; Guest, J. R., *Biochem. Biophys. Res. Commun.* **1996,** *229*, 635-642.
(123) Gladyshev, V. N.; Khangulov, S. V.; Stadtman, T. C., *Biochemistry* **1996,** *35*, 212-223.
(124) Yano, T.; Chu, S. S.; Sled, V. D.; Ohnishi, T.; Yagi, T., *J. Biol. Chem.* **1997,** *272*, 4201-4211.
(125) Canne, C.; Stephan, I.; Finsterbusch, J.; Lingens, F.; Kappl, R.; Fetzner, S.; Hüttermann, J., *Biochemistry* **1997,** *36*, 9780-90.
(126) Luykx, D. M.; Duine, J. A.; de Vries, S., *Biochemistry* **1998,** *37*, 11366-11375.
(127) Hänzelmann, P.; Meyer, O., *Eur. J. Biochem.* **1998,** *255*, 755-765.
(128) Day, A. L.; Parsons, B. M.; Dailey, H. A., *Arch. Biochem. Biophys.* **1998,** *359*, 160-169.
(129) Müller, K.; Matzanke, B. F.; Schünemann, V.; Trautwein, A. X.; Hantke, K., *Eur. J. Biochem.* **1998,** *258*, 1001-1008.
(130) Atta, M.; Lafferty, M. E.; Johnson, M. K.; Gaillard, J.; Meyer, J., *Biochemistry* **1998,** *37*, 15974-15980.
(131) Gallagher, S. C.; Cammack, R.; Dalton, H., *Biochem. J.* **1999,** *339*, 79-85.
(132) Chatelet, C.; Gaillard, J.; Pétillot, Y.; Louwagie, M.; Meyer, J., *Biochem. Biophys. Res. Commun.* **1999,** *261*, 885-889.
(133) Olson, J. W.; Agar, J. N.; Johnson, M. K.; Maier, R. J., *Biochemistry* **2000,** *39*, 16213-16219.
(134) Armengaud, J.; Gaillard, J.; Timmis, K. N., *J Bacteriol* **2000,** *182*, 2238-2244.
(135) Sugimori, D.; Ichimata, T.; Ikeda, A.; Nakamura, S., *Biometals* **2000,** *13*, 23-28.
(136) Verhagen, M. F. J. M.; O'Rourke, T. W.; Menon, A. L.; Adams, M. W. W., *Biochim. Biophys. Acta* **2001,** *1505*, 209-219.
(137) Zu, Y.; Di Bernardo, S.; Yagi, T.; Hirst, J., *Biochemistry* **2002,** *41*, 10056-10569.
(138) Dermoun, Z.; De Luca, G.; Asso, M.; Bertrand, P.; Guerlesquin, F.; Guigliarelli, B., *Biochim. Biophys. Acta* **2002,** *1556*, 217-225.
(139) Iwasaki, T.; Kounosu, A.; Aoshima, M.; Ohmori, D.; Imai, T.; Urushiyama, A.; Cosper, N. J.; Scott, R. A., *J. Biol. Chem.* **2002,** *277*, 39642-39648.
(140) Meyer, J.; Clay, M. D.; Johnson, M. K.; Stubna, A.; Münck, E.; Higgins, C.; Wittung-Stafshede, P., *Biochemistry* **2002,** *41*, 3096-3108.
(141) Mitou, G.; Higgins, C.; Wittung-Stafshede, P.; Conover, R. C.; Smith, A. D.; Johnson, M. K.; Gaillard, J.; Stubna, A.; Münck, E.; Meyer, J., *Biochemistry* **2003,** *42*, 1354-1364.
(142) Pan, G.; Menon, A. L.; Adams, M. W. W., *J. Biol. Inorg. Chem.* **2003,** *8*, 469-474.
(143) Mohsen, A. W.; Rigby, S. E. J.; Jensen, K. F.; Munro, A. W.; Scrutton, N. S., *Biochemistry* **2004,** *43*, 6498-6510.
(144) Barquera, B.; Nilges, M. J.; Morgan, J. E.; Ramirez-Silva, L.; Zhou, W.; Gennis, R. B., *Biochemistry* **2004,** *43*, 12322-12330.
(145) Türk, K.; Puhar, A.; Neese, F.; Bill, E.; Fritz, G.; Steuber, J., *J. Biol. Chem.* **2004,** *279*, 21349-21355.
(146) More, C.; Asso, M.; Roger, G.; Guigliarelli, B.; Caldeira, J.; Moura, J.; Bertrand, P., *Biochemistry* **2005,** *44*, 11628-11635.
(147) Alhapel, A.; Darley, D. J.; Wagener, N.; Eckel, E.; Elsner, N.; Pierik, A. J., *Proc. Natl. Acad. Sci. U. S. A.* **2006,** *103*, 12341-12346.

(148) Martínez-Espinosa, R. M.; Richardson, D. J.; Butt, J. N.; Bonete, M. J., *FEMS Microbiol. Lett.* **2007,** *277*, 50-55.
(149) Wu, C. H.; Jiang, W.; Krebs, C.; Stubbe, J., *Biochemistry* **2007,** *46*, 11577-11588.
(150) Reda, T.; Barker, C. D.; Hirst, J., *Biochemistry* **2008,** *47*, 8885-8893.
(151) Ewen, K. M.; Hannemann, F.; Khatri, Y.; Perlova, O.; Kappl, R.; Krug, D.; Hüttermann, J.; Müller, R.; Bernhardt, R., *J. Biol. Chem.* **2009,** *284*, 28590-28598.
(152) Germer, F.; Zebger, I.; Saggu, M.; Lendzian, F.; Schulz, R.; Appel, J., *J. Biol. Chem.* **2009,** *284*, 36462-36472.
(153) Schilhabel, A.; Studenik, S.; Vödisch, M.; Kreher, S.; Schlott, B.; Pierik, A.; Diekert, G., *J. Bacteriol.* **2009,** *191*, 588-599.
(154) Dikanov, S. A.; Samoilova, R. I.; Kappl, R.; Crofts, A. R.; Hüttermann, J., *Phys. Chem. Chem. Phys.* **2009,** *11*, 6807-6819.
(155) Roessler, M. M.; King, M. S.; Robinson, A. J.; Armstrong, F. A.; Harmer, J.; Hirst, J., *Proc. Natl. Acad. Sci. U. S. A.* **2010,** *107*, 1930-1935.
(156) Voss, I.; Goss, T.; Murozuka, E.; Altmann, B.; McLean, K. J.; Rigby, S. E.; Munro, A. W.; Scheibe, R.; Hase, T.; Hanke, G. T., *J. Biol. Chem.* **2011,** *286*, 50-59.
(157) García, L. L.; Rivas-Marín, E.; Floriano, B.; Bernhardt, R.; Ewen, K. M.; Reyes-Ramírez, F.; Santero, E., *J. Biol. Chem.* **2011,** *286*, 1709-1718.
(158) Abdalla, J. A.; Bowen, A. M.; Bell, S. G.; Wong, L. L.; Timmel, C. R.; Harmer, J., *Phys. Chem. Chem. Phys.* **2012,** *14*, 6526-6537.
(159) Mapolelo, D. T.; Zhang, B.; Naik, S. G.; Huynh, B. H.; Johnson, M. K., *Biochemistry* **2012,** *51*, 8071-8084.
(160) Johnson, T. W.; Li, H.; Frigaard, N. U.; Golbeck, J. H.; Bryant, D. A., *Biochemistry* **2013,** *52*, 1331-1343.
(161) Banci, L.; Ciofi-Baffoni, S.; Mikolajczyk, M.; Winkelmann, J.; Bill, E.; Pandelia, M. E., *J. Biol. Inorg. Chem.* **2013,** *18*, 883-893.
(162) Martin, D.; Charpilienne, A.; Parent, A.; Boussac, A.; D'Autreaux, B.; Poupon, J.; Poncet, D., *FASEB J.* **2013,** *27*, 1074-1083.
(163) Kolaj-Robin, O.; Noor, M. R.; O'Kane, S. R.; Baymann, F.; Soulimane, T., *PLoS One* **2013,** *8*, e53559.
(164) Singh, A. K.; Shin, J. H.; Lee, K. L.; Imlay, J. A.; Roe, J. H., *Mol. Microbiol.* **2013,** *90*, 983-996.
(165) Banci, L.; Ciofi-Baffoni, S.; Gajda, K.; Muzzioli, R.; Peruzzini, R.; Winkelmann, J., *Nat. Chem. Biol.* **2015,** *11*, 772-778.
(166) Rajakovich, L. J.; Norgaard, H.; Warui, D. M.; Chang, W. C.; Li, N.; Booker, S. J.; Krebs, C.; Bollinger, J. M., Jr.; Pandelia, M. E., *J. Am. Chem. Soc.* **2015,** *137*, 11695-11709.
(167) Netz, D. J.; Genau, H. M.; Weiler, B. D.; Bill, E.; Pierik, A. J.; Lill, R., *Biochem. J.* **2016,** *473*, 2073-2085.
(168) Birrell, J. A.; Laurich, C.; Reijerse, E. J.; Ogata, H.; Lubitz, W., *Biochemistry* **2016,** *55*, 4344-4355.
(169) Watanabe, S.; Tajima, K.; Matsui, K.; Watanabe, Y., *Biosci. Biotechnol. Biochem.* **2016,** *80*, 2371-2375.
(170) Maiti, B. K.; Moura, I.; Moura, J. J. G.; Pauleta, S. R., *Biochim. Biophys. Acta* **2016,** *1857*, 1422-1429.
(171) Beilschmidt, L. K.; Ollagnier de Choudens, S.; Fournier, M.; Sanakis, I.; Hograindleur, M. A.; Clemancey, M.; Blondin, G.; Schmucker, S.; Eisenmann, A.; Weiss, A.; Koebel, P.; Messaddeq, N.; Puccio, H.; Martelli, A., *Nat. Commun.* **2017,** *8*, 15124.
(172) Barr, I.; Stich, T. A.; Gizzi, A. S.; Grove, T. L.; Bonanno, J. B.; Latham, J. A.; Chung, T.; Wilmot, C. M.; Britt, R. D.; Almo, S. C.; Klinman, J. P., *Biochemistry* **2018,** *57*, 1306-1315.
(173) Dörner, K.; Vranas, M.; Schimpf, J.; Straub, I. R.; Hoeser, J.; Friedrich, T., *Biochemistry* **2017,** *56*, 2770-2778.
(174) Dunham, W. R.; Bearden, A. J.; Salmeen, I. T.; Palmer, G.; Sands, R. H.; Orme-Johnson, W. H.; Beinert, H., *Biochim. Biophys. Acta* **1971,** *253*, 134-152.
(175) Kuzmann, E.; Hommonay, Z.; Nagy, S.; Nomura, K., Mössbauer spectroscopy. In *Handbook of nuclear chemistry*, 2nd ed.; Vértes, A.; Nagy, S.; Klencsár, Z.; Lovas, R. G.; Rösch, F., Eds. Springer: Boston, 2011; pp 1379-1446.
(176) Cooke, R.; Tsibris, J. C.; Debrunner, P. G.; Tsai, R.; Gunsalus, I. C.; Frauenfelder, H., *Proc. Natl. Acad. Sci. U. S. A.* **1968,** *59*, 1045-1052.
(177) Cammack, R.; Rao, K. K.; Hall, D. O.; Johnson, C. E., *Biochem. J.* **1971,** *125*, 849-856.
(178) Münck, E.; Debrunner, P. G.; Tsibris, J. C.; Gunsalus, I. C., *Biochemistry* **1972,** *11*, 855-863.
(179) Werber, M. M.; Bauminger, E. R.; Cohen, S. G.; Ofer, S., *Biophys. Struct. Mech.* **1978,** *4*, 169-177.
(180) Barata, B. A.; Liang, J.; Moura, I.; Legall, J.; Moura, J. J. G.; Huynh, B. H., *Eur. J. Biochem.* **1992,** *204*, 773-778.
(181) Khoroshilova, N.; Popescu, C.; Münck, E.; Beinert, H.; Kiley, P. J., *Proc. Natl. Acad. Sci. U. S. A.* **1997,** *94*, 6087-6092.
(182) Boll, M.; Fuchs, G.; Meier, C.; Trautwein, A.; El Kasmi, A.; Ragsdale, S. W.; Buchanan, G.; Lowe, D. J., *J. Biol. Chem.* **2001,** *276*, 47853-47862.

(183) Krebs, C.; Agar, J. N.; Smith, A. D.; Frazzon, J.; Dean, D. R.; Huynh, B. H.; Johnson, M. K., *Biochemistry* **2001,** *40*, 14069-14080.
(184) Wu, G.; Mansy, S. S.; Hemann, C.; Hille, R.; Surerus, K. K.; Cowan, J. A., *J. Biol. Inorg. Chem.* **2002,** *7*, 526-532.
(185) Ollagnier-de Choudens, S.; Nachin, L.; Sanakis, Y.; Loiseau, L.; Barras, F.; Fontecave, M., *J. Biol. Chem.* **2003,** *278*, 17993-18001.
(186) Wollenberg, M.; Berndt, C.; Bill, E.; Schwenn, J. D.; Seidler, A., *Eur. J. Biochem.* **2003,** *270*, 1662-1671.
(187) Lin, P. C.; Puhar, A.; Türk, K.; Piligkos, S.; Bill, E.; Neese, F.; Steuber, J., *J. Biol. Chem.* **2005,** *280*, 22560-22563.
(188) Smith, A. D.; Jameson, G. N.; Dos Santos, P. C.; Agar, J. N.; Naik, S.; Krebs, C.; Frazzon, J.; Dean, D. R.; Huynh, B. H.; Johnson, M. K., *Biochemistry* **2005,** *44*, 12955-12969.
(189) Lillig, C. H.; Berndt, C.; Vergnolle, O.; Lönn, M. E.; Hudemann, C.; Bill, E.; Holmgren, A., *Proc. Natl. Acad. Sci. USA* **2005,** *102*, 8168-8173.
(190) Bandyopadhyay, S.; Gama, F.; Molina-Navarro, M. M.; Gualberto, J. M.; Claxton, R.; Naik, S. G.; Huynh, B. H.; Herrero, E.; Jacquot, J. P.; Johnson, M. K.; Rouhier, N., *EMBO J.* **2008,** *27*, 1122-1133.
(191) Gupta, V.; Sendra, M.; Naik, S. G.; Chahal, H. K.; Huynh, B. H.; Outten, F. W.; Fontecave, M.; Ollagnier de Choudens, S., *J. Am. Chem. Soc.* **2009,** *131*, 6149-6153.
(192) Wu, S. P.; Bellei, M.; Mansy, S. S.; Battistuzzi, G.; Sola, M.; Cowan, J. A., *J. Inorg. Biochem.* **2011,** *105*, 806-811.
(193) Bhave, D. P.; Hong, J. A.; Lee, M.; Jiang, W.; Krebs, C.; Carroll, K. S., *J. Biol. Chem.* **2011,** *286*, 1216-1226.
(194) Bhave, D. P.; Hong, J. A.; Keller, R. L.; Krebs, C.; Carroll, K. S., *ACS Chem. Biol.* **2012,** *7*, 306-315.
(195) Bräutigam, L.; Johansson, C.; Kubsch, B.; McDonough, M. A.; Bill, E.; Holmgren, A.; Berndt, C., *Biochem. Biophys. Res. Commun.* **2013,** *436*, 491-496.
(196) Gao, H.; Subramanian, S.; Couturier, J.; Naik, S. G.; Kim, S. K.; Leustek, T.; Knaff, D. B.; Wu, H. C.; Vignols, F.; Huynh, B. H.; Rouhier, N.; Johnson, M. K., *Biochemistry* **2013,** *52*, 6633-6645.
(197) Guo, Y.; Yoda, Y.; Zhang, X.; Xiao, Y.; Cramer, S. P., Synchotron radiation based nuclear resonant scattering: applications to bioinorganic chemistry. In *Mössbauer spectroscopy: Applications in chemistry, biology, and nanotechnology*, 1 ed.; Sharma, V. K.; Klingelhöfer, G.; Nishida, T., Eds. Wiley: Hoboken, 2013; pp 249-271.
(198) Bouvier, D.; Labessan, N.; Clémancey, M.; Latour, J. M.; Ravanat, J.-L.; Fontecave, M.; Atta, M., *Nucleic Acids Res.* **2014,** *42*, 7960-7970.
(199) Folgosa, F.; Camacho, I.; Penas, D.; Guilherme, M.; Frois, J.; Ribeiro, P. A.; Tavares, P.; Pereira, A. S., *Radiat. Environ. Biophys.* **2015,** *54*, 111-121.
(200) Rietzschel, N.; Pierik, A. J.; Bill, E.; Lill, R.; Mühlenhoff, U., *Mol. Cell. Biol.* **2015,** *35*, 370-378.
(201) Saichana, N.; Tanizawa, K.; Pechousek, J.; Novak, P.; Yakushi, T.; Toyama, H.; Frebortova, J., *J. Biochem.* **2016,** *159*, 87-99.
(202) Tanner, A. W.; Carabetta, V. J.; Martinie, R. J.; Mashruwala, A. A.; Boyd, J. M.; Krebs, C.; Dubnau, D., *Mol. Microbiol.* **2017,** *104*, 837-850.
(203) Grell, T. A. J.; Kincannon, W. M.; Bruender, N. A.; Blaesi, E. J.; Krebs, C.; Bandarian, V.; Drennan, C. L., *J. Biol. Chem.* **2018,** *293*, 17349-17361.
(204) Agar, J. N.; Krebs, C.; Frazzon, J.; Huynh, B. H.; Dean, D. R.; Johnson, M. K., *Biochemistry* **2000,** *39*, 7856-7862.
(205) Chandramouli, K.; Unciuleac, M. C.; Naik, S.; Dean, D. R.; Huynh, B. H.; Johnson, M. K., *Biochemistry* **2007,** *46*, 6804-6811.
(206) Fox, N. G.; Chakrabarti, M.; McCormick, S. P.; Lindahl, P. A.; Barondeau, D. P., *Biochemistry* **2015,** *54*, 3871-3879.
(207) Fleischhacker, A. S.; Stubna, A.; Hsueh, K. L.; Guo, Y.; Teter, S. J.; Rose, J. C.; Brunold, T. C.; Markley, J. L.; Munck, E.; Kiley, P. J., *Biochemistry* **2012,** *51*, 4453-4462.
(208) Ferecatu, I.; Goncalves, S.; Golinelli-Cohen, M. P.; Clemancey, M.; Martelli, A.; Riquier, S.; Guittet, E.; Latour, J. M.; Puccio, H.; Drapier, J. C.; Lescop, E.; Bouton, C., *J. Biol. Chem.* **2014,** *289*, 28070-28086.
(209) Golinelli-Cohen, M.-P.; Lescop, E.; Mons, C.; Goncalves, S.; Clémancey, M.; Santolini, J.; Guittet, E.; Blondin, G.; Latour, J.-M.; Bouton, C., *J. Biol. Chem.* **2016,** *291*, 7583-7593.
(210) Pellicer Martínez, M. T. Studies of iron- sulfur cluster containing regulators of the Rrf2 family. PhD, University of East Anglia, Norwich, 2017.
(211) Schünemann, V.; Trautwein, A. X.; Illerhaus, J.; Haehnel, W., *Biochemistry* **1999,** *38*, 8981-8991.
(212) Geary, P. J.; Dickson, D. P., *Biochem. J.* **1981,** *195*, 199-203.
(213) Müller, C. S.; Auerbach, H.; Stegmaier, K.; Wolny, J. A.; Schünemann, V.; Pierik, A. J., *Hyperfine Interact.* **2017,** *238*, 102.

(214) Fee, J. A.; Findling, K. L.; Yoshida, T.; Hille, R.; Tarr, G. E.; Hearshen, D. O.; Dunham, W. R.; Day, E. P.; Kent, T. A.; Münck, E., *J. Biol. Chem.* **1984,** *259*, 124-133.
(215) Rao, K. K.; Cammack, R.; Hall, D. O.; Johnson, C. E., *Biochem. J.* **1971,** *122*, 257-265.
(216) Bill, E.; Bernhardt, F. H.; Trautwein, A. X., *Eur. J. Biochem.* **1981,** *121*, 39-46.